Elucidation of the molecular pathways of lifespan extension by dietary restriction in yeast

Joseph R Delaney

A dissertation

submitted in partial fulfillment of the

requirements for the degree of

Doctor of Philosophy

University of Washington

2012

Reading Committee:

Matt Kaeberlein, Chair

Peter Rabinovitch

Maitreya Dunham

Program Authorized to Offer Degree:

Molecular and Cellular Biology

Abstract:

In this dissertation, we demonstrate strong support for the antagonistic pleiotropy view of aging, reveal the illusion of sirtuin mediated longevity in 32 long lived alleles (hopefully steering the field farther from sirtuin research and toward more interesting things), show that there is indeed a conserved aging factor between CLS and RLS, indicate that aging in yeast is complex like any other organism and use phenotype clustering to show *afg3*Δ was within the Gcn4 pathway of lifespan extension, and finally bring nuclear tRNA and Gln3 into the light- showing that these could positively affect lifespan without reducing translation.

Table of contents:

List of figures:

List of tables:

General Introduction

Studies of dietary restriction date back to the 1800s, where it was found that a single spider which did not eat or drink remained remarkably healthy for 204 days [1]. While such low powered studies nowadays do not reach the editors of the journal Science as this one did, studies of dietary restriction and aging are indeed increasing in importance to molecular biologists and indeed society as a whole. In particular, our lab and others have proposed the target of rapamycin, or TOR, pathway as being integral to the increased longevity imparted by dietary restriction, and Pubmed reveals an exponential trend with the number of papers associating TOR with longevity:

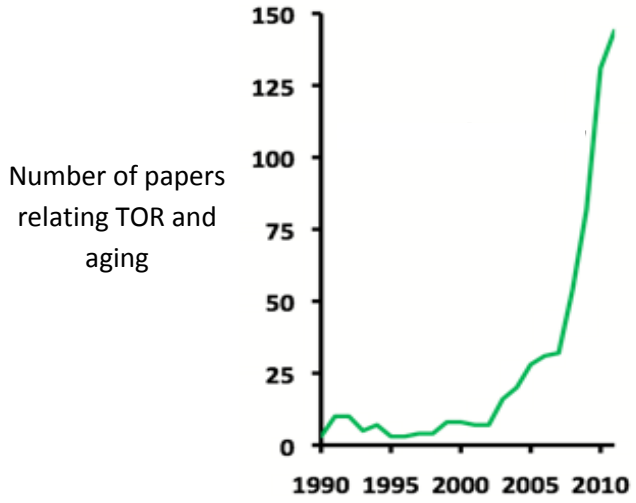

This dissertation will analyze how the TOR pathway and dietary restriction interact with a variety of factors to influence aging. As a dissertation, it will of course primarily focus on the research I and my colleagues have performed directly.

Since, as Theodosius Dobzhansky wrote in a famous essay, nothing in biology makes sense except in the light of evolution, I will begin our discussion with the first rigorous testing of a popular aging theory in yeast. Section I describes my first publication in the Kaeberlein lab which improved our understanding of the theory of antagonistic pleiotropy. First proposed in 1957 by Dr. George Williams, the theory

proposed that there may be an energetic tradeoff between an organism being able to live long and an organism being able to reproduce efficiently[2]. A few studies had shown that for a favorite longevity allele, be it *daf-2*[3] or *age-1*[4], individuals were able to live long at the cost of their reproductive capacity. But these studies were limited to a single gene; nobody had systematically tested a set of long lived mutants for their ability as a group to uphold the theory of antagonistic pleiotropy. I filled this gap in the literature through testing 48 long lived deletions (and one overexpression) in yeast for their ability to compete with wild type yeast. If wild type yeast could outcompete them, then it would be reasonable to conclude that for these alleles, longevity was indeed a tradeoff for fitness. Even in our simple assay testing only the ability to grow quickly and maintain a short stationary phase, 32 out of the 49 mutants were outcompeted by wild type yeast. In addition, no other study showed a statistical enrichment over a control set; experiments had only tested a single gene at a time and hence there was never a legitimate control other than wild type. We took our results an extra step and tested ten random mutants without a long lifespan and found that while many were outcompeted by wild type, only one out of ten reached the magnitude of fitness defect that 25 out of 49 long lived mutants did. This test demonstrates a clear enrichment for genes fitting the antagonistic pleiotropy hypothesis. It is our prediction that if our fitness assays were able to test for other things which may occur in nature, such as resistance to environmental stresses, there may be an even greater enrichment of poor fitness in the long lived set. This was the first systematic study to widely support the view that aging evolved due to a tradeoff between fitness and longevity.

While longevity evolves in a biological sense, it seems as though the study of aging evolves as well. While my mentor Dr. Matt Kaeberlein has authored or coauthored a variety of studies which focus on the positive relationship between Sirtuins and longevity, he has since fought hard to show that the field is wrought with poor interpretations and shoddy data. Indeed, the drug resveratrol has been widely disputed to have any effects either on Sirtuins or on aging and has frustrated many scientists over the years (I will always remember Dr. Richardson presenting mouse lifespan data from three institutes: he showed a single

slide with thousands of mice treated with a range of resveratrol concentrations with no effect. Then he switched to the rapamycin slide, which showed wonderfully consistent lifespan extension). The fluorophore used to find Sirtuin activators was shown to be selectively cleaved when resveratrol was added to the experiment, but resveratrol had no effect on native histone substrates[5]. Furthermore, even though Sir2 was published and widely cited to be "necessary" for dietary restriction to function to extend lifespan[6,7], Dr. Kaeberlein showed that it was in fact dispensable for lifespan extension when a form of yeast specific damage was removed through deletion of *FOB1*[8]. While Sirtuins are undoubtedly interesting proteins, there seems to be little evidence that they mediate lifespan extension by dietary restriction. In an attempt to put one of the final nails in the coffin to Sir2, we published a paper showing that 32 long lived single-gene deletion mutants in yeast in a variety of pathways could not extend a *sir2*Δ mutant. While one hypothesis is that ALL 32 require Sir2 for lifespan extension, we instead posit that *sir2*Δ mutants produce a form of damage that does not occur during normal aging and thus alleles which slow aging cannot rescue the mutant's short lifespan. In addition, we show seven of these long lived deletions and four forms of dietary restriction can extend a *sir2*Δ mutant when FOB1 is deleted as well, giving support to our non-aging related damage limiting hypothesis. This study is represented in Section II.

It may be noted that the studies I have pursued in the lab mostly pertain to studying mutants which extend replicative lifespan. However, many yeast labs study a different form of "aging": chronological lifespan (CLS). Our lab has thoroughly demonstrated why chronological aging, at least as studied by most of the field, may be a yeast specific phenomenon. On a molecular basis, CLS is determined primarily by nutrient conditions reducing the formation of acetic acid to "extend" lifespan[9]. Chris Burtner and Chris Murakami therefore proposed that transferring yeast to water during CLS may better detect yeast strains which age slowly without having acetic acid complicate the interpretation. It is theoretically possible that humans are affected by some form of cellular extrinsic lowering of the pH, accompanied by a similarly detrimental metabolite, but the evidence for this is sparse[10]. More importantly, Burtner and Murakami

tested a random assortment of 550 genes for CLS and for acidification of culture media. While these mutants were highly enriched for long CLS within the strains which did not acidify the media, there was no statistical enrichment for a conservation of long lived (by CLS) strains with replicatively long lived strains, nor did knockdowns of their homologues in *Caenorhabditis elegans* tend to be long lived[11]. Combining these two results would seem to suggest CLS is a poor measure of aging in the sense that it is not valuable to study conserved mechanisms. However, there is a strong enrichment in long lived knockdowns in *Caenorhabditis elegans* that tend to also be long lived in our replicative lifespan assay for yeast homologous deletions [12] [13]. Thus it seems the RLS assay is more promising for finding conserved longevity pathways, and this is the reason we spend so much effort elucidating pathways through this technique.

That being said, we present novel findings relating CLS to RLS in Section III. It appears that if cells are aged chronologically, their replicative lifespan is also shortened, as has been previously shown in a brief report [14]. We were able to confirm that aging cells in two of the most commonly utilized chronological aging medias, synthetic complete (2% glucose) and YEPD, were able to have subsequent effects on shortening replicative lifespan. Furthermore, two methods which extend CLS, reducing glucose in the media to 0.05% and buffering the media to a pH of 6.0, were both able to drastically attenuate the decrease in replicative lifespan noted for later chronological age time points. It would appear that there is some molecular phenotype which is indeed conserved between CLS and RLS, and that damage of this component reduces the lifespan in both conditions. One possibility for this damage was something referred to as DNA replication stress, a model pushed by the Burhans lab [15]. We found that indeed, chronologically aged cells were subject to this phenomenon as evidenced by their inappropriate DNA synthesis as they age, despite the lack of nutrients to complete a cell division. Furthermore this effect was reduced in longer lived media conditions. Cells which were budded were exclusively in the dead fraction of cells aged chronologically, however, suggesting that replication stress (or conversely, DNA stability) is not the conserved factor between CLS and RLS. We are still searching for what this

conserved factor may be, and are looking at proteotoxic stress and mitochondria health as the two most promising forms of stress which may be conserved between the two methods. Nonetheless, this study substantially advances our understanding of the differences and potential similarities between CLS and RLS.

There are any number of papers in the aging field which may point out that proteotoxic stress and mitochondria health are obvious directions to look for something which universally affects aging [16 17 18 19]. Yet, no comprehensive study on long lived alleles in any organism has ever attempted to look for a universal stress which long lived strains are better able to handle. If there were a single stress, it would be more convincing that this form of stress is a primary component of the stochastic aging process. With the wealth of data I was able to produce from assaying the 49 long lived alleles in the antagonistic pleiotropy project, I felt that our yeast system could finally address this point. My undergraduate Umema Ahmed undertook this project with me to determine systematically the ability of different stresses to affect the growth rates of long lived alleles. The results are expanded upon in Section IV. This study was somewhat complicated by the fact that many long lived yeast grow slowly, so we determined how a stress would slow yeast division both in terms of percent change in growth rate as well as in absolute changes in doubling times. Complications aside, these sets of data directly compared longevity alleles with their ability to grow in media which could affect DNA damage rates (by addition of the alkylating agent MMS or survivability after UV treatment), oxidative and mitochondria stress (by addition of paraquat, an ETC inhibitor which produces free radicals), endoplasmic reticulum based proteotoxic stress (by addition of tunicamycin, which results in a buildup of proteins with inadequate glycosylation), and general proteotoxic stress (by heat shock). For better or worse, no individual stress was universally resisted by these long lived strains. This indicates that even lowly yeast have a complex regulation of lifespan which likely involves multiple forms of damage, and RLS is not simply an assay for a single form of damage but rather a legitimate measure of the aging process. Nonetheless, we did in fact find that the subset of genes which affect both translation and lifespan in yeast were resistant to additional growth rate inhibition by

addition of paraquat or tunicamycin and were also resistant to heat shock. Surprisingly, a single mutant clustered with these translation mutants which we felt should not necessarily belong: the AAA metalloprotease *afg3*Δ mutant, which is involved in mitochondria complex formation. It also has a defect in translation and we were able to use these clustered phenotypes to place it in the translation reduction pathway of lifespan extension. Like other translation mutants, it required Gcn4 for its lifespan extension and the lifespan extension in *afg3*Δ was not additive with that of *rpl20b*Δ. We stress in this report that clustering based on phenotypes may be a way to place mutants within known longevity pathways, as evidenced by the *afg3*Δ example.

While I have thoroughly described how sirtuins are not part of the dietary restriction pathway and how *afg3*Δ may act similar to dietary restriction mimetics (reduction of translation mutants), I felt there was a large gap in our understanding of how dietary restriction functions to extend lifespan. In particular, even though *tor1*Δ could be thought to reduce translation, it in fact has no effect on cell growth in yeast, despite having an extended lifespan. I was curious if I could find a signal downstream of reduced translation which converged with *tor1*Δ and dietary restriction. The way I eventually figured out this signal was through exploring the reasons why a tRNA nuclear exporter mutant [20], *los1*Δ, was long lived.

In Section V, I present my cornerstone project which will have the most impact on the aging field. We found that *los1*Δ was long lived (by RLS), even though the mutant had no reduced translation, similar to *tor1*Δ. It was known that buildup of nuclear tRNA occurs during many forms of DR [21 22], so it seemed logical that *los1*Δ may overlap with the DR pathway. In fact, *los1*Δ and DR are non-additive in their lifespan extension, suggesting they work by similar mechanisms. I discovered that the localization of Los1p could be controlled by DR and that the translocation of Los1 from the nucleus to the cytoplasm by DR was entirely dependent on the DNA damage signal amplification factor Rad53. Rad53 itself was upregulated by DR, although not to the same levels as when stressed by MMS. We performed a microarray analysis of *los1*Δ mutant yeast and found that 60 genes were upregulated compared to wild

type control yeast. Of these genes, 88% were regulated by Gcn4 and 22% were regulated by Gln3. We already knew Gcn4 was partially required for lifespan extension by DR, but it was certainly not the only factor. We found that Gln3 was entirely necessary for lifespan extension by DR, and that low copy overexpression of Gln3 was sufficient to extend RLS by an astounding 80%. With these data, I was able to construct a complete pathway starting with DR, leading into Rad53 and Los1, and terminating on upregulation of the transcription factor Gln3. This is the greatest leap in the yeast DR field since 2008, when Gcn4 was first identified as an aging regulator.

In summary, I have had an incredibly rewarding experience in the Kaeberlein lab. I have been able to attack questions of the basic biology of aging to an extent I never thought I would be able to do in four years at the University of Washington. We demonstrated strong support for the antagonistic pleiotropy view of aging, revealed the illusion of sirtuin mediated longevity in 32 long lived strains (hopefully steering the field farther from sirtuin research and toward more interesting things), found that there is indeed a conserved aging factor between CLS and RLS, showed that aging in yeast is complex like any other organism and used phenotype clustering to show afg3Δ was within the Gcn4 pathway of lifespan extension, and finally brought nuclear tRNA and Gln3 into the light- showing that these could positively affect lifespan without reducing translation. I know these findings have advanced our understanding of aging and will continue to push for further understanding in my future career. Please enjoy the expanded description of these exciting results in the sections which follow.

Section I: Quantitative evidence for early life fitness defects from 32 longevity-associated alleles in yeast

The following section is based on this publication[23].

Abstract:

Reduced fecundity has been associated with some alleles that enhance longevity in invertebrate and mammalian models. This observation has been suggested to support the antagonistic pleiotropy theory of aging, which predicts that alleles of some genes promoting fitness early in life have detrimental effects later in life that limit survival. In only a few cases, however, has the relative fitness of long-lived mutants been quantified through direct competition with the wild type genotype. Here we report the first comprehensive analysis of longevity/fitness trade-offs by measuring the relative fitness of 49 long-lived yeast variants in a direct competition assay with wild type cells. We find that 32 (65%) of these variants show a significant defect in fitness in this competition assay. In 26 (81%) of these cases, this reduction in fitness can be partially accounted for by reduced maximal growth rate during early life, usually resulting from a G0/G1-specific cell cycle defect. A majority of the less fit longevity-enhancing variants are associated with reduced mRNA translation. These findings are therefore consistent with the idea that enhanced longevity often comes with a fitness cost and suggest that this cost is often associated with variation in a subset of longevity factors, such as those regulating mRNA translation, growth, and reproduction.

Introduction:

The antagonistic pleiotropy model of aging posits that aging results from the action of genetic variants that are beneficial early in life, but detrimental later[2]. Natural selection favors those variants that promote survival to reproductive age or enhance reproductive output, but the effect of these same variants on post-reproductive survival is relatively unimportant, since the force of natural selection is no longer significant late in life. Evidence consistent with this model has been provided by the observation that many mutations associated with increased life span also cause a reduction in fecundity. Several examples of this "trade-off" have been noted in different species, including bacteria[24], nematodes[3,25,26], flies[27,28], and mice[29]. In particular, a number of fruit fly experiments were designed to increase lifespan through artificial selection and mutants which resulted from this selection were also shown to have reduced rates of larval development or egg laying[30-34]. This relationship is not universal, however, since other longevity enhancing alleles have been isolated that do not significantly reduce fecundity[35,36]. Reproduction under optimal conditions is not the only measure of fitness that determines evolutionary success, however, and it may be that longevity-associated variants without fecundity defects reduce evolutionary fitness in other ways.

One way to quantify fitness is to allow different genetic variants to compete against each other under conditions that mimic the natural environment. A few experiments along these lines have been performed in invertebrate organisms to test the prediction that mutations causing slower aging also reduce fitness. For example, Jenkins *et al.* showed that *C elegans* mutants with decreased function of the insulin-like-receptor DAF-2 resulted in decreased fitness when co-cultured with wild type animals[37]. There are also cases where long-lived mutants only have reduced fitness under certain conditions. For example, Walker *et al.* examined the relative fitness of long-lived *age-1(hx546)* mutant nematodes, which also have reduced insulin-like signaling, and found that under standard laboratory conditions *age-1(hx546)* mutant animals were not outcompeted by wild type animals[4]. However, when a cyclic period

of starvation was introduced into the experimental design, the wild type animals outcompeted the *age-1(hx546)* mutants, although the mechanistic basis for this was not determined. A similar observation was made using long-lived *Indy* mutant fruit flies which only showed reduced fitness when food was calorie poor[38], although it should be noted that the longevity and fitness phenotypes of these flies is likely not due to mutation at the *Indy* locus[39]. Despite the plethora of longevity alleles known in biology, very few additional studies have directly addressed the prevalence or mechanistic basis of fitness trade-offs among long-lived variants via direct competition assays.

The budding yeast *Saccharomyces cerevisiae* is an important model system for aging-related research, complementing the other invertebrate and mammalian model organisms[19]. The replicative life span (RLS) of a yeast mother cell is defined as the number of daughter cells produced prior to senescence, and can be measured by physical separation of the daughter cells away from the mother cell. Many different cellular processes have been implicated in RLS determination, including ribosomal DNA stability, nutrient response signaling, mitochondrial function, oxidative stress resistance, and mRNA translation[19,40]. As part of an ongoing genome-wide analysis of yeast aging, we have reported more than 50 genetic variations that cause increased RLS in one strain background[8,41-46]. Each of these variants is a single-gene deletion mutant contained in the yeast ORF deletion collection, with one exception: overexpression of the Sir2 protein deacetylase[47-49]. This collection of long-lived deletion mutants provides a unique opportunity to systematically test the prediction that genetic variants associated with longevity result in reduced fitness.

Here we describe the first large scale examination of the fitness costs associated with enhanced longevity by directly quantifying the relative fitness of 49 replicatively long-lived yeast variants in direct competition assays with the parental wild type strain. While our competition assay does not account for every challenge experienced by yeast in nature, such as the need for sexual reproduction and sporulation, the fitness assay nonetheless tests the strains under common conditions of rapid growth

followed by periods of starvation[50]. Of the 49 long-lived mutants, more than half were found to be significantly less fit than the wild type strain. In most cases, the longevity-associated fitness defect could be attributed to an elongated cell division cycle under optimal growth conditions, a measure of fecundity. Interestingly, this fecundity defect could largely be attributed to a delay in the G0/G1 phase of the cell cycle, further defining the molecular nature of the trade-off between longevity and fitness in yeast.

Results:

Increased replicative life span is associated with reduced fitness in yeast

As an initial attempt to explore whether enhanced RLS is associated with decreased fitness, we competed 49 long-lived mutant strains against wild type cells in a fitness assay designed to mimic three cycles of growth and starvation (see **Materials and Methods**). Each cycle lasted for one week and was accomplished by growing mixed cultures containing wild type and one long-lived mutant through exponential phase into stationary phase in rich media. Roughly equal numbers of wild type and mutant cells were inoculated into the mixed culture at the initial time point, and relative viable cell number in each culture was quantified at the initial time point and weekly thereafter for three iterations. The strains chosen for this study were comprised from 52 previously reported long-lived yeast strains in the BY4742 genetic background[8,41-46], 51 of which are single-gene deletion mutants plus one overexpression strain (*SIR2-OX*) (**Table 1**). Three strains were excluded from the study because our flow cytometric analysis indicated that these strains from our *MAT*α haploid ORF deletion collection were, in fact, diploid (described in **Materials and Methods**).

We used a measure of relative fitness (RF) defined as the log base 2 ratio of mutant to wild type relative to the initial ratio, such that RF = 0 indicates no change in the ratio of mutant to wild type, an RF = 1 corresponds to twice as many mutant cells as wild type cells relative to the initial ratio, while an RF = -1 corresponds to twice as many wild type cells as mutant cells. Those strains for which no mutant cells were counted (ones which were completely outcompeted by wild type) at a non-zero time point were assigned an RF value of -7.

As an additional control, we compared the RF of wild type cells (BY4742) to a second 'wild type' BY4742 strain engineered with a single additional selectable marker at its endogenous locus (*LYS2*). The *LYS2* selectable marker allows for quantitation of the ratio of cells at each time point (see **Materials and Methods**). As expected, there was no significant difference in RF at the end of this control competition experiment between BY4742 and the *LYS2* strain (RF = -0.11±0.12), demonstrating relatively low intrinsic variance in the assay. Following three weeks of competition, 32 out of 49 long-lived strains showed a significant fitness defect compared to the *LYS2* control (**Table 1**).

In order to determine whether the RF of long-lived mutants differs from randomly selected deletion strains, we also determined RF for 20 randomly selected single-gene deletion mutants using identical assay conditions (**Fig. S2b, Table S1,** online at Cell Cycle). Based on a rank-sum comparison of final RF values, the set of long-lived mutants had significantly greater fitness defects than the randomly selected strains (p=8.41E-5). The difference in magnitude of the defect can also be seen from the fact only that 2/20 (10%) randomly selected deletion strains have an RF < -3, whereas, 25/49 (51%) in the long lived set reach an RF < -3. In addition, a g-test shows these data are from a sufficiently large sample size to show enrichment for competitive defect (p=7.12E-4).

The findings from the competitive fitness analysis indicate that single gene deletions causing enhanced RLS in yeast result, on average, in a more severe fitness defect than randomly selected gene deletions. The distribution of RF values for the two sets of gene deletions is noteworthy, however. The randomly selected gene deletions show a distribution of RF values that is normal (By Anderson-Darling test, p=0.223), while the long-lived mutants show a non-normal distribution of RF values that appears to be bimodal (p=3.17E-5, **Fig. 1C**). This distribution is suggestive of two types of long-lived mutants: one set that has a fitness profile similar to randomly selected deletion mutants and a second set that has a severe fitness defect.

Replicative longevity is associated with reduced maximal growth rate

A common trait associated with longevity enhancing mutations or interventions in higher eukaryotes is a reduced rate of reproduction or reduced maximal reproductive potential (reviewed in [51] and [52]). This observation has been interpreted to suggest that there is a trade-off between reproduction and somatic maintenance[53]. Since RLS is defined as the number of daughter cells an individual mother cell is capable of producing under optimal growth conditions, the doubling time of the cell is a measure of reproductive fitness under identical conditions. Variants with a shorter doubling time (faster growth rate) will produce more genetically identical progeny in a given period of time, relative to slower growing variants.

To assess whether slower growth rate is associated with reduced fitness in long-lived yeast strains, the doubling times of all 49 long-lived mutants was quantified using a Bioscreen C MBR machine (see **Materials and Methods**). Strikingly, 26 out of 32 (81%) of the long-lived mutants with significant fitness defects also exhibited a significant ($p<0.05$) increase in doubling time relative to the parental wild-type

strain (**Fig. 2a, Table 1)**. Among all of the long-lived strains tested, 28 out of 49 (57%) were slow growing. For comparison, only 14 out of 50 (28%) randomly selected single gene deletion strains showed a significant growth rate defect, and most defects were much lower in magnitude. These data indicate that reduced maximal growth rate, analogous to reduced fecundity of multicellular eukaryotes, is more common in long-lived variants compared to random deletion mutants and likely contributed to reduced fitness among a subset of these variants. Not all long-lived yeast strains are slow growing, however, nor are all slow-growing yeast strains long-lived. Thus, slow growth is neither necessary nor sufficient for enhanced replicative longevity.

Reduced maximal growth rate explains a majority of the observed fitness defects in long-lived mutants

In order to determine whether growth rate is sufficient to account for the observed RF defects of long-lived mutants, we performed *in silico* simulations of the competition assay in which the cell ratio of mutant to wild type was calculated as a function of the number of cell division cycles, taking into account maximal growth rate and RLS of each cell type. The cell count for wild type and mutant at each cell division round can be estimated by the following two formulas:

$$C_{wt}(d) = 2C_{wt}(d-1) - \frac{C_{wt}(d-1)}{2^{RLS_{wt}+1}}$$

and

$$C_{mut}(d) = \left(1 + \frac{\Delta_{wt}}{\Delta_{mut}}\right) C_{mut}(d-1) - \frac{C_{mut}(d-1)}{2^{RLS_{mut}+1}}$$

where $C_{wt}(d)$ and $C_{mut}(d)$ are the absolute cell counts for wild type and mutant at each wild type cell division (d), RLS_{wt} and RLS_{mut} are the experimentally determined mean RLS values for wild type and mutant, and Δ_{wt} and Δ_{mut} are the experimentally determined doubling times (maximal growth rates) for wild type and mutant.

An initial characterization of the global behavior of this simulation demonstrates that growth rate is a much more substantial determinant of fitness than is RLS in populations of dividing cells (**Fig. 3a,b**). We estimate that in our competitive fitness assay, the initial cells in each outgrowth phase are able to complete approximately 13 cell divisions prior to reaching saturation. Since three periods of growth and quiescence were used in the competitive fitness assay, we estimate a total of approximately 40 cell division cycles occurred during the course of each experiment. Even if we assume that a mutant strain has a wild type RLS of 52, which is approximately double that of the wild type strain, the effect on RF after 40 divisions is negligible as long as maximal growth rate of the mutant and wild type strains are equal (RLS_{mut} = 52, RLS_{wt} = 26, (Δ_{wt} = 90, Δ_{mut} = 90):

$$RF(40) = \log_2\left[\frac{C_{mut}(40)}{C_{wt}(40)}\right] = 2.15x10^{-7}$$

Indeed, based on this simulation, the effect of life span extension will never have a significant positive effect on RF of the mutant over the first 40 population doublings, and a reduced life span will only result in an RF < -3 when RLS of the mutant falls below 3, an approximately 90% reduction in mean RLS.

In contrast to the negligible effect of RLS on RF, if the maximal growth rate of the mutant strain is 10 minutes slower than the wild type (RLS_{mut} = 26, RLS_{wt} = 26, (Δ_{wt} = 90, Δ_{mut} = 100), our simulation predicts that it would result in a significant decrease in RF over the course of the competitive fitness assay:

$$RF(40) = \log_2\left[\frac{C_{mut}(40)}{C_{wt}(40)}\right] = -3.0$$

This simulation strongly supports the assertion that maximal growth rate, rather than replicative potential, is an appropriate measure of fecundity in this system, since replicative potential is essentially free from the force of natural selection.

We next compared the predicted RF values from our *in silico* simulation with the experimentally observed RF values for two mutants with a significant reduction in maximal growth rate. For both *sch9Δ*, and *dbp3Δ* , the RF values predicted by our algorithm closely parallel the actual RF values observed in the competitive fitness assay, based solely on the experimentally observed doubling times and RLS values (**Fig. 3C, S1,** online at Cell Cycle). These data further support the idea that, at least for a subset of long-lived mutants, the observed fitness defect can be primarily attributed to reduced fecundity.

Reduced maximal growth rate is most apparent early in the replicative lifespan

An important aspect of the antagonistic pleiotropy theory is that natural selection maximizes vigor early in life at the expense of vigor late in life[2]. A logical extension of this prediction is that life span extending alleles may reduce vigor specifically during early life stages. To test this possibility, we examined the relative growth rate of mother cells over the course of their RLS. This was accomplished by micromanipulation of daughter cells away from mother cells and quantification of the number of daughter cells removed from each mother cell at each time-point during a standard RLS assay. Relative

to wild type mother cells, the 32 long-lived mutants for which a competitive defect was observed show a significant decrease in the number of daughter cells produced during the first time-point, which corresponds to the first 1-2 budding cycles of the cell life span (**Fig. 4a**). This defect in vigor is also observed, although reduced in magnitude, at the second time-point of the life span experiment, corresponding to budding cycles 2-4 of the mother cell life span. By the third time-point, there is no significant difference between wild type and long-lived mutants. This early life loss of vigor in some long-lived mutants is further illustrated by quantifying the cumulative number of daughter cells produced as a function of time over the entire life course for *dbp3Δ*, *rpl31aΔ* and *sch9Δ* mother cells, which have a substantial reduction in competitive fitness, relative to wild type cells (**Fig. 4b**). Importantly, these long-lived mutants show improved vigor relative to wild type cells late in life. These data suggest that the reduced vigor associated with life span extension in these mutants is specific for the early stage of life and that late life vigor is enhanced, consistent with the antagonistic pleiotropy theory of aging.

Long-lived, slow growing mutants tend to have a G0/G1-specific cell cycle delay

We further explored the nature of the growth defect observed for the slow-growing, long-lived variants by examining their cell cycle profiles by flow cytometry (**Table 1, Fig. S1,** online at Cell Cycle). Interestingly, the growth defects associated with extended life span could be attributed almost exclusively to a delay in the G0/G1 phase of the cell cycle (**Table 1**). Many long-lived variants in yeast are known to have reduced levels of global mRNA translation[54], which can result in an elongated G0/G1 phase of the cell cycle due to delayed accumulation of G1 cyclins[55-57]. Consistent with this idea, all of the slow-growing translation-related mutants examined, with the exception of *tor1Δ*, showed a significant enrichment in the percentage of cells in the G0/G1 phase of the cell cycle (**Fig. 5, Table 1**). These long-

lived variants also showed evidence of reduced cell size, as assayed by forward scatter in the flow cytometer (**Fig. S3,** online at Cell Cycle), although this may be attributed in part to a greater percentage of smaller G0/G1 cells in the population.

While G0/G1 delay could account for slow growth in a majority of long-lived variants, three mutants showed abnormal cell cycle profiles without a substantial enrichment in G0/G1 cells (**Fig. S1,** online at Cell Cycle). Only the long-lived *ELP4* deletion strain has an increase in S-phase cells, consistent with an S-phase delay. Elp4 is subunit of the Elongator complex, a histone acetyltransferase component of the RNA polymerase II holoenzyme. Cells lacking *ALG12* or *SPT4* were enriched for G2 phase cells. Like Elp4, Spt4 also functions in transcriptional elongation by RNA polymerase II; however, *spt4Δ* cells are known to also have a high rate of chromosome missegregation, which could account for the observed polyploidy and the G2 enrichment. Alg12 adds a mannose group to asparagine residues in the endoplasmic reticulum, and its role in the cell cycle is unclear. Two other mutants (*pmr1Δ, sps1Δ*) had increased doubling times, but had no specific cell cycle defect that we could detect.

Among the randomly selected deletion strains, *bud22Δ* showed a strong growth defect that was accompanied by a significant increase in G0/G1 cells (**Fig. 6a**). Deletion of *BUD22* failed to increase RLS, however, demonstrating that not all mutants with elongated G0/G1 are long-lived (**Fig. 6b**). Similar to *bud22Δ* cells, deletion of the small ribosomal subunit protein *RPS0B* also leads to an increase in G0/G1 cells but does not increase RLS (**Fig. 6b**). This data is consistent with our prior report that depletion of the large ribosomal subunit, but not the small ribosomal subunit, is associated with increased RLS by a mechanism that is partially dependent on the stress- and nutrient-responsive transcription factor Gcn4[43]. Among translation-related longevity mutants, there is a trend toward correlation of enrichment for G0/G1 cells with the magnitude of replicative lifespan extension (**Fig. 6c**). This trend is not strong,

however, suggesting that the magnitude of the translation defect (and hence G0/G1 delay) is not the sole factor determining longevity.

Discussion:

In this study, we have shown that over half the known long-lived variants in the BY4742 background have a significant fitness defect relative to the parental strain. In other words, the wild type allele of each of these genes functions to promote fitness at the expense of longevity. This represents, by far, the most extensive analysis of the relationship between fitness and longevity in any model system to date and provides experimental data consistent with antagonistic pleiotropy. Among the long-lived variants with detectable fitness defects, a majority contain mutations that impair global mRNA translation. The overwhelming majority of these variants show a similar defect in maximal growth rate, a reduction in cell size, and a specific delay in cell cycle progression resulting in an accumulation of G0/G1 phase cells.

We have suggested here that maximal growth rate is an appropriate measure of fecundity for the replicative aging model in *Saccharomyces cerevisiae*. The logic behind this assertion is that in a mixed population of asymmetrically dividing cells, the primary determinant of relative fitness is growth rate, not replicative potential. To demonstrate this, *in silico* simulations were used to estimate the relative importance of RLS and maximal growth rate in a competitive fitness assay based solely on exponential growth. While this simulation does not reflect the importance of survival during quiescence, it does adequately recapitulate the experimentally observed RF values for slow growing mutants, suggesting that, at least in these cases, maximal growth rate is the primary determinant of fitness. Importantly, extended RLS plays essentially no role in determining fitness, even when the simulation is carried out to more than 100,000 population doublings (**Fig. S5,** online at Cell Cycle**)**. We note that this lack of

selection on replicative capacity adequately reflects the reduction in selection on post-reproductive longevity of chronologically aging multicellular organisms. Thus, in a replicative aging paradigm, growth rate is an appropriate measure of fecundity while replicative potential is not.

Our observations suggest that while decreased RF is generally associated with reduced fecundity, this need not always the case. For example*, idh1Δ, idh2Δ, sam1Δ, sok1Δ, tma19Δ,* and *ure2Δ* have normal doubling times, but were outcompeted by wild type in the fitness assay (**Table 1**). One possibility is that these mutants are outcompeted specifically during the phase of the fitness competition in which cells are not growing exponentially (i.e. entry into or survival during stationary phase). Indeed, *idh1Δ* and *idh2Δ* cells are respiratory-deficient and yeast cells rely heavily on respiratory metabolism during the shift from logarithmic growth to stationary phase (**Fig. S1,** online at Cell Cycle). Such mutants may be akin to the long-lived *age-1* mutants in *C. elegans*, which are outcompeted by wild type animals specifically during starvation periods[4].

It is noteworthy that 17 out of 49 (35%) long-lived variants showed no significant effect on fitness. While it may be that our assay was not sufficiently sensitive to detect more subtle defects, at least two additional explanations for this observation exist. First, it may be that these mutants are not less fit than wild type cells and it is possible to slow aging without large fitness costs. Alternatively, it may be that the competition assay employed did not sample a sufficient spectrum of conditions experienced by yeast in the natural environment to detect the fitness defects associated with these mutants. For example, variants defective for sporulation would be substantially less fit in a natural context, but would not necessarily show a fitness defect in the assays used here. Consistent with this idea, 14 out of 49 long-lived strains are annotated to have reduced sporulation efficiency, compared to only 4 out of 50 randomly selected strains. Altered resistance to temperature fluctuation, susceptibility to

environmental toxins, or reduced ability to utilize alternative carbon sources could also lead to substantially reduced fitness in the natural environment and were not queried here. Further studies will be required to adequately address this question.

In summary, we have identified 32 long-lived yeast mutants with significant defects in fitness through direct competition assays. This is, by far, the most comprehensive analysis of the prevalence of longevity-associated fitness trade-offs in any model system, expanding by roughly an order of magnitude the number of such mutants identified. These less fit, long-living variants tend to be defective for regulating cell size, growth rate, and mRNA translation. Taken together, these data support the idea that enhanced life span is often associated with an early life fitness cost and suggest that such costs may be more likely to result from mutations in genes that modulate specific molecular processes related to growth control and mRNA translation.

Materials and Methods

Yeast strains used:

Unless otherwise indicated, all yeast strains were derived from the *MAT*α ORF deletion collection and are isogenic to the parental BY4742 strain[48,49]. The *LYS2* strain was generated by sporulation of diploid cells from a cross between a BY4741 *MAT**a*** deletion strain and wild type BY4742. The resulting spore clone was verified as *MAT*α *his3Δleu2Δ LYS2 met15Δ ura3Δ*. The *SIR2-OX* strain is a tandem two copy *SIR2* strain with a *URA3* marker generated by integration of a second copy of *SIR2* in BY4742 as previously described[47]. A few strains (*adh1*Δ, *rom2*Δ, and *rpl20b*Δ) were excluded from our analysis upon finding the strains had undergone spontaneous diploidization (**Fig. S4a,** online at Cell Cycle). A

remade *rpl20bΔ* strain was generated by replacing the *RPL20B* open reading frame with *HIS3* and was verified to have an extended replicative lifespan (**Fig. S4b,** online at Cell Cycle). All gene disruptions were verified by PCR.

Competition assay:

In an effort to simulate a periodic growth and starvation cycle similar to what yeast might experience in the natural environment and analogous to what has been previously studied in *Caenorhabditis elegans*[4], we developed a competition assay consisting of inoculating yeast into fresh YPD followed by intermediate periods of starvation. Test strains were first inoculated into 150 µL YPD in individual wells of a 96 well plate and incubated at 30°C for two days. 8µl of these cultures were then serially diluted in 150µl YPD twice and then 8µl of this dilution was inoculated into 150 µL of fresh YPD in a single well of a new 96 well plate. An equal volume of BY4742 was similarly inoculated into the same well, providing a roughly equal number of mutant and wild type cells in each culture. This is defined as the initial time-point for each experiment. Every 7 days the individual cultures were serially diluted in an identical fashion into a well containing fresh YPD in a 96 well plate. The procedure allowed for about 50,000 cells to be re-inoculated into fresh culture, thereby preventing any bottlenecks, and to divide 13 times before the next round of fresh YPD.

Each long-lived mutant is marked with the selectable KanMX marker (except the *SIR2-OX* strain, which is *URA3* marked), allowing convenient quantification of the ratio of mutant to wild type cells in the mixed culture. For each weekly time point, the competition culture was serially diluted four times (8µl of culture into 150µl YPD) and then all 158µl was plated onto YPD agar, yielding 150-300 total colony forming units (CFUs) per plate. After 2 days of growth at 30°C, the total number of CFUs per plate was counted, and then replica plated onto YPD supplemented with G418 to select for the KanMX

marker (or SD–LYS media for the *LYS2* strain, or SD–URA media for the *SIR2-OX* strain). The number of CFUs on each selective media plate was then counted after 1 day of incubation. The ratio of mutant to wild type cells in the mixed culture can then be defined as the number of CFUs grown on selective media divided by the number of CFUs unable to grow on selective media (calculated by $CFU_{WT}= CFU_{YPD}- CFU_{selective\ media}$).

Relative fitness was calculated using the following equation:

$$\text{Relative fitness}= \log_2((CFU^x_{mutant}/CFU^x_{WT})/(CFU°_{mutant}/CFU°_{WT}))$$

Where CFU^x is the CFU count at the end of week x and CFU° is the CFU count at initial inoculation (day zero). This allowed us to normalize for changes between cultures in the mutant/wild type ratio depending on initial inoculation. While most cultures were inoculated near the 50/50 ratio, we confirmed that even intentionally large changes in the starting ratio did not significantly change the results of the assay (**Fig. S2a**). Statistical significance was determined by a two-tailed Student's t-test at the end of week three, comparing relative fitness of long lived mutant cultures to the *LYS2* control competition cultures for a minimum of triplicate biological replicates for each strain.

Growth rate analysis:

Yeast growth rates were analyzed with a Bioscreen C MBR machine (Growth Curves USA) as previously described using the Yeast Outgrowth Data Analyzer (YODA)[58]. Reported doubling times in 30°C YPD are taken from interval readings from the $OD_{420-580}$=0.2-0.6 range of maximum growth rate. Significance was tested with a two-tailed Student's t-test of mutant doubling times compared to wild type doubling times. Error bars are shown as standard error of the mean (s.e.m.). Each experiment was performed in biological triplicates per run (three cultures, three Bioscreen C Honeycomb Plate wells)

and the runs were performed on at least three biological replicate cultures (independently grown from different colonies on different days) for each mutant (**Table 1**).

Flow cytometry:

Samples were prepared following a protocol modified from that previously described[59]. The modifications were as follows: no pepsin digestion was used and SYTOX® Green (Invitrogen, S7020) was utilized at a 2μM final concentration. All yeast strains were inoculated into fresh YPD from an overnight culture with an initial $OD_{540} < 0.05$. Cells were allowed to grow logarithmically for at least two cell cycles and were harvested with a final OD_{600} between 0.4 and 0.6 in 70% ethanol. All strains shown, unless otherwise indicated, were grown, harvested, processed, stained, and analyzed for at least three biological replicates from independent cultures grown and analyzed on different days. The flow cytometer used was a BD Biosciences Influx Cell Sorter. The relative percentages of cells in G1, S, and G2 phase were calculated using WinCycle. Forward scatter was analyzed in FCS Express and mean values were used to compare relative cell size.

Replicative lifespan:

Replicative lifespan assays were performed as previously described[41,60]. 2% glucose YPD plates were used, and statistical significance was determined by a Wilcoxon Rank-Sum test (MATLAB "ranksum" function). RLS values shown in Table 1 are derived from prior studies[8,41-46]. Growth curves from replicative lifespans were constructed by averaging across all mother cells the sum of daughter cells that had budded before each time point during the lifespan assay (**Fig. 4b**).

Acknowledgements - This work was supported by NIH Grant R01AG025549. Flow Cytometry was performed through the University of Washington Nathan Shock Center of Excellence in the Basic Biology

of Aging Imaging Core (NIH Grant P30AG013280). JD is supported by NIH Training Grant T32AG000057. MK is an Ellison Medical Foundation New Scholar in Aging.

Figures and Tables:

Table 1: Relative fitness, maximal growth rate, and flow cytometry analysis of cell cycle progression for 49 long-lived mutants

Life span percent change is the relative increase in life span for each mutant compared to experiment matched wild type controls. G1 delay is shown as the percent increase in cells in G1 during log phase for each mutant relative to wild type. Mean values and standard error of the mean (s.e.m) for at least triplicate biological replicates for each assay are shown. *p < 0.05, **p < 0.01

Strain	Lifespan (% Change)	Relative Fitness (RF)		Doubling Time (min)		G1 Delay (%)	
afg3	20.4	-7.00 ± 0.00	**	128.5 ± 2.9	**	45.8 ± 9.8	**
alg12	24.7	-0.37 ± 0.44		92.6 ± 0.2		-22.1 ± 1.6	**
dbp3	33.6	-6.78 ± 0.65	**	116.5 ± 1.6	**	44.8 ± 5.7	**
elp4	34.8	-7.00 ± 0.00	**	116.8 ± 1.4	**	5.8 ± 11.3	
fob1	23.5	0.27 ± 0.16		92.7 ± 1.6		8.6 ± 6.8	
gpa2	36.1	-2.12 ± 0.28	**	107.5 ± 2.3	**	6.8 ± 2.3	*
gpr1	21.1	0.62 ± 0.52		93.8 ± 0.8		4.4 ± 3.6	
hse1	25.5	-0.94 ± 1.13		90.3 ± 0.4		9.0 ± 13.0	
idh1	35.1	-1.02 ± 0.38	*	94.1 ± 1.3		-5.4 ± 5.7	
idh2	25.3	-1.37 ± 0.16	**	94.3 ± 1.0		9.6 ± 11.0	
inp51	13.2	0.05 ± 0.09		91.6 ± 0.5		11.9 ± 8.7	
inp53	30.7	-0.38 ± 0.11		93.4 ± 3.1		3.4 ± 9.4	
msw1	30.2	-0.41 ± 0.28		90.3 ± 0.9		-3.9 ± 2.2	*
pkh2	22.2	3.36 ± 1.86	**	93.4 ± 1.8		1.7 ± 7.4	
pmr1	37.0	-5.18 ± 0.74	**	109.4 ± 4.4	**	-4.3 ± 11.8	
rei1	37.5	-3.96 ± 1.84	**	129.3 ± 6.2	**	45.4 ± 12.5	**
rim1	13.7	0.16 ± 0.54		92.9 ± 1.9		-3.6 ± 2.4	
rpl13a	27.0	-6.75 ± 0.22	**	115.3 ± 2.8	**	46.6 ± 5.0	**
rpl19a	28.4	-3.92 ± 0.79	**	117.2 ± 3.7	**	52.5 ± 4.7	**
rpl21b	54.5	-6.36 ± 0.78	**	112.3 ± 2.7	**	46.0 ± 3.7	**
rpl22a	34.5	-7.00 ± 0.00	**	144.8 ± 6.3	**	73.6 ± 8.8	**
rpl23a	29.5	-7.00 ± 0.48	**	115.1 ± 2.7	**	30.7 ± 11.2	**
rpl29	28.0	-4.22 ± 0.44	**	109.0 ± 3.1	**	41.0 ± 0.9	**
rpl31a	34.1	-7.00 ± 0.00	**	287.7 ± 3.4	**	127.2 ± 16.9	**
rpl37b	35.1	-6.72 ± 0.15	**	116.8 ± 2.3	**	46.0 ± 6.6	**
rpl43b	37.5	-2.71 ± 1.02	**	96.0 ± 1.0	*	23.7 ± 0.5	**
rpl6b	13.9	-5.21 ± 1.79	**	117.2 ± 3.9	**	48.5 ± 7.2	**
rpl7a	39.3	-5.79 ± 0.66	**	112.3 ± 2.0	**	30.1 ± 2.7	**
rpl9a	29.4	-6.41 ± 0.31	**	111.6 ± 3.8	**	54.1 ± 2.8	**
rpp2b	54.2	-7.00 ± 0.00	**	144.9 ± 2.3	**	68.0 ± 2.7	**
sam1	37.9	-1.31 ± 0.71	*	92.9 ± 2.7		-2.6 ± 2.4	
sch9	42.8	-7.00 ± 0.00	**	170.2 ± 3.5	**	87.0 ± 3.2	**
sip2	18.0	0.42 ± 0.39		93.4 ± 1.9		6.3 ± 7.8	
SIR2OX	25.0	0.26 ± 0.16		91.4 ± 1.9		3.5 ± 5.9	
sis2	47.8	-0.68 ± 0.29		95.2 ± 0.7	*	6.6 ± 6.3	

sok1	37.2	-0.93	±	0.38	*	94.7	±	3.2		6.1	±	3.0	*
sps1	23.8	-3.93	±	1.03	**	106.0	±	5.9	*	-4.4	±	6.3	
spt4	46.3	-6.53	±	0.47	**	118.2	±	5.5	**	-49.5	±	14.0	**
tif1	13.1	-0.07	±	0.55		94.3	±	1.4		29.4	±	5.0	**
tif2	18.1	-0.02	±	0.21		90.6	±	1.5		18.3	±	2.7	**
tif4631	18.0	-4.62	±	1.03	**	111.6	±	3.1	**	27.8	±	4.2	**
tis11	32.2	0.81	±	0.30	**	92.2	±	2.3		-5.5	±	3.5	
tma19	31.8	-1.25	±	0.67	*	98.0	±	3.8		28.6	±	8.4	**
tor1	30.8	-0.85	±	0.78		92.8	±	1.9		0.5	±	1.2	
ure2	29.5	-5.40	±	0.82	**	95.7	±	3.5		3.6	±	5.8	
ybr238c	49.7	-3.57	±	0.15	**	98.2	±	2.4	*	9.7	±	5.2	*
ybr255w	33.9	-0.29	±	0.18		96.8	±	1.9	*	-0.9	±	5.1	
ybr266c	37.0	-6.96	±	0.04	**	122.6	±	2.6	**	63.6	±	4.0	**
ypt6	30.3	-4.02	±	0.36	**	107.0	±	3.7	**	17.1	±	1.2	**
LYS2	N/A	-0.11	±	0.12		90.0	±	0.8		-0.6	±	0.4	
BY4742	N/A		N/A			91.0	±	1.3		0.0	±	1.6	

Figure 1: Direct competition reveals a fitness defect in 32 long-lived yeast strains.

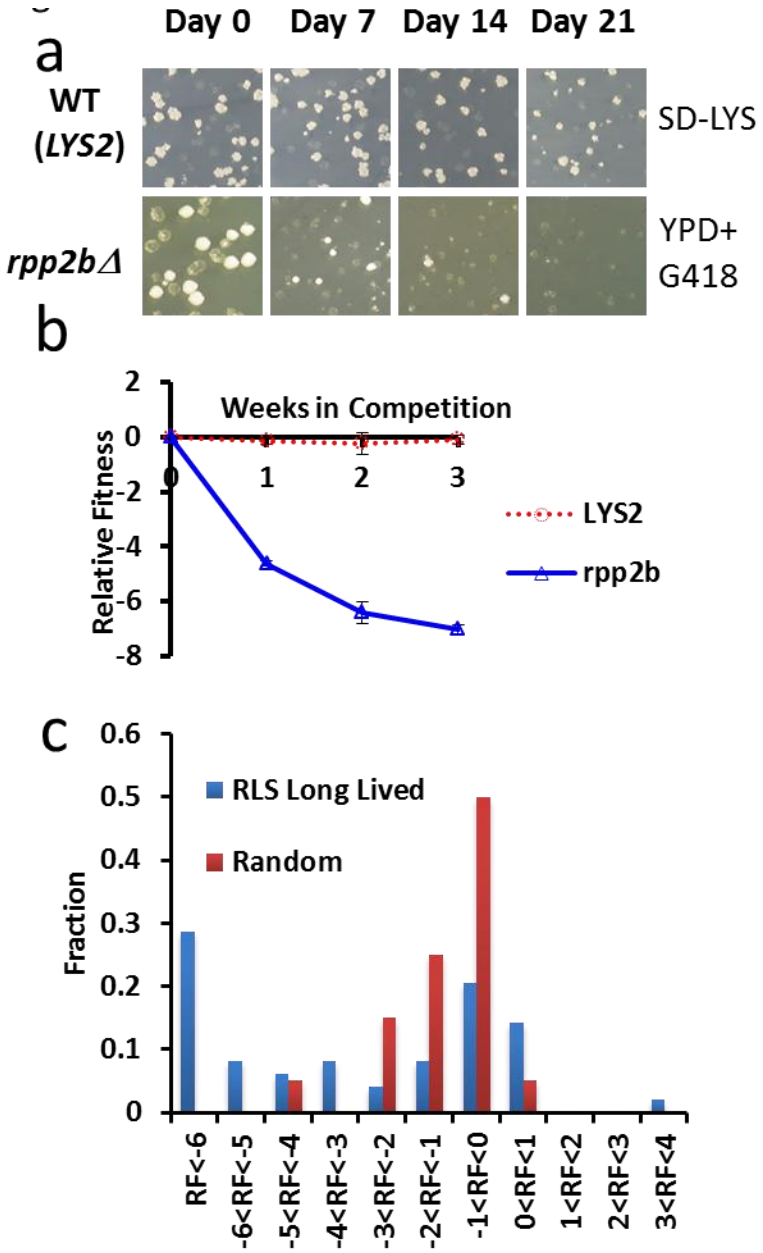

a) Representative example of colony forming units (CFUs) from a fitness competition. Cells were plated from a mixed culture of control (BY4742) and a mutant (*rpp2bΔ* is a long lived mutant example, *LYS2* is a wild type mimetic control example) onto YPD medium to ascertain a total CFU count and then replica plated onto selective media to gather a mutant CFU count (SD-LYS top panel, YPD+G418 bottom panel).

b) Relative fitness of *LYS2* control and *rpp2bΔ* compared to wild type (BY4742) during the competition experiment.

c) Histogram showing the observed relative fitness values at the end of the assay for long-lived deletion strains and randomly selected deletion strains.

Figure 2: Long-lived yeast are enriched for slow growth.

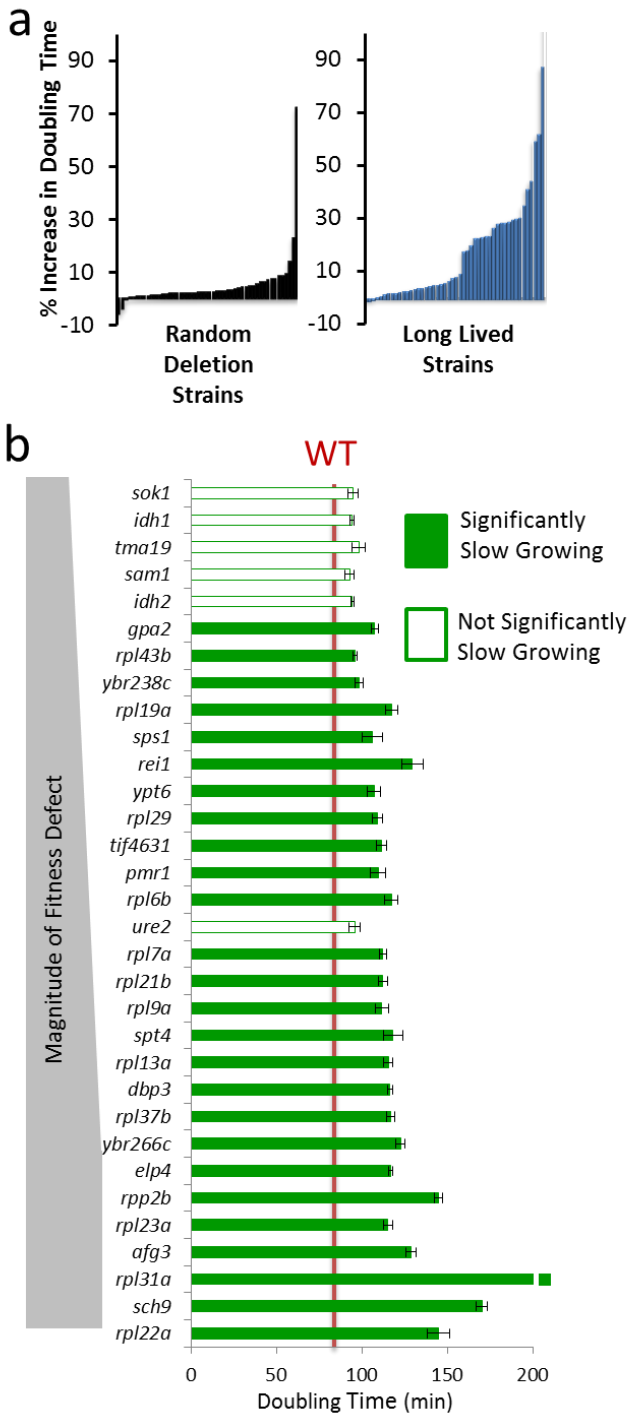

a) Percent increase in maximal doubling time relative to wild type cells for 50 randomly selected deletion strains and 49 long-lived strains. Each bar represents one strain.

b) Comparison of the long lived mutants' doubling time to the magnitude of their respective relative fitness defects. Strains with a fitness defect are shown.

Figure 3: Simulation of the relative importance of growth rate and replicative potential on fitness of yeast cells after 40 wild type cell division cycles.

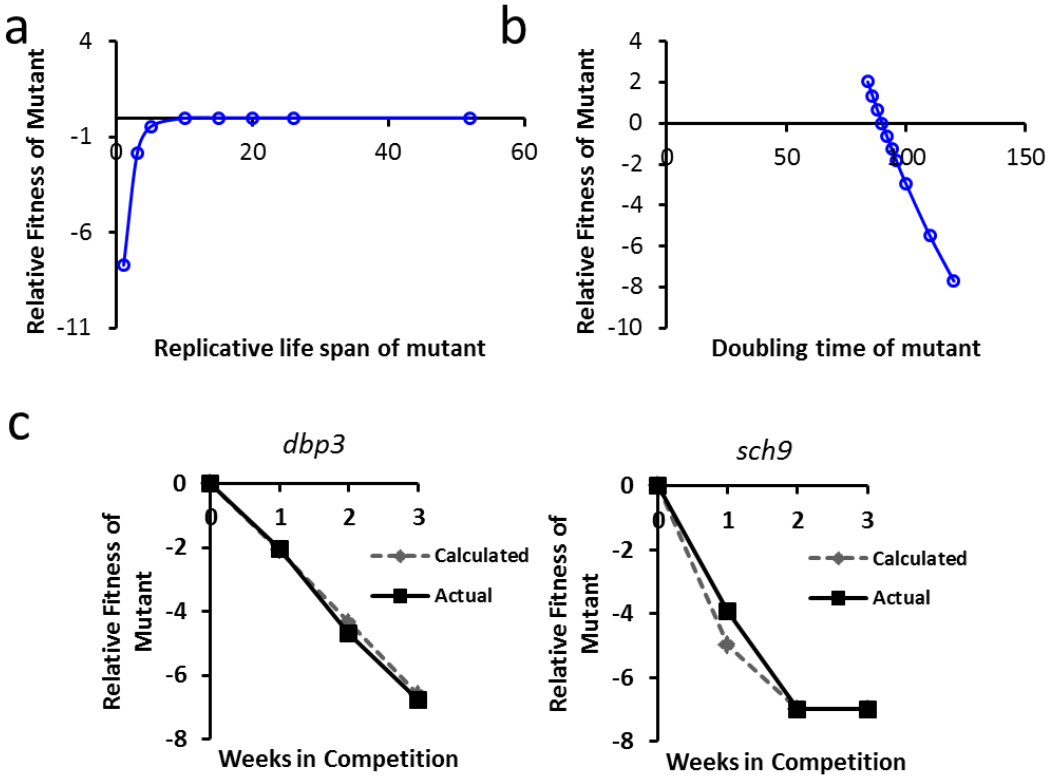

a) The replicative life span of a mutant has relatively little effect on fitness, except in cases where life span is reduced to less than about 3 generations. Replicative life span for wild type is set at 26 generations. Doubling time for mutant and wild type is defined as equal (90 minutes).

b) Doubling time of the mutant has a relatively large effect on relative fitness. Wild type doubling time is set at 90 minutes. Replicative life span for mutant and wild type is defined as equal (26 generations).

c) Comparison of the *in silico* predicted relative fitness for *dbp3Δ* and *sch9Δ* cells based on experimentally measured replicative life span and doubling time values with the experimentally

measured relative fitness of these mutants. Comparisons of the remaining mutants to *in silico* calculations can be found in Figure S1 (online at Cell Cycle).

Figure 4: Reduced vitality of long-lived mutants occurs early in life.

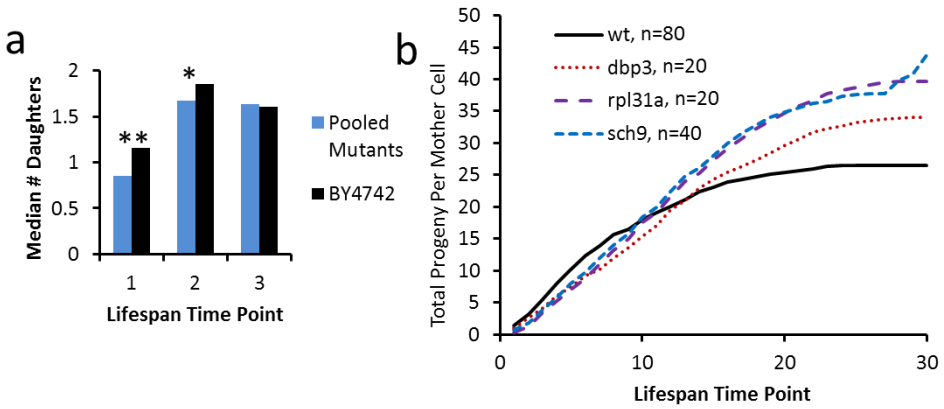

a) The median number of daughters produced per mother cell over the first three time-points in a standard replicative life span assay is shown for experimentally-matched wild type (BY4742) and long-lived mutants (pooled data for 32 strains showing a significant defect in relative fitness). Each time point corresponds to removal of daughter cells by microdissection after 90-150 minutes of incubation at 30°C. *$p < 0.05$, **$p < 0.01$

b) Cumulative daughter cell production per mother cell derived from a replicative lifespan experiment. Experimental time points are the same as described in (a).

Figure 5: Slow growth is due to a G0/G1 delay in long-lived translation-related mutants.

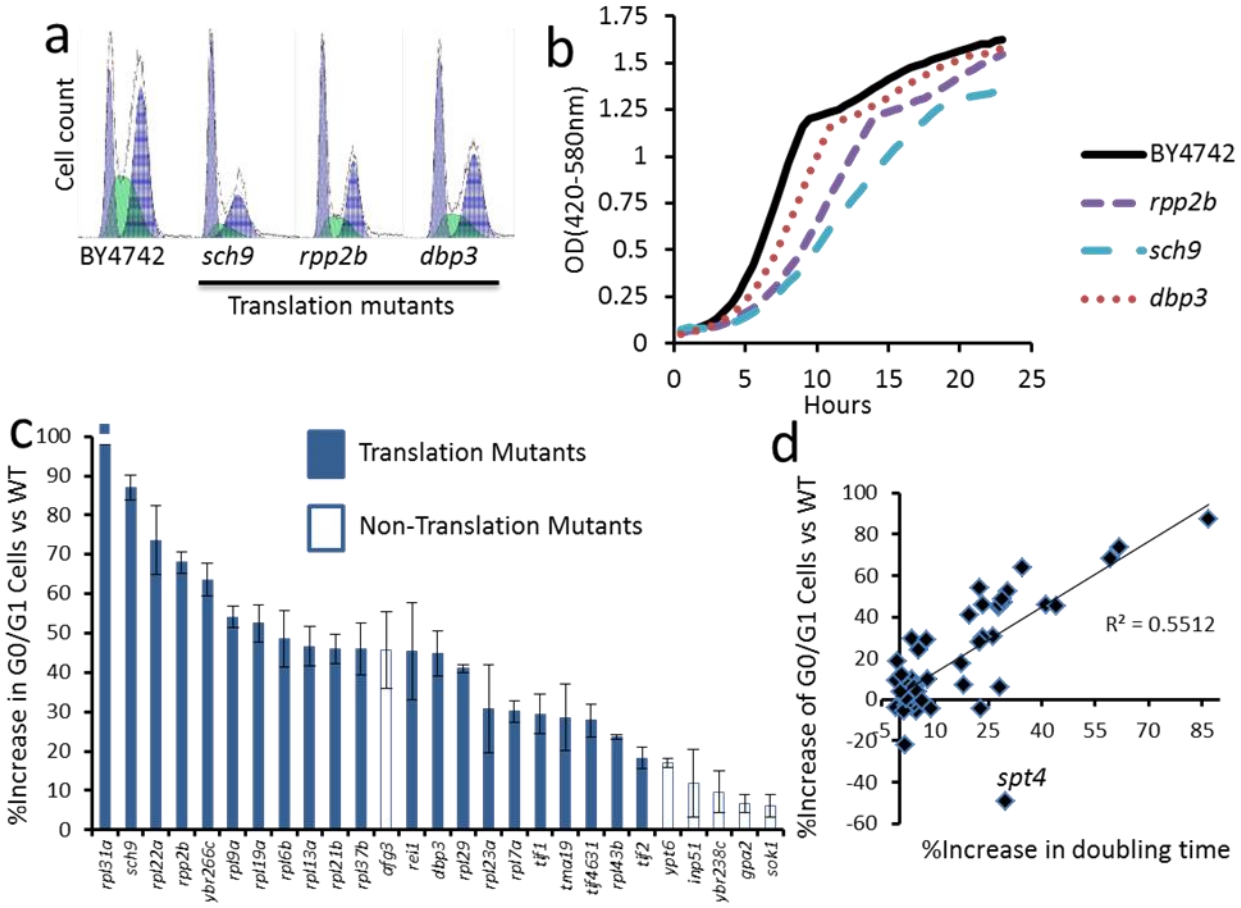

a) Representative flow cytometry profiles of log phase yeast cells stained with SYTOX Green. Higher values on the x-axis indicate increased fluorescence.

b) Representative growth curves obtained from a Bioscreen C MBR machine. Cells were grown at 30°C in YPD.

c) Long-lived strains with a significant G0/G1 delay.

d) Relationship between G0/G1 delay and growth rate for all 49 long-lived strains.

Figure 6: G0/G1 delay is not sufficient to increase lifespan

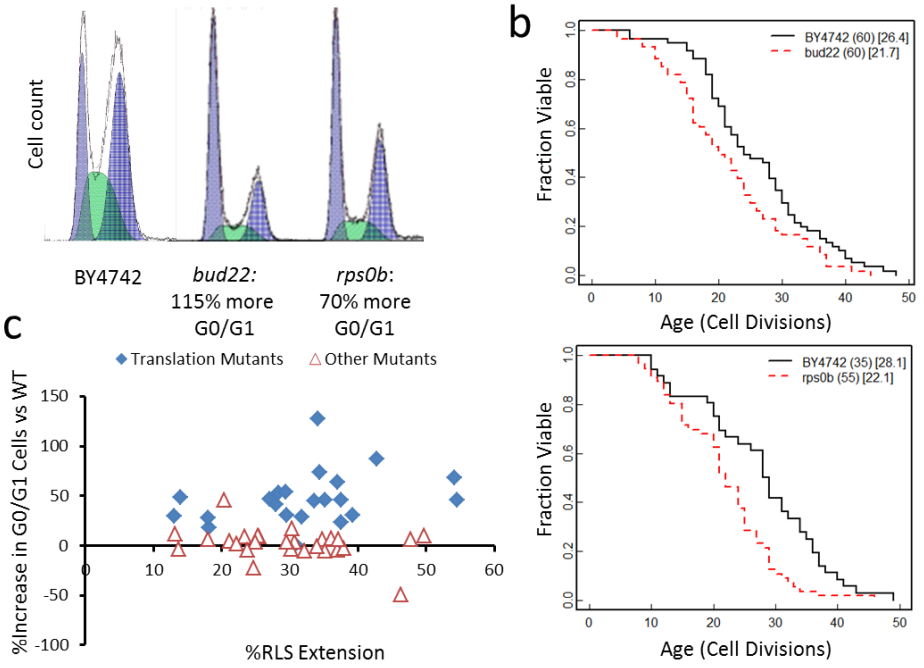

a) Flow cytometry profiles *bud22Δ* and *rps0bΔ* log phase cells. Cells deleted for *BUD22* were found to be the slowest growing of our 50 randomly selected strains while small ribosomal subunits have been previously published as not long lived,[43] and *rps0b* was chosen as a sample mutant. Higher values on the x-axis indicate increased fluorescence.

b) Replicative lifespan data of *bud22Δ* and *rps0bΔ.* The number of mother cells is shown in (), mean lifespan in [].

c) Comparison between G0/G1 delay and life span among translation-related long-lived mutants (filled diamonds) and the remaining long-lived mutants with no clear role in mRNA translation (open triangles).

Section II: Sir2 deletion prevents lifespan extension in 32 long-lived mutants

Transitioning introduction:

As with biological evolution, science continuously evolves through numerous labs testing individual theories until one survives and thrives. The study of aging is no different. Sirtuins once thrived as the most promising transducer of dietary restriction. Since then many studies have called these results into question and alternative molecules appear to be the primary mediators of aging. Sirtuins no doubt are interesting proteins to study, but the following section explains why they are unlikely to be the mediators of lifespan extension by dietary restriction.

The following section is based on this publication[61].

Abstract

Activation of Sir2-orthologs is proposed to increase lifespan downstream of dietary restriction (DR). Here we describe an examination of the effect of 32 different lifespan-extending mutations and four methods of dietary restriction on replicative lifespan (RLS) in the short-lived *sir2*Δ yeast strain. In every case, deletion of *SIR2* prevented RLS extension; however, RLS extension was restored when both *SIR2* and *FOB1* were deleted in several cases, demonstrating that *SIR2* is not directly required for RLS extension. These findings indicate that suppression of the *sir2*Δ lifespan defect is a rare phenotype among longevity interventions and suggest that *sir2*Δ cells senesce rapidly by a mechanism distinct from that of wild-type cells. They also demonstrate that failure to observe life span extension in a short-lived background, such as cells or animals lacking sirtuins, should be interpreted with caution.

Introduction:

Combining two or more longevity-altering interventions and determining the resulting effect on lifespan is a common method for examining the relationship between such interventions. An important subset of this type of analysis occurs when one of the factors under study promotes longevity, such as *daf-16* in *Caenorhabditis elegans* or *SIR2* in *Saccharomyces cerevisiae*. For both of these genes, several studies have combined a lifespan shortening null allele with an intervention that extends lifespan. A resulting lifespan similar to that of the short-lived single mutant has generally been interpreted as suggesting that the factors act in the same pathway. In contrast, an intervention extending the lifespan of the short-lived mutant has been interpreted as suggesting that the factors act in genetically distinct pathways. Specific examples of this type of comparison are studies in which DR fails to extend lifespan in yeast [62], invertebrates [63,64], and mice [65] when Sir2-orthologs are mutated. These data have been, and continue to be, interpreted by some to support a model in which DR promotes longevity and healthspan through activation of sirtuins [66].

Results:

It has been previously reported that deletion of *SIR2* blocks RLS extension from DR by reduction of glucose and in strains lacking *GPA2* or *HXK2*, two genetic mimics of DR, but not in a strain lacking the rDNA replication fork block protein, *FOB1* [8]. In order to examine the influence of deleting *SIR2* on RLS extension more generally, we generated 30 additional double mutant strains in which a RLS extending deletion was combined with deletion of *SIR2*. We also tested three additional methods of DR involving growth on alternative carbon sources (ethanol,

glycerol, or raffinose). Strikingly, none of these interventions resulted in a significant RLS extension relative to *sir2*Δ cells (**Figure 1**; **Figure S2; Table S1,** online at Aging Cell).

One possible interpretation of these data is that each of the RLS-extending interventions acts upstream of Sir2, perhaps by promoting Sir2 activity. Two observations are inconsistent with this model. First, at least eight of these mutations, and all four forms of DR, significantly extend the RLS of *sir2*Δ *fob1*Δ cells (**Figure S1A; Figure S2; Table S1,** online at Aging Cell), demonstrating that *SIR2* is not absolutely required for RLS extension in these cases. Second, at least five long-lived deletion mutants show no indication of enhanced Sir2 activity *in vivo*, as measured by rDNA recombination or rDNA silencing (**Figure S3,** online at Aging Cell). A similar lack of increased Sir2 activity has been previously reported in cells subjected to DR [5,67,68]. Interestingly, deletion of *TOR1* caused a significant decrease in rDNA recombination, but this effect was independent of *SIR2* (**Figure S3A**, online at Aging Cell).

An alternative explanation for these data is that loss of *SIR2* alters aging such that molecular processes that do not limit RLS in wild-type cells become limiting in *sir2*Δ cells. Sir2 has multiple functions, including repression of extrachromosomal rDNA circle formation [47], enhancing global rDNA stability and silencing [69,70], promoting asymmetric inheritance of damaged proteins [71], and maintaining telomeric chromatin during aging [72]. The observation that only deletion of *FOB1* (shown here) or overexpression of Hsp104[73] is sufficient to suppress the short RLS of *sir2*Δ cells suggests that (1) the RLS-limiting defect is likely related to rDNA stability or asymmetric segregation of proteins and (2) none of the 32 deletions tested that slow aging in wild-type cells is able to overcome this defect.

While it is likely that many of the genes examined in this study do not require Sir2 for their effect on RLS, we do not believe that all of the 32 long-lived single gene deletion mutants examined here necessarily act via Sir2-independent mechanisms. For example, deletion of *SAS2*, a histone acetyltransferase known to antagonize Sir2 effects on chromatin [72], extends wild-type RLS but fails to extend the RLS of *sir2*Δ *fob1*Δ cells (**Figure S2b**, online at Aging Cell). Thus, both functional and genetic evidence suggest that Sas1 likely acts in the same longevity pathway as Sir2.

Discussion:

This study provides a clear demonstration of the challenges associated with interpreting longevity epistasis data. In particular, the failure of a longevity-intervention to extend lifespan in a short-lived background may not be informative regarding the mechanism of lifespan extension in the wild-type context. In the absence of strong evidence indicating that the lifespan shortening is caused by acceleration of the wild-type aging process, caution is warranted when interpreting these types of data.

Figure 1. Single-gene deletions that extend RLS in wild-type cells do not extend RLS of *sir2Δ* cells.

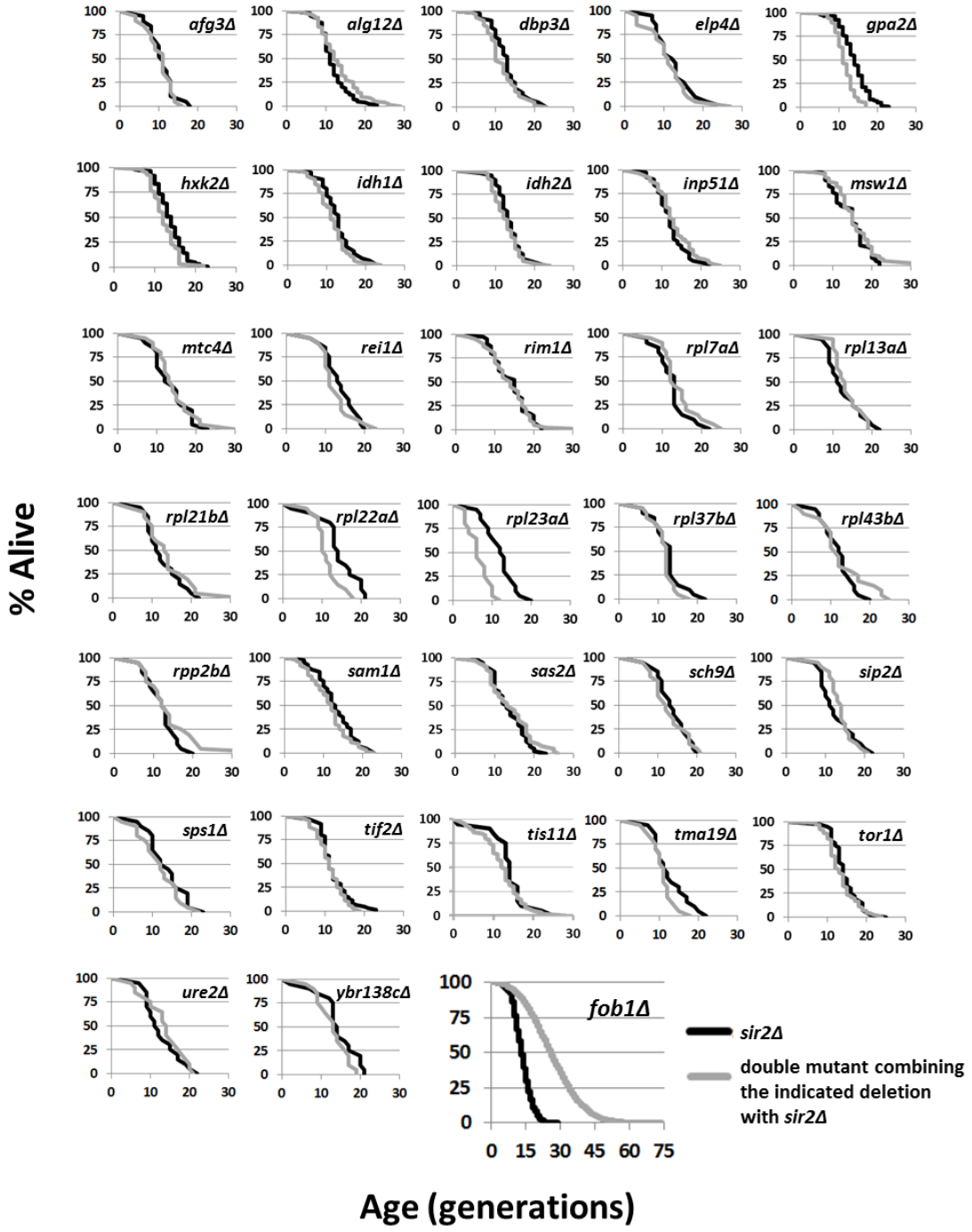

Replicative survival curves are provided for 33 double mutant strains combining a known long-lived gene deletion with deletion of *SIR2*.

Section III: Dietary restriction or pH neutralization attenuates the reduction in replicative lifespan following chronological aging in yeast

Transitioning introduction:

While we were debunking Sir2 as a mediator of lifespan extension by dietary restriction, we were making strong efforts to ascertain what aspects of dietary restriction are indeed conserved and potentially important mechanisms. In particular, many research labs use chronological lifespan to study aging in yeast even though it is our belief that replicative aging is probably more relevant [11,44]. While chronological aging is clearly distinct from replicative aging, we know that dietary restriction can improve both chronological lifespan and replicative lifespan. It was also known that chronologically aged cells exhibit a replicative defect. We examined the interaction between chronological lifespan and replicative lifespan in much greater detail than ever before, and placed it in the context of dietary restriction. The main findings are described below, and will be published in the near future.

Abstract:

Chronological and replicative aging have been studied in yeast as alternative paradigms for post-mitotic and mitotic aging, respectively. It has been known for more than a decade that cells aged chronologically in rich medium in one strain background have reduced replicative life span relative to chronologically young cells. Here we report replication of this observation in the diploid BY4743 strain background and extend this finding in several ways. First, we show that the reduction in replicative lifespan from chronological aging is accelerated when cells are chronologically aged under standard conditions in synthetic complete medium rather than rich medium. This loss of replicative potential is attenuated by two different interventions previously shown to extend chronological life span: buffering the pH of the medium to 6.0 or dietary restriction by reducing the glucose concentration of the medium to 0.05%. We see that within

the live populations a larger cell correlates with a shortened replicative lifespan. Chronologically aged cells also progress through the cell cycle into G2, and this progression is attenuated by buffering to pH 6.0 or by reducing glucose to 0.05%. These observations suggest that the detrimental effects of extracellular medium acidification on chronological lifespan result in intracellular damage that reduces the subsequent replicative capacity of the chronologically aged cells and demonstrate that dietary restriction is sufficient to prevent this reduction in replicative capacity following chronological aging.

Introduction:

The budding yeast has been used extensively as a model system to understand the processes that influence cellular aging [19]. Two distinct methods for aging of yeast cells have been developed. Yeast chronological aging is a model of post-mitotic aging where lifespan is defined by the length of time that a yeast cell can survive in a non-dividing, quiescent-like state [74,75]. Yeast replicative aging, in contrast, is a replicative model of mitotic capacity where lifespan is defined by the number of daughter cells a mother cell can produce [76,77].

Replicative life span (RLS) is typically measured in the laboratory by isolating individual cells on rich medium (YPD), allowing those cells to proceed through the cell cycle at 30°C, and using a micromanipulator with a fiber optic needle to physically remove daughter cells after every 1-2 divisions until the mother cell reaches senescence [60]. There is variation in the RLS of different laboratory strains, with typical average wild type RLS values ranging from 15-35 generations. In the genetic background of the yeast ORF deletion collection, haploid cells (BY4742 *MATα* or BY4741 *MAT***a**) have an RLS of approximately 25 generations, while diploid cells (BY4743)

have an average RLS of approximately 35 generations [78]. The mechanisms underlying the difference in RLS between haploid and diploid cells in this background is not known; however, in other strain backgrounds haploids and diploids can have a similar average RLS [79 80].

A variety of slightly different methods have been used to measure chronological life span (CLS) in yeast. The most commonly used protocol involves culturing cells under aeration in liquid synthetic defined medium with an initial glucose concentration of 2% [74,75]. Under these conditions, cells undergo fermentative exponential growth where ethanol is produced from glucose, followed by a metabolic shift to respiration upon glucose depletion. Within 48 hours, a majority of cells exit the cell cycle as unbudded, quiescent cells. Viability over time is then quantified by removing small aliquots of cells and plating for colony forming units (CFUs) on YEPD. A higher-throughput method for quantifying CLS has also been described in which the cells are still aged in SC medium, but the relative proportion of viable cells is determined based on outgrowth kinetics in YEPD rather than CFU determination [81,82]. Several variations on the CLS assay have been described involving either changing the composition of the initial culture medium in which the cells are aged, transferring the cells to water following entry into quiescence, or altering the temperature at which the cells are aged ([83]). In every case, both commonly used methods for determining viability over time (CFU determination or outgrowth kinetics) are equally applicable.

Although the detailed mechanisms of chronological aging remain unknown, there is abundant evidence that aging in this system is associated with an increasing burden of oxidative stress, damage to mitochondria, and an induction of the yeast apoptotic-like response [84-86].

Chronological life span can be extended under certain conditions by activation of stress response pathways or overexpression of antioxidant enzymes, further supporting a role for oxidative damage in chronological aging [87,88]. We and others have also shown that acidification of the extracellular culture medium contributes to chronological senescence when cells are cultured in SC medium, as buffering the culture medium to pH 6.0 or neutralizing the pH with NaOH is sufficient to significantly extend life span in several common laboratory strains [9,89,90]. We also showed that CLS extension from dietary restriction (DR) by reducing the glucose concentration of the culture medium from 2% to 0.5% or 0.05% can be explained by attenuation of medium acidification and reduced secretion of acetic acid into the extracellular milieu [9]. These initial observations have since been extended to the vineyard yeast strain RM11, as well as several alternative carbon sources [91]. In both the laboratory isolate and the vineyard isolate, there is a significant inverse correlation between the pH of the culture at day 2 or day 4 of the experiment (which is highly dependent upon the carbon source) and the CLS of the cells.

In a seminal study published in 1998, Ashrafi et al. [14] showed that chronologically aging cells in YEPD results in a reduction of their replicative life span that is proportional to the chronological age of the cells. They provided evidence that the depression of RLS following chronological aging is not mediated by accumulation of extrachromosomal rDNA circles, but the mechanism behind this phenomenon has remained otherwise unstudied. Since CLS is so dependent upon the pH of the culture medium, this raises the question as to whether cell extrinsic factors may play a role in the reduction in RLS observed during chronological aging. Here we describe an initial attempt to replicate the initial observation in the BY4743 diploid yeast strain and to directly address this question.

Results:

Buffering to pH 6.0 or dietary restriction suppresses the reduction in RLS associated with chronological aging

In order to determine the effect of chronological aging on subsequent RLS, we chronologically aged diploid BY4743 cells under four different culture conditions and measured the RLS of cells that were chronologically aged for 2, 4, 9, 16, or 23 days. The four conditions utilized were (1) SC medium with 2% glucose, (2) YEPD medium with 2% glucose, (3) DR by reducing the glucose from 2% to 0.05% in SC medium, and (4) SC medium buffered to a pH of 6.0. At each age-point, chronological survival was also determined in two ways: by our standard Bioscreen C MBR CLS assay [82,92] and by directly quantifying the number of aged cells that were capable of re-entering the cell cycle when plated on YEPD during the RLS analysis. As expected, medium acidification was attenuated by culture in YEPD, DR, or buffering, and CLS was extended under each of these conditions, relative to cells aged in SC 2% glucose (**Figure 1**, **Table 1**).

As previously reported [14], cells aged chronologically in YEPD showed a reduction in subsequent RLS, and the negative effect on RLS was enhanced by greater chronological age (**Figure 2A**). This effect was also observed in cells aged in SC 2% glucose, although the reduction in RLS was somewhat accelerated relative to YEPD, consistent with the reduced CLS in SC 2% relative to YEPD (**Figure 2B**). Cells aged in SC buffered to pH 6.0 showed a reduced effect of chronological aging on RLS, relative to cells aged in SC 2% glucose (**Figure 2C**), and DR

almost completely prevented the reduction in RLS associated with chronological aging up to 23 days (**Figure 2D**)

During the course of these experiments, we noted an increase with chronological age in the number of cells that were only able to complete one cell division during the RLS experiment, particularly for those cells aged in SC 2% glucose. Not censoring these cells from the subsequent RLS analysis does not substantially change the results, however.

A direct comparison of the reduction in RLS during chronological aging indicates that cells aged chronologically in SC 2% glucose lose replicative capacity more rapidly than cells aged chronologically in any of the other media conditions tested, while cells aged in YEPD show an intermediate rate of loss of replicative capacity with increasing chronological age. This can be seen from a plot of the mean RLS as a function of the chronological age of the cells at the start of the RLS experiment (**Figure 3A**). Cells aged chronologically in SC 2% glucose, YEPD, or SC 2% glucose pH6.0 show a statistically significant ($p<0.05$) negative correlation between chronological age and RLS, while no significant decrease in RLS during the first 23 days of chronological aging was detected for cells subjected to DR (**Figure 3B**). However, the slope of this regression correlation was drastically reduced in pH6.0 buffered SC 2% glucose medium as well as in YEPD, and both sets of data are significantly different from SC 2% glucose aged cells in ANOVA tests (**Figure 3B**). Thus, buffering the culture medium to pH 6 and DR both attenuate the reduction in RLS associated with chronological age as well as extend CLS.

A complex relationship between cell size and aging

Based on a recent report suggesting that cell size may limit RLS under some conditions [93], we measured the cell size of chronologically aged yeast in order to determine whether the reduction in RLS correlates with increased cell size during chronological aging. Cell size was estimated by quantifying the area of the cell when lying flat on the surface of YEPD agar (see Methods). Unexpectedly, the average size of cells grown in SC 2% glucose decreased during chronological aging; however, this effect could be attributed to an increasing number of exceptionally small cells accumulating in the population. This smaller sub-population consisted of cells that were unable to reenter the cell cycle, as determined during the replicative life span analysis (**Figure 4A**). When the cells which failed to bud were censored from the data set, the SC 2% glucose cultured yeast were as large cells aged in SC 2% glucose buffered to pH 6 or in YEPD (**Figures 4B, C, D**).

For those mother cells that were able to divide at least once, smaller cell size following chronological aging was significantly correlated with greater subsequent RLS when cells were aged in unbuffered SC 2% glucose **(p<8.3E-5)**, SC 2% glucose buffered to pH 6 **(p<1.1E-2)**, or YEPD **(p<8.8E-7)** (**Figure 4E**,). There was an opposite correlation between cell size after chronological aging and RLS for cells subjected to DR **(p<2.1E-3)**, perhaps since these cells are smaller on average to begin with.

Chronological Cell Death is Associated with Apparent Failure to Maintain G1 Arrest

As an additional characterization of cell viability during chronological aging, cells were treated with the dye SYTOX Green, which serves two purposes in this study. First, SYTOX Green differentiates live from dead cells, as it is excluded from cells with an intact plasma membrane [94] [95]. Second, SYTOX Green binds nuclear DNA, providing a measure of cell cycle progression [59] [61]. As expected from its vital dye capability, the proportion of cells stained brightly with SYTOX Green increased dramatically with chronological age when cells were aged in in unbuffered SC 2% glucose (**Figure 5**). Consistent with the survival data, this increase was attenuated for cells aged in YEPD, SC 2% glucose buffered to pH 6, or subjected to DR (**Figure 6A**). By measuring forward scatter, an indicator of relative cell size, the SYTOX Green staining also supported the cell size measurements obtained by microscopy; the cells subjected to DR were smaller than cells aged in other conditions, and the live cells in unbuffered SC2% glucose cultures were approximately 20% larger than the dead cells in the same culture.

During our analysis, we noted that the DNA content of the brightly staining cells aged in unbuffered SC 2% glucose appeared to increase with chronological age (**Figure 6B**). This suggests that cell death in unbuffered SC 2% glucose is associated with a loss of DNA replication control, since SYTOX Green staining is proportional to DNA content only in dead cells. A similar trend can be seen in cells aged in YEPD, SC 2% glucose buffered to pH 6, or DR medium after 36 days of chronological aging (**Figure 6C**). Thus, although survival is extended under these conditions, exit from G1 and initiation of DNA replication appears to be associated with cell death in all cases. These data are further supported by analysis of budding index. Cells were gated based on SYTOX Green staining into “live” and “dead” fractions and budding morphology was determined by microscopy for each fraction. In every case, the dead

population contained significantly more budded cells (around 20%) than the live fraction (**Figure 6D**).

Discussion:

The primary goals of this study were to verify the report that chronological aging of yeast cells reduces RLS and to determine whether changes in the extracellular environment that influence CLS would also influence subsequent RLS. Both of these goals were achieved. Chronological aging of diploid BY4743 yeast cells in YEPD medium was found to reduce RLS, with our observed effects quite similar to those reported by Ashrafi et al. [14]. The vast majority of published CLS studies do not use YEPD as the aging medium, however, and instead use SC 2% glucose. Importantly, we observed that cells aged under these more commonly used conditions also show a reduction in RLS that is even more severe than cells aged in YEPD, correlating with their relatively shorter CLS. Two interventions known to extend CLS, buffering the SC 2% glucose medium to pH 6.0 or DR by reducing the glucose to 0.05%, prevented the reduction in RLS during chronological aging out to 23 days of age. Taken together, these observations suggest a strong link between the rate of chronological aging and the resulting reduction in RLS.

It has been proposed that chronological aging in yeast is associated with DNA replication stress, and that DR may extend CLS by promoting a more efficient G1 arrest [15]. Our observations that dead cells in the chronologically aging population show indications of release from G1 arrest and partial DNA synthesis are consistent with this model. This failure to maintain cell cycle arrest was only observed in dead cells, however, as evidenced by the high proportion of unbudded cells

in the live cell fraction of the populations under all conditions and age-points examined. It remains unclear whether escape from G1 is a cause or consequence of cell death during chronological aging. It is important to note, however, that this cell cycle progression is distinct from the 'gasping' phenomenon described in prior studies [89], where a small fraction of the population escapes from cell cycle arrest and undergoes several cell divisions. Indeed, the fact that an overwhelming proportion of the live cells in our experiments were unbudded indicates that gasping did not occur in the long-lived cell populations, and we suggest that this type of analysis may be a useful way to control for gasping in these types of experiments.

A key question for future studies will be to determine the nature of the molecular damage that accumulates during chronological aging to reduce the cell's replicative capacity. It is well-established that chronologically aging yeast cells undergo an apoptotic-like response [96 97]; however, apoptotic cells are unable to resume cell division and do not contribute to the shortened RLS. It may also be that replication stress and failure to maintain a G1 arrest contribute to reduced RLS; however, as with apoptosis, this phenomenon appears to be restricted to that portion of the population that is unable to complete even one replication event. Instead, we speculate that oxidative damage to cytoplasmic proteins and/or mitochondria occurring during chronological aging may underlie the reduction in RLS. Several lines of evidence support this idea. First, nuclear extrachromosomal rDNA circles do not accumulate in cells during chronological aging [14], indicating that the reduction in RLS is unlikely to be related to rDNA instability. Second, oxidative damage to mitochondria and proteins does accumulate during chronological aging [98 99], and these types of damage are asymmetrically segregated to the mother cell during normal replicative aging [71,73,100,101]. Third, extracellular acetic acid can induce

intracellular oxidative stress during chronological aging [102], and preventing acidification by buffering the culture medium to pH 6.0 during chronological aging attenuates RLS reduction. Taken together, these data suggest a model whereby acidification of the extracellular environment induces oxidative stress and the accumulation of oxidatively damaged macromolecules that are asymmetrically inherited by the mother cell upon resumption of cell division, resulting in a reduced RLS (**Figure 7**).

A compelling feature of this model is that it explains an apparent paradox regarding why such a system of asymmetric segregation should have evolved in budding yeast. In natural populations, the vast majority (>99.9%) of cells in any natural population will be fewer than 10 generations old (less than the median RLS of a mother cell), and half of all cells will have produced at most one daughter cell. Thus, inheritance of damage is unlikely to have a significant effect on fitness for the vast majority of individuals in rapidly dividing populations [61]. In non-dividing populations, however, damage will accumulate over time. By retaining this damage in the mother cell upon resumption of cell division, the fitness of the daughter cell is maximized. Thus, we propose that the selection for asymmetry arises due to the natural cycle of quiescence, followed by growth, followed by quiescence. A recent report suggests that a similar process of damage clearance may occur during sporulation, based on the observation that replicatively aged mother cells induced to undergo sporulation give rise to daughter cells that are free from age-related oxidative damage [103]. By the same logic as above, this meiotic asymmetry is unlikely to have evolved based on replicative age, since aged mother cells represent a vanishingly small proportion of any population. Instead, such a mechanism may be more relevant for cells that undergo sporulation following a prolonged period of quiescence. It will therefore be of

substantial interest to determine whether spore clones arising from chronologically aged cells show a similar reduction in damage and restoration of normal replicative capacity.

Experimental Procedures

Yeast strains and media

The diploid BY4743 strain was obtained from Open Biosystems**.** CLS assays were performed as previously described using the Bioscreen C MBR (Growth Curves Inc., Piscataway, NJ, USA) automated shaker/incubator/plate reader to determine viability [81,82,92]. A second measure of viability following chronological aging was obtained from the percentage of cells that were able to complete at least one mitotic division during the replicative aging assay. All chronological aging cultures were initiated by seeding a 5 ml liquid culture of YEPD with a single colony from a freshly streaked strain grown on YEPD agar at 30°C. A 1:100 dilution of the YEPD culture was made into synthetic complete (SC) medium, containing 2% glucose, unless otherwise noted. Basic medium is 1.7g/L Yeast Nitrogen Base (-AA/-AS) (BD Difco™, Franklin Lakes, NJ, USA) and 5g/L $(NH_4)_2SO_4$. Components of the SC medium used in this study have been described elsewhere in detail [82,91]. All strain auxotrophies were compensated with a four-fold excess of amino acids. Cultures were grown and aged in a roller drum enclosed in a water-jacketed incubator at 30˚C. YEPD was 20g/L Bacto Peptone and 10g/L Yeast Extract (BD Difco™, Franklin Lakes, NJ, USA), supplemented with glucose at the indicated concentrations. For alternative carbon source experiments, the glucose was replaced with the indicated carbon source at the indicated concentration. For growth in buffered medium, a citrate

phosphate buffer (64.2mM Na_2HPO_4 and 17.9mM citric acid, pH 6.0) adjusted to pH 6.0 was added to the medium prior to inoculation.

pH Determinations

Aging cultures were prepared as described above, with a 1:100 dilution of a YEPD culture being inoculated into synthetic medium containing the appropriate carbon source. pH of cultures was measured after 30 days of aging using an Accumet XL 15 pH meter (Fisher Scientific, Pittsburgh, PA, USA). Between readings, the meter was rinsed with ethanol, sterile deionized water, and patted dry with a laboratory tissue wipe.

Chronological lifespan analysis

Unless otherwise stated, CLS was determined using a Bioscreen C MBR (Growth Curves Inc., Piscataway, NJ, USA) automated incubator/plate reader to monitor the outgrowth kinetics of chronologically aged cultures in a synthetic complete medium supplemented with 2% glucose, as previously described [81,82,92]. Chronological viability was calculated from growth curves of aging cultures using the Yeast Outgrowth Data Analyzer (YODA, www.sageweb.org/yoda)[104]. The survival integrals were calculated using the YODA "cleaned" algorithm on YODA and the doubling time was calculated by the "interval" method. The calculation parameters were as follows: Threshold ODs (Min = 0.100, Max = 2.000); Doubling Time Interval OD (Min = 0.200, Max = 0.500); Doubling Time Adjustment (Delay OD = 0.500, Slope = 0.0261, Min Delay (sec) = 500); Survival Time Shift (OD = 0.300). Survival integral (SI) is defined as the area under the mortality curve and provides a quantitative measure of the CLS that allows for statistical analysis between experimental and control groups [81,92]. A Student's T-test was used to calculate p-values.

For all experiments, outgrowth data was normalized to the initial time point collected on the second day of chronological aging.

Replicative lifespan analysis

RLS was determined using a standard yeast tetrad dissection scope as previously described [60], with the modification that virgin daughter cells were not specifically selected by allowing a cell division cycle to occur prior to initiating the experiment. Instead, 5 µL of the chronological aging culture was spotted onto 2% glucose YPD plates, allowed to dry into the plates, and 60-1080 cells (depending on the predicted viability of the culture at that point) were randomly selected for RLS analysis. Selected cells were moved to the middle of the YPD plates and the RLS of those cells was measured. Statistical significance for lifespan differences was determined using the Wilcoxon Rank-Sum test. Regression statistics were performed using Microsoft Excel Analysis Toolpak's "Regression" function, and regression lines were compared (Figure 3) using Microsoft Excel Analysis Toolpak's "ANOVA: two factor with replication" function using individual lifespans as the replicates.

Direct cell size analysis

Cell sizes were determined through two methods: direct photography and outlining of cells present on replicative lifespan plates as well as forward scatter measurements by flow cytometry. For the former, pictures of the cells measured in the replicative lifespans (shown in **Figure 2**) were taken by a Zeiss SteREO Lumar.V12 (Thornwood, NY, USA) at 150X zoom using bright field settings. Axiovision was then used to draw a perimeter around the cell and the cell area was automatically calculated. Results are shown as the mean average of the sizes of at

least 60 cells for each condition tested. Regression statistics were performed using Microsoft Excel Analysis Toolpak's "Regression" function.

Flow cytometry

All flow cytometry experiments were performed in the University of Washington Nathan Shock Center of Excellence in the Basic Biology of Aging Imaging Core using a BD Biosciences Influx Cell Sorter. Cell were aged chronologically and then 5 x 10^7 cells were harvested for flow cytometric analysis. Cells were spun down (7k rpm 1 minute) and the supernatant removed. Cells were washed in sterile 50 mM Na citrate buffer, spun down again, and the supernatant discarded. Cells were resuspended in 50 mM Na citrate containing 2µM SYTOX® Green (Invitrogen, S7020, Grand Island, NY, USA). Cells were kept on ice and immediately run through the flow cytometer. Readings were optimized to maximize the spread of live and dead cells to ease subsequent analysis. 20,000 cells were used in each biological replicate measurement.

Cell cycle profiles were generated by gating dead cells and then by creating plots in FCS Express (DeNovo software, Los Angeles, CA, USA). Cell sizes from flow cytometry were determined by gating live or dead cells and then by using the mean forward scatter (a relative cell size measurement) value for comparisons between biological replicates. Budding indices were formed from gating the live or dead cells after 13 days of aging and then using the cell sorting capability of the instrument to separate the two into separate eppendorf tubes, each containing at least 500 cells, 100 of which were used to determine budding percentages.

Figures:

Table 1. Effect of culture medium on pH. Cells were aged in synthetic complete medium with 2% glucose, synthetic complete medium with 0.05% glucose, synthetic complete medium with 2% glucose buffered to pH 6.0, or rich YEPD medium. pH was determined using an Accumet XL 15 pH meter after 30 days of chronological aging between three biological replicates.

Medium	**Day 30 pH**
SC 2% glucose	2.78 ± 0.01
SC 0.05% glucose	6.03 ± 0.04
SC 2% glucose pH 6.0	5.19 ± 0.01
YEPD	4.55 ± 0.00

Figure 1: Chronological lifespan accurately measures the ability of cells to reenter the cell cycle.

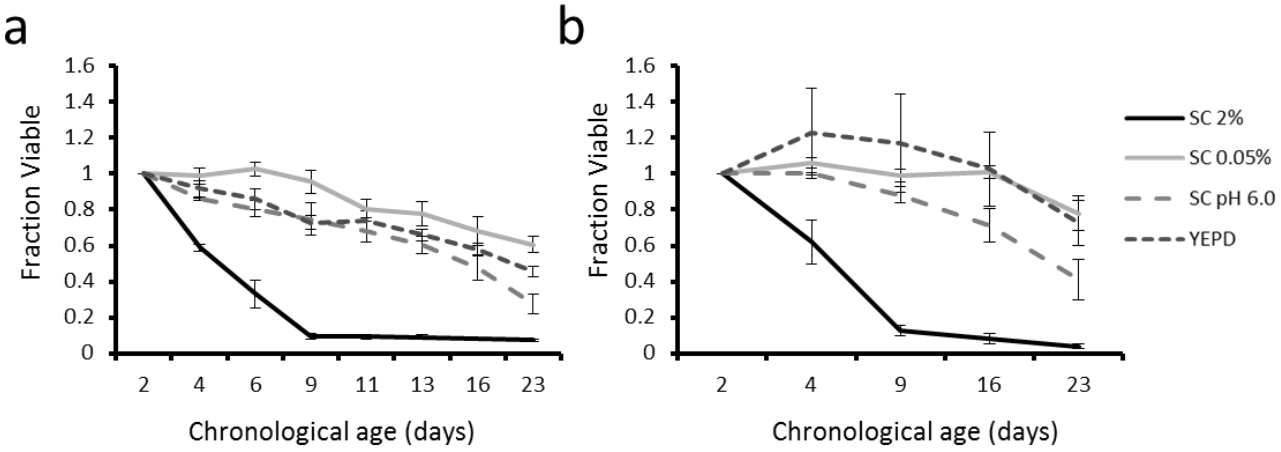

(a) Chronological lifespans of cells aged in SC 2% glucose, SC 0.05% glucose, SC 2% glucose pH6.0, and YEPD measured using the Bioscreen C MBR machine. The data represents six biological replicates with error bars representing standard error. (b) Fraction of cells able to

complete more than one division after chronological aging as determined by replicative lifespan measurements. The data represents six biological replicates with error bars representing standard error.

Figure 2: Conditions which rescue accelerated chronological aging also rescue shortened replicative lifespan.

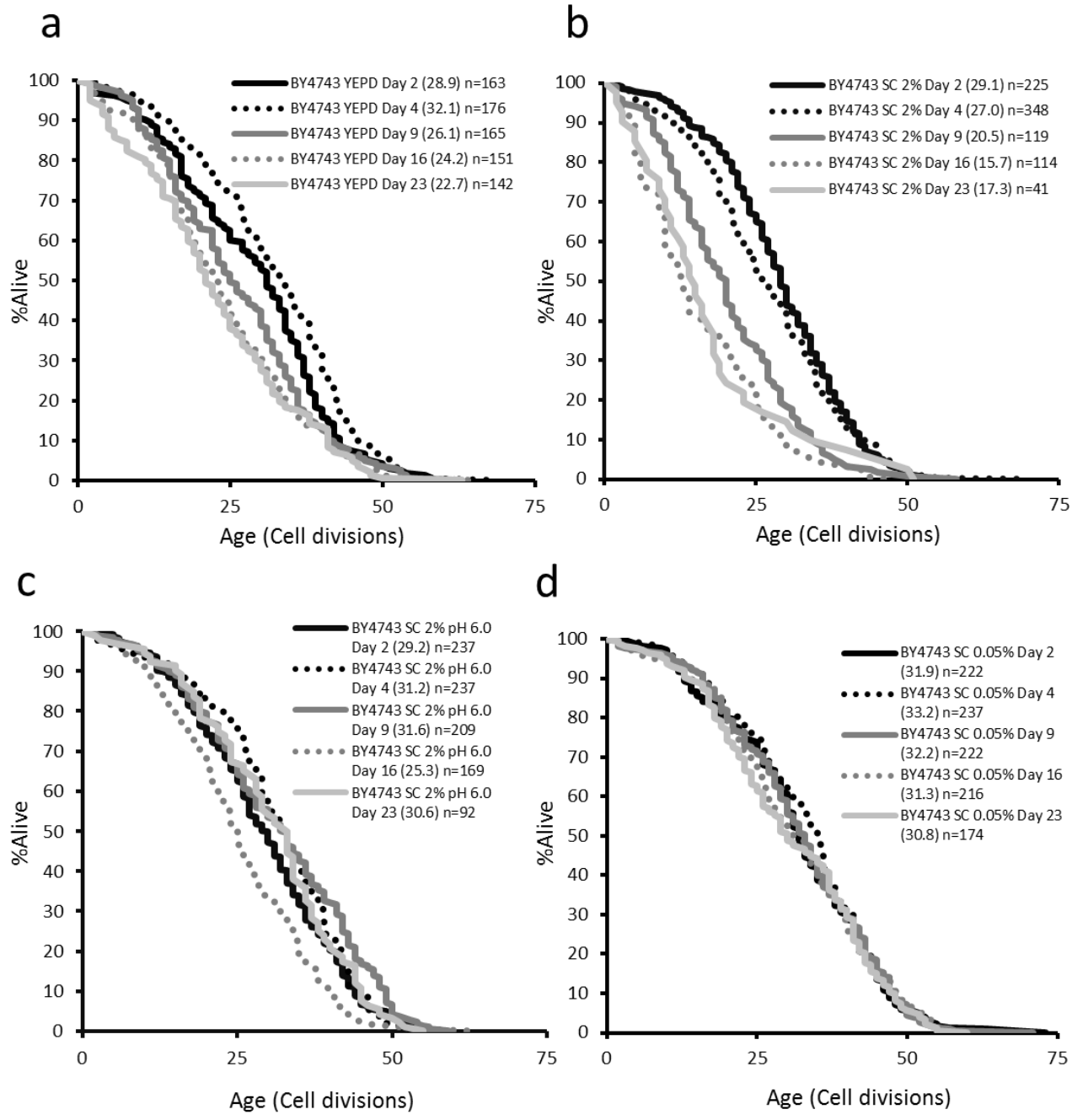

Replicative lifespan curves of cells aged chronologically in (a) YEPD, (b) SC 2% glucose, (c) SC 2% glucose pH 6.0, and (d) SC 0.05% glucose. Cells which did not divide or divided once are not included (see uncensored lifespans in Supplemental Figure 2).

Figure 3: Plotting mean RLS versus chronological age shows a decreased rate of lifespan shortening in SC 0.05% glucose and SC 2% glucose pH 6.0 media.

a

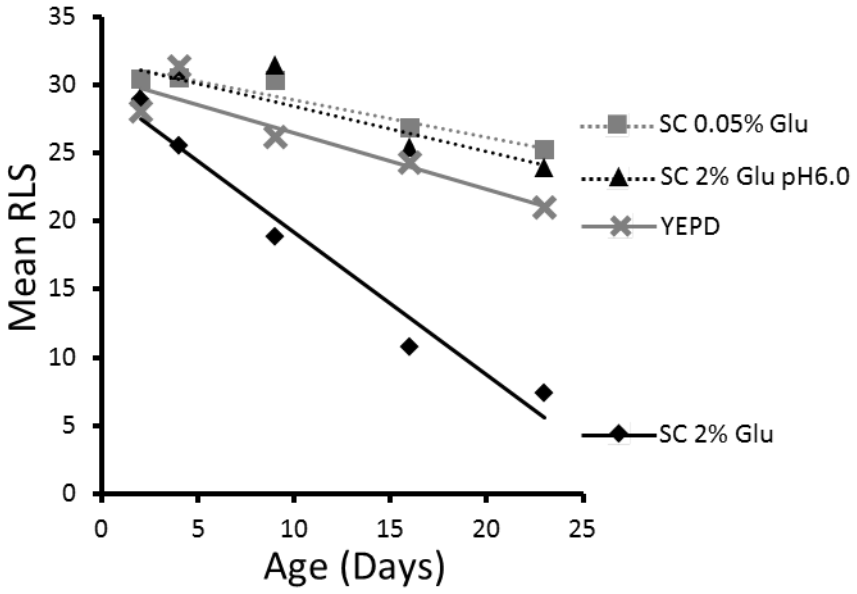

b

Trendline statistics:

	Slope	Regression p	ANOVA p (2%)	p (0.05%)	p (2% pH6)
SC 2% Glu	-1.0	7.5E-14			
SC 0.05% Glu	-0.27	0.14	2.2E-08		
SC 2% Glu pH6.0	-0.33	2.7E-04	6.1E-17	0.77	
YEPD	-0.41	1.3E-06	1.4E-14	0.11	0.010

(a) Trend lines created from mean replicative lifespans following chronological aging are shown here. (b) Statistics and slope measurements of the regression trendlines in (a).

Figure 4: The interrelationship of cell size and replicative lifespan.

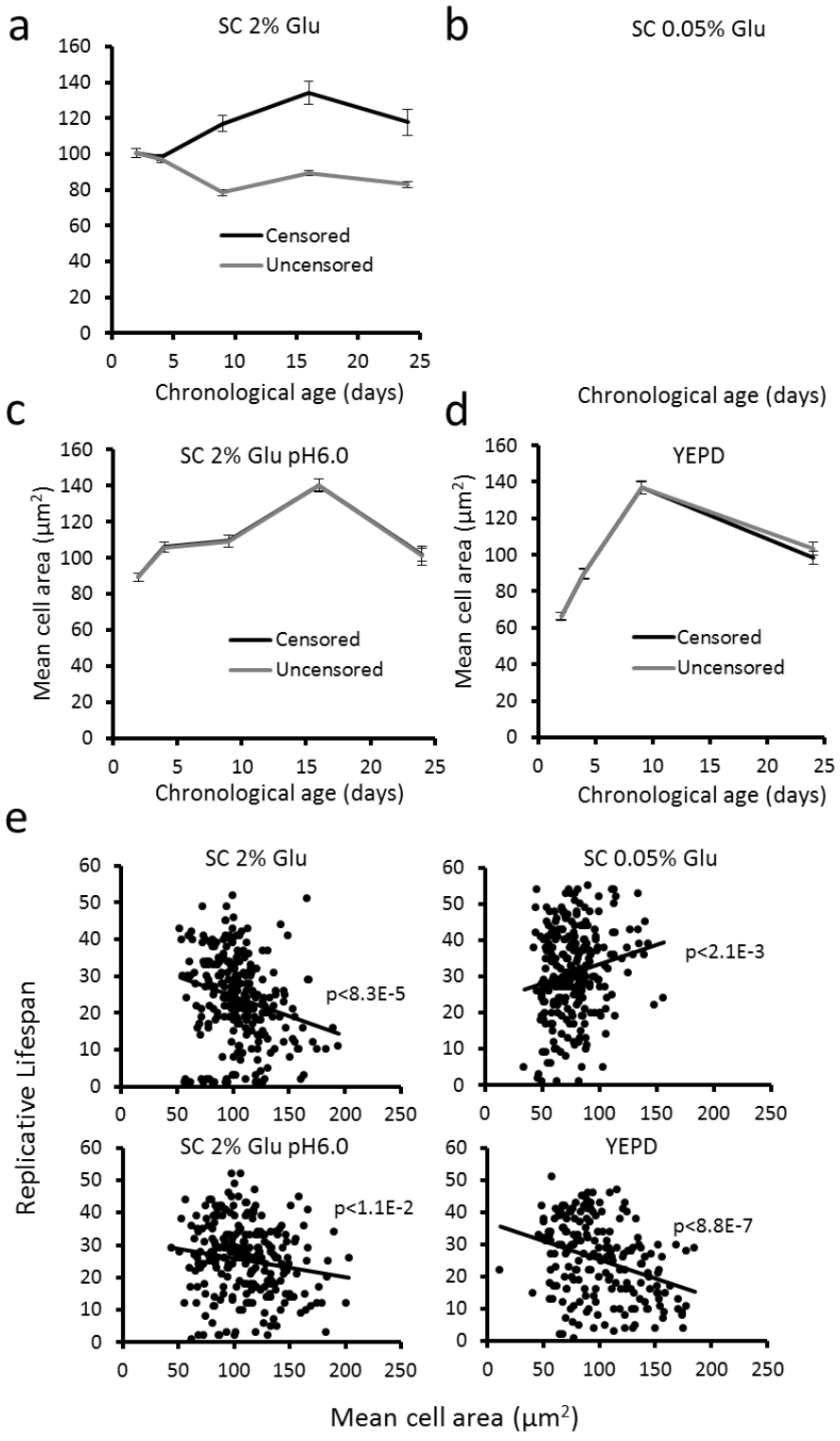

(a) Cell size measurements of aged cultures prior to replicative lifespan analysis. Cell size of those which divide one or more times (censored) is greater than that of the population mostly containing dead cells (uncensored) in SC 2% glucose, but not the other conditions (b-d). (e) Scatter plots of cell sizes taken from images at the beginning of replicative lifespan compared to their corresponding replicative lifespan. p values represent significant correlations between size and replicative lifespan.

Figure 5: Uptake of vital dye SYTOX Green during chronological aging.

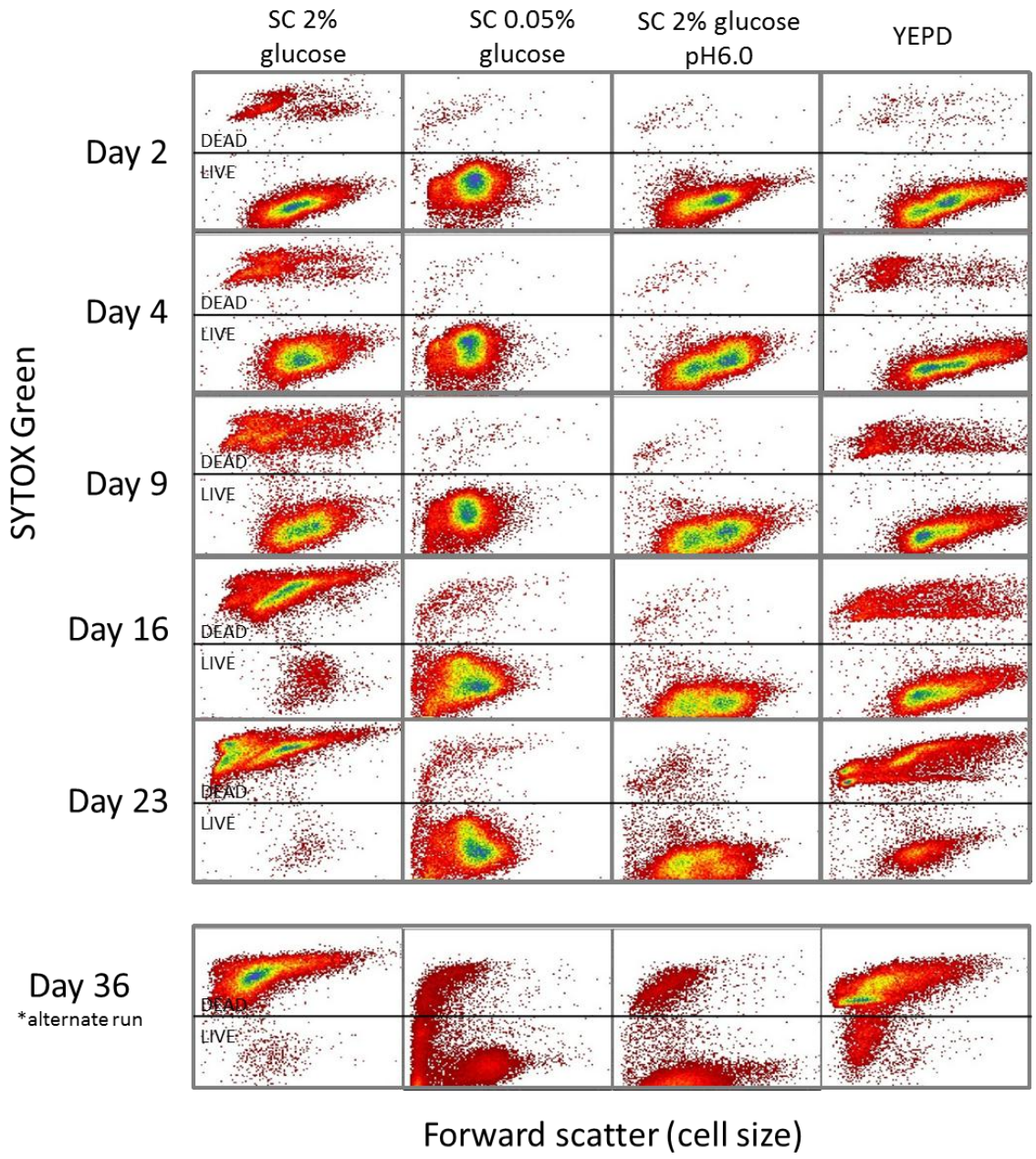

SYTOX Green stained cells were run through a flow cytometer and assayed for relative fluorescence. Since dead cells are able to uptake the dye and allow it to bind DNA, live and dead cell gates were constructed based on SYTOX staining. Forward scatter measures relative cell size.

Figure 6: Shorter lived cells undergo enhanced replication stress.

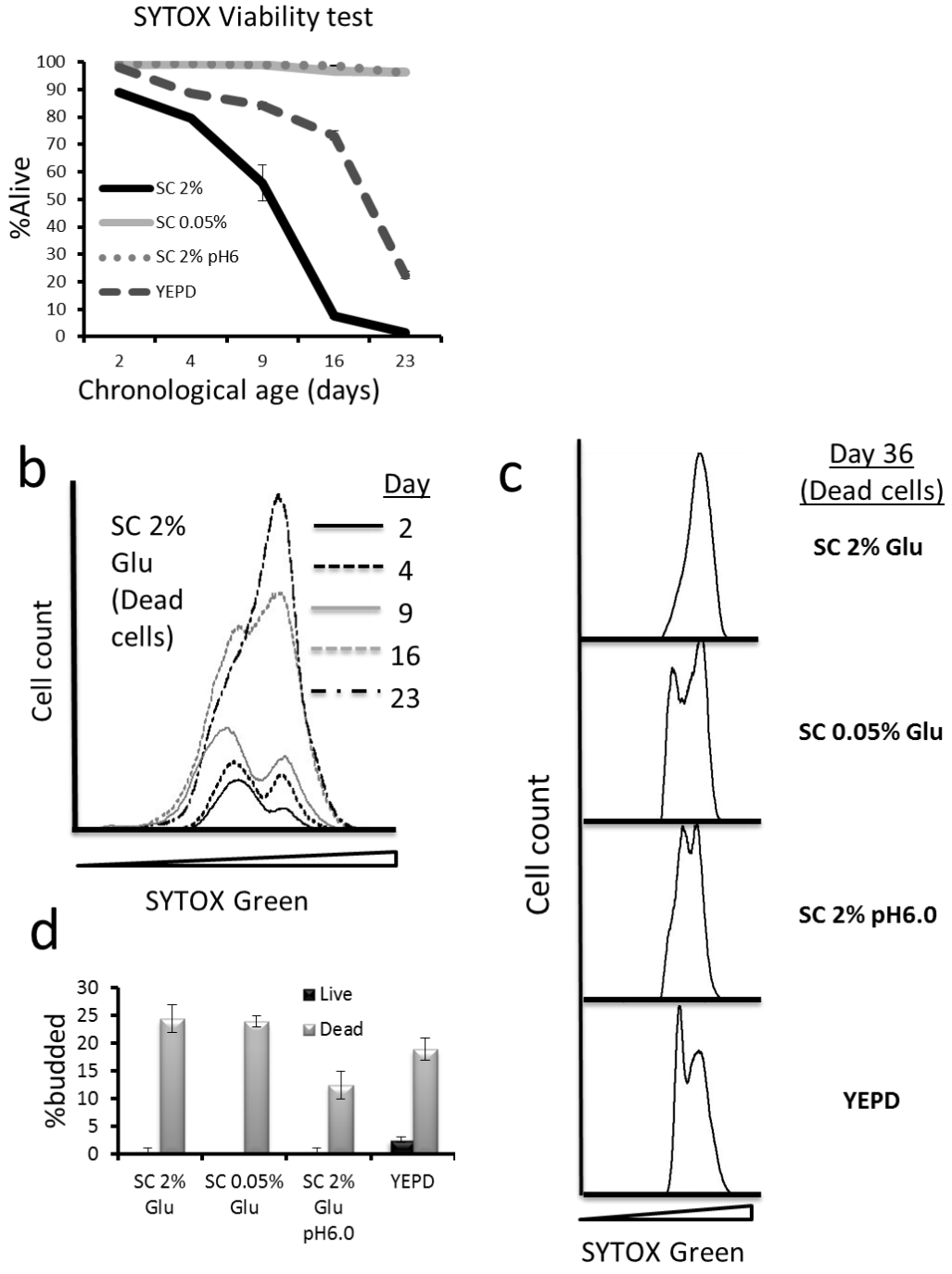

(a) SYTOX Green stained cells analyzed after chronological aging are gated as in Figure 5 and the viability measurements are shown here. (b) Dead gated SC 2% glucose cells are analyzed

for cell cycle profiles during chronological aging. (c) Dead gated cells of all types of chronologically aged cultures are analyzed for cell cycle profiles after 36 days of aging. (d) Gated live and dead cells were sorted for analysis after 13 days of chronological aging and visually assayed for budding state, with the percent budded of each type shown here.

Figure 7: Model for unique and shared forms of damage in yeast aging

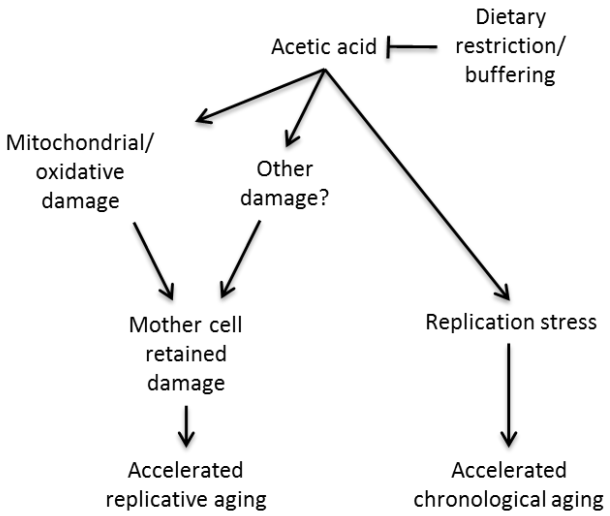

Section IV: Stress profiling of longevity mutants identifies Afg3 as a mitochondrial determinant of cytoplasmic mRNA translation and aging

Abstract:

While environmental stress likely plays a significant role in promoting aging, the relationship remains poorly understood. In order to characterize this interaction in a comprehensive manner, we performed a systematic analysis of the stress response profiles for 46 long-lived yeast mutant strains across four different stress conditions (oxidative, ER, DNA damage, and thermal), grouping genes based on their associated stress response profiles. Unexpectedly, cells lacking the mitochondrial AAA protease gene *AFG3* clustered strongly with long-lived strains lacking cytosolic ribosomal proteins of the large subunit. Similar to these ribosomal protein mutants, *afg3Δ* cells show reduced cytoplasmic mRNA translation, enhanced resistance to tunicamycin that is independent of the ER unfolded protein response, and Sir2-independent but Gcn4-dependent life span extension. These data demonstrate an unexpected link between mitochondrial protein quality control, cytoplasmic mRNA translation, and aging.

Introduction:

Defining the molecular mechanisms of aging is one of the most challenging problems in modern biology. Hundreds of life span-extending mutations have been discovered in yeast, nematodes, and fruit flies, and a handful of conserved longevity pathways have been identified [13,18,105]. For the vast majority of these genes, however, the pathways in which they act, and the mechanisms by which they modulate aging, remain poorly understood.

One feature that has been observed to correlate with longevity, both across species and among individuals of the same species, is altered resistance to different forms of stress. In general, long-lived mutants across a variety of species tend to be stress-resistant; however, there is specificity depending on the type(s) of stress applied and the longevity pathway(s) under study [16]. For example, cell lines derived from long-lived species show enhanced resistance to several forms of stress, but also show enhanced sensitivity to other forms of stress [106-108]. In yeast, nematodes and fruit flies, many long-lived mutants are resistant to oxidative and thermal stress. For example, in yeast, long-lived cells deleted for the S6 kinase homolog *SCH9* or the mammalian target of rapamycin homolog *TOR1*, up-regulate stress-responsive transcription factors, and also show enhanced stress resistance [87,109]. To date, however, no comprehensive analysis of the relationship between stress resistance and longevity has been performed in any system.

The budding yeast *Saccharomyces cerevisiae* provides an ideal model for exploring the relationship between stress resistance and longevity. The availability of collections containing individual single gene deletions for a majority of yeast genes has allowed for genome-scale studies of sensitivity and resistance for multiple forms of environmental stress [110,111]. Replicative life span (RLS) in yeast is defined as the number of daughter cells produced by a mother cell before cessation of cell division [76]. Several types of molecular damage are asymmetrically inherited by the mother cell and are proposed to limit RLS, including nuclear ribosomal DNA circles, cytoplasmic protein aggregates, and damaged mitochondria [19,77]. Over the past several years, we have been screening strains derived from the yeast ORF deletion collection to identify single-gene deletions that increase RLS [112]. This has resulted in the identification of several dozen long-lived mutants [8,12,41-43,45,46].

One well-studied longevity pathway in yeast consists of long-lived mutants with reduced nutrient signaling and impaired mRNA translation. *TOR1* and *SCH9* are nutrient responsive kinases that regulate ribosome biogenesis and mRNA translation in response to nutrient availability. Under conditions of nutrient restriction, such as dietary restriction, reduced signaling through Tor1 and Sch9 along with other factors, coordinate a reduction in mRNA translation, an increase in autophagy, and a metabolic shift from fermentation to respiration [113]. Deletion of either *TOR1* or *SCH9* is sufficient to increase RLS, and subjecting these mutants to dietary restriction fails to further increase life span [41]. The particular importance of mRNA translation in this pathway was suggested by the finding that deletion of multiple ribosomal protein genes is also sufficient to increase RLS [43]. With one exception [114], life span extension from ribosomal protein gene deletions in yeast appears to be specific for large ribosomal subunit (60S) genes that result in a deficiency of mature large ribosomal subunits [43]. Like *tor1Δ* or *sch9Δ* cells, RLS extension in mutants deficient for large ribosomal subunits is non-additive with dietary restriction and independent of the Sir2 protein deacetylase [43,115]. Although general mRNA translation is impaired, it is thought that RLS extension in these mutants results primarily from increased translation of the Gcn4 transcription factor under conditions where large ribosomal subunits are limiting [43]. This increase in Gcn4 translation has been attributed to the presence of inhibitory upstream open reading frames in the Gcn4 mRNA 5' untranslated region [116], and Gcn4 is required for life span extension in several of the long-lived ribosomal large subunit gene deletion mutants [43].

We have performed a systematic analysis of the stress response profiles for 46 long-lived deletion strains across four different stress conditions. The growth properties of each strain were assessed under conditions designed to induce ER stress (tunicamycin), oxidative stress (paraquat), DNA damage stress (methyl methanesulfonate, or MMS), or thermal stress (heat shock). Although long-lived mutants were often resistant to one or more stressors, relative to the parental wild type strain (BY4742), none of the

stressors elicited a similar response across the entire panel of long-lived strains. Analysis of the stress response profiles using cluster algorithms successfully grouped long-lived strains into distinct classes. One such class included several large subunit ribosomal protein deletion strains that showed resistance to growth inhibition by tunicamycin and paraquat, as well as resistance to heat shock. Also included in this class was a strain lacking the gene coding for the mitochondrial m-AAA protease Afg3 (also referred to as Yta10). Afg3 is known to play an important role in regulating electron transport chain complexes and is also required for maturation of the mitochondrial ribosomal protein Mrpl32 [117,118]

In this study, deletion of *AFG3* was found to cause a profound reduction in cytoplasmic mRNA translation and an increase in resistance to tunicamycin that was independent of the ER unfolded protein response transcription factor Hac1. Similar to deletion of *RPL20B*, life span extension from deletion of *AFG3* is independent of both Hac1 and Sir2, but requires Gcn4. These observations demonstrate an important new role for the mitochondrial protease Afg3 in modulating cytoplasmic mRNA translation and ER stress resistance, and suggest that Afg3 modulates longevity in yeast by a mechanism similar to ribosomal large subunit proteins.

Results:

Quantitative determination of stress induced growth rate changes among long-lived mutants

In order to quantitatively assess the stress response profiles of long-lived yeast deletion strains, we utilized a Bioscreen C MBR machine to determine doubling time in the presence or absence of a stressor for 46 long-lived mutants. The Bioscreen C MBR is a combined shaker, incubator, and plate reader that has been shown to provide high quality growth rate determinations for yeast cells maintained under a

variety of conditions [9,11,81,82,92,119,120]. Since many long-lived deletion strains have doubling times that differ from the wild type control [23], we normalized growth rate changes induced by stress (GRC_s) by normalizing to the growth rate under untreated conditions using the following equation:

$$GRC_s = \frac{D_s - D_u}{D_u} * 100$$

where D_s is the doubling time of the strain in rich growth medium (YPD) in the presence of the stressor and D_u is the doubling time of the strain in the same medium in the absence of the stressor. Using this method, we determined the growth inhibition stress responses for each of 46 long lived mutants as well as wild type and control sensitive strains to three different chemical stress conditions: ER stress induced by tunicamycin, oxidative stress induced by paraquat, and DNA damage stress induced by MMS. It should be noted that each of these chemicals may induce additional forms of stress in addition to those described above. Resistance to thermal stress was also assessed as the percent of cells that maintained viability following a heat shock.

Quantitative determination of tunicamycin induced growth rate changes among long-lived mutants

Growth inhibition in response to ER stress was determined by monitoring outgrowth kinetics in the presence of 1 ug/mL tunicamycin, an inhibitor of N-linked protein glycosylation that causes an accumulation of proteins in the ER and induces the ER unfolded protein response [121]. This concentration of tunicamycin was sufficient to increase the doubling time of wild type BY4742 cells by nearly 200% (**Figure 1a**). In order to validate the method, we included as a control cells lacking *HAC1*, which encodes a transcription factor required for induction of many proteins involved in the ER unfolded protein

response [122]. As expected, *hac1Δ* cells showed extreme growth inhibition by 1 µg/mL tunicamycin, such that not even a single doubling in cell density was observed over 24 hours (**Figure 1a**).

Of the 46 long-lived mutants tested, 22 had a lower GRC_s than wild type BY4742 (WT) cells in the presence of tunicamycin, 4 showed greater growth inhibition (higher GRC_s), and 20 had no significant change from WT ($p < 0.05$ in each case, **Figure 1a**). Notably, all ten long-lived large ribosomal protein deletion strains had significantly lower GRC_s than WT. Three additional mutants with known defects in large ribosomal subunit biogenesis or function (*rei1Δ*, *rpp2bΔ*, and *dbp3Δ*) showed a similar resistance to tunicamycin growth inhibition, while mutations in the signaling kinases that regulate mRNA translation (*tor1Δ* and *sch9Δ*) did not.

Afg3 encodes a component of a mitochondrial inner membrane AAA protease that functions to maintain proteostasis in the mitochondria and promote proper assembly of electron transport chain complexes [118,123,124]. Interestingly, long-lived *afg3Δ* cells showed reduced growth inhibition in the presence of tunicamycin that was comparable to the large subunit ribosomal protein deletion mutants, such as *rpl20bΔ* (**Figure 1b-d**). This resistance to growth inhibition is particularly evident at higher concentrations of tunicamycin, such as 2.5 µg/mL, where the doubling time of *afg3Δ* (156 min) and *rpl20bΔ* (185 min) was faster than that of WT cells (284 min), despite both mutants being slow-growing in unstressed conditions. The absence of respiratory growth in *afg3Δ* cells is evident from the flat growth curve after glucose has been consumed. The Bioscreen C MBR machine provides a linear estimate of cell density from approximately OD 0.1-1.0, so anything above this range is an underestimate of the cell density. Across the entire panel of 46 long-lived mutants, there was no significant correlation between tunicamycin growth rate changes and lifespan (**Figure 1e**).

Quantitative determination of paraquat induced growth rate changes among long-lived mutants

The effect of oxidative stress on growth inhibition was determined by culturing cells in the presence of the superoxide-generating chemical paraquat. Addition of 5 mM paraquat was sufficient to increase the doubling time of wild type cells by 69% (**Figure 2a**). As controls, we examined growth inhibition for three strains previously annotated as sensitive to oxidative stress: *ctt1Δ*, *cta1Δ*, and *sod1Δ* [125,126]. *CTT1* and *CTA1* encode cytosolic and peroxisomal catalase enzymes necessary for detoxification of hydrogen peroxide, respectively, while *SOD1* encodes the cytosolic superoxide dismutase that is primarily responsible for converting superoxide to hydrogen peroxide ([127]). Cells deleted for *SOD1* are significantly shorter-lived than BY4742 wild type cells, while cells lacking either *CTT1* or *CTA1* have a lifespan that does not differ significantly from wild type in this background (**Figure 8**).

Among the 46 long-lived strains examined, eight were significantly more growth inhibited by paraquat, relative to the wild type control, while twenty-one were less inhibited ($p<0.05$ in each case, **Figure 2a**). The remaining 17 long-lived mutants showed changes in doubling time (GRC_s values) that did not differ significantly from that of wild type cells**.** As was observed for tunicamycin, *afg3Δ* and *rpl20bΔ* cells were significantly less growth inhibited by paraquat compared to WT (**Figures 2b-d**). No significant correlation was observed between the effect of paraquat on growth and magnitude of life span extension across the 43 long-lived strains (**Figure 2e**).

Quantitative determination of MMS induced growth rate changes among long-lived mutants

The DNA alkylating agent methyl methanesulfonate (MMS) was utilized to assay for the effect of DNA damage stress on growth inhibition. At 0.01%, MMS increased the doubling time of WT cells by 66% (**Figure 3a**). As a control, we included *rad52Δ* cells defective for homologous recombination (Herzberg et al., 2006). The same concentration of MMS increased the doubling time of *rad52Δ* by 506%.

Of the 46 long-lived mutants, 15 showed a significant reduction in growth inhibition compared to WT, while 6 had a higher GRC_s ($p<0.05$ in each case, **Figure 3a**). The long-lived *fob1Δ* strain showed less growth inhibition by MMS (**Figure 3a**), perhaps related to the enhanced genomic stability of this strain at the ribosomal DNA [128]. Once again, *afg3Δ* and *rpl20bΔ* showed a similar response to MMS, although in this case both strains trended toward enhanced growth inhibition rather than reduced growth inhibition, relative to WT (**Figures 3b-d**). As with tunicamycin and paraquat, no significant correlation between growth inhibition in the presence of MMS and longevity was observed (**Figure 3e**).

Quantitative determination of heat shock stress profiles among long-lived mutants

Resistance to thermal stress was assessed by quantifying viability following a 10 minute transient 55°C heat shock. After thermal stress, 15.8% of wild type control cells from an overnight culture retained viability. Within the set of 46 long-lived mutants, 23 had a higher survival than wild type whereas only 4 showed increased death ($p < 0.05$, **Figure 4a**). No significant difference in survival was detected for 19 long-lived mutants. As expected, the control sensitive mutants, heat shock response factor double mutant *msn2Δ msn4Δ* and ER stress response factor deletion *hac1Δ*, were sensitive to heat shock.
As with growth inhibition from tunicamycin, many long-lived ribosomal protein deletion mutants showed resistance to heat shock, relative to WT. Also, once again, *afg3Δ* clustered with the ribosomal protein deletion mutants, such as *rpl20bΔ* (**Figure 4b**); however, no significant correlation between heat shock resistance and lifespan was detected across all 46 long-lived strains (**Figure 4c**).

Stress response profiling places afg3Δ cells into the mRNA translation longevity pathway

We next asked whether the stress response profiles of long-lived mutants could be informative regarding potential mechanisms of lifespan extension. To assess this, we applied the Array Track™ clustering algorithm [129] to the stress response profiles for each strain subjected to the four stress inducers (**Figure 5**). We utilized the "complete linkage analysis" option to maximize distances between clusters in order to identify distinct pathways. Although the power of this approach is likely to be limited be the relatively small number of conditions examined, we noted that many of the mutants with known defects in mRNA translation clustered together (**Cluster I**). These included several strains lacking ribosomal proteins of the large subunit or rRNA processing factors (*dbp3Δ* and *rei1Δ*) that were characterized by significantly reduced growth inhibition from paraquat, tunicamycin, and heat shock. Cells lacking *AFG3* were also contained in this Cluster.

The remaining genes could be classified into three additional clusters (II-IV). Unlike Cluster I, the functional and mechanistic relationships among the grouped genes were less clear. Cluster II differed from Cluster I primarily in the response to paraquat, with strains in this group showing stronger growth inhibition than wild type following oxidative stress. Cluster II contained the recently characterized *ubr2Δ* mutant, which extends life span by up-regulation of proteasome gene expression and activity [120], as well as *mtc4Δ*, *spt4Δ*, and *elp4Δ*. Cluster III comprises mutants largely unaffected (less growth rate changes) by paraquat but growth-inhibited by tunicamycin. This cluster contains the *tor1Δ* strain, as well as translation initiation factor deletion strains, *tif1Δ* and *tif2Δ*. The remaining Group IV is more likely an unspecific group rather than a *bona fide* cluster, since it contains a variety of mutants that generally showed similar growth inhibition as WT across the different stress conditions.

Deletion of AFG3 promotes resistance to tunicamycin by a HAC1-independent mechanism

Based on the significant resistance to growth inhibition from tunicamycin observed for *afg3Δ* cells in liquid culture, we asked whether this phenotype could be recapitulated using traditional spot assays on solid agar medium. Cells deleted for *AFG3* were also found to be resistant to tunicamycin in agar plates, although *rpl20bΔ* cells appeared to be even more resistant (**Figure 6a,c**). We reasoned that resistance to tunicamycin in *afg3Δ* cells could be caused by constitutive induction of the ER unfolded protein response. To test this possibility we deleted *HAC1*, which is required for induction of the ER unfolded protein response, in *afg3Δ* cells. Interestingly, *afg3Δ hac1Δ* double mutants still showed enhanced resistance to tunicamycin, relative to *hac1Δ* cells, demonstrating that loss of *AFG3* promotes resistance to ER stress by a mechanism that is at least partially independent of the canonical unfolded protein response. Consistent with these observations, life span extension from deletion of *AFG3* did not require *HAC1* (**Figure 6b**). These results are similar to our recent studies of cytoplasmic ribosomal protein deletions, where deletion of *RPL20B* showed a similar HAC1-independent resistance to tunicamycin (as in **Figure 6c**) and life span extension [130].

Deletion of AFG3 reduces cytoplasmic translation and extends lifespan by a Gcn4-dependent mechanism

Based on the stress response studies described above, we speculated that deletion of *AFG3* might extend life span by a similar mechanism to that of cells deficient for ribosomal large subunits. We have previously shown that life span extending mutations resulting in large subunit deficiency, such as *rpl20bΔ*, decrease overall mRNA translation as measured by polysome analysis [43]. Similar to *rpl20bΔ* cells, *afg3Δ* cells showed a significant decrease in mRNAs with 2 or more ribosomes bound, consistent with a dramatic decrease in overall cytoplasmic mRNA translation (**Figure 7a, b**). In contrast, however, no significant change in the relative abundance of free large ribosomal subunits (or small subunits) was

detected. This suggests that, while overall mRNA translation is reduced, the mechanism of translation inhibition in *afg3Δ* cells does not involve specific depletion of large ribosomal subunits.

We have previously shown that life span extension from deletion of *RPL20B* or other large ribosomal subunit genes occurs by a mechanism that is independent of the Sir2 protein deacetylase and involves activation of the Gcn4 transcription factor [43,115]. In order to assess whether *AFG3* is modulating aging by a similar mechanism, we determined the RLS of *afg3Δ sir2Δ fob1Δ* triple mutant mother cells and *afg3Δ gcn4Δ* double mutant cells. As is the case for cells lacking large ribosomal protein subunits [115], deletion of *AFG3* further extends the RLS of cells lacking both *SIR2* and *FOB1* (**Figure 7c**), but fails to extend RLS in cells lacking *GCN4* (**Figure 7d**). Combining deletion of *AFG3* with deletion of *RPL20B* also fails to result in an additive increase in RLS (**Figure 7**e). Along with the stress response and polysome data, these longevity data support the model that deletion of the mitochondrial protease gene *AFG3* unexpectedly reduces cytoplasmic mRNA translation and increases life span by a mechanism similar to deletion of large subunit ribosomal protein genes.

Discussion:

The relationship between stress resistance and longevity is complex. A systematic analysis of stress response for 43 long-lived yeast deletion strains across 4 different stress conditions revealed that a majority of mutants show altered response to one or more types of stress. More often than not, the change in stress response was toward enhanced resistance and decreased growth inhibition, although there were many observed cases of increased sensitivity or growth inhibition in the long-lived mutants, and no significant correlation between longevity and altered stress resistance was detected for any of the stress conditions tested. Despite the complexity of the data, this analysis allowed for successful classification of long-lived mutants by their stress response profiles. In particular, the striking similarly in

stress response of *afg3Δ* cells with ribosomal protein gene deletions led us to uncover a previously unsuspected role for this mitochondrial protease in cytoplasmic mRNA translation, ER stress resistance, and Gcn4-dependent longevity control. Thus, successful classification of Afg3 represents proof-of-principle that this type of stress response profiling approach can be used to predict the longevity pathway for unknown factors, as well as uncover novel cellular functions.

It should be noted that our method for quantitatively assessing growth inhibition in responses to paraquat, tunicamycin, and MMS differs from traditional methods such as spot assays or plating for colony forming units. Unlike these traditional methods, which identify changes in sensitivity of about 2-fold, we were able to reproducibly quantify changes in doubling time of less than 10% using this method. Two possible interpretations can explain a difference in growth rate in these assays. One is simply that a different percentage of cells are dying and cannot give rise to the next generation, thereby influencing the doubling time of the population as a whole. This interpretation is supported by the fact that all of our sensitive mutant controls displayed longer doubling times. Another possibility is that the drug is inducing a slowed cell cycle and that while most cells are indeed viable, the population doubling time increases due to more cells reaching a damage level that activates a cellular response or checkpoint. Either case is physiologically relevant. It is possible that differing stress response profiles, and the resulting clusters, would be obtained if alternative methods that directly measure cell death rather than growth inhibition were used. In the case of tunicamycin, however, we observed similar resistance in both growth inhibition assays and less sensitive spot assays for *rpl20bΔ* and *afg3Δ*.

The finding that loss of Afg3 results in reduced cytoplasmic mRNA translation and enhanced resistance to tunicamycin was unexpected, as prior studies had indicated purely mitochondrial functions for Afg3 in yeast, as well as its orthologs in mammals [131,132]. Although it is possible that Afg3 may also function in the cytoplasm to modulate mRNA translation, we know of no evidence to support this model. Instead,

we speculate that the mitochondrial function of Afg3 indirectly promotes cytoplasmic mRNA translation, perhaps by ensuring appropriate regulation of mitochondrial mRNA translation. In support of this idea, it has been shown that cleavage of the mitochondrial ribosomal protein Mrpl32 by Afg3 is required for assembly of ribosome particles in the mitochondria [117]. It may be that failure to properly assemble mitochondrial ribosomes or other mitochondria complexes induces a signal from the mitochondria to the cytoplasm to inhibit cytoplasmic mRNA translation. Further support for this idea is provided by the observation that *mrpl32Δ* cells are also slow-growing and long-lived (**Figure 10**). Such a response may be important for preventing an imbalance between nuclear encoded mitochondrial proteins and mitochondrially encoded proteins under conditions where mitochondrial translation is impaired.

A possible alternative explanation for our data is that the inability to carry out mitochondrial respiration directly causes a deficit in mRNA translation due to depletion of ATP needed to synthesize ribosomes and new proteins. We do not favor this model, however, since not all respiratory deficient mutants show growth defects and RLS extension similar to *afg3Δ* cells (**Figure 9**). A second alternative explanation is the possibility that loss of *AFG3* induces yeast cells to lose their mitochondrial DNA (become rho^0), which can reduce growth rate and has previously been shown to extend RLS in some strain backgrounds [133]. We have ruled out this possibility by crossing our long-lived *afg3Δ* haploid to a rho^0 haploid of the opposite mating type and observing that the resulting diploid is able to carry out mitochondrial respiration as evidenced by growth on the non-fermentable carbon source glycerol (**Figure 10**). One prior study reported resistance to oxidative stress and RLS extension in cells lacking the mitochondrial ribosomal protein Afo1 [134]. It is tempting to speculate that the mechanism of RLS extension and stress resistance is similar between deletion of *AFG3* and *AFO1*. Unlike the case for *afg3Δ* cells, however, *afo1Δ* cells were reported to have a normal growth rate (and presumably normal mRNA

translation). Further studies will be needed to establish the precise relationship between Afo1 and Afg3 with respect to longevity, stress resistance, and cytoplasmic mRNA translation.

In addition to RLS, a second type of aging (referred to as chronological aging) is studied in yeast by culturing the cells into stationary phase and monitoring viability over time [74]. Many chronologically long-lived mutants are resistant to multiple forms of stress; however, unlike RLS, the vast majority of respiratory-deficient mutants have reduced chronological life span, likely as a result of an inability to properly enter stationary phase. Consistent with this, *afg3Δ* cells also have reduced chronological lifespan [11].

The Hac1-independent tunicamycin resistance displayed by *afg3Δ* cells can likely be attributed to the profound reduction in cytoplasmic mRNA translation, since *rpl20bΔ* cells showed an even more pronounced tunicamycin-resistance. The mechanism accounting for this phenotype in *rpl20bΔ* and *afg3Δ* cells is not known, but may simply reflect reduced flux of proteins through the ER [130]. Since tunicamycin induces ER stress by inhibiting glycosylation of ER proteins, it may be that simply reducing translation of proteins destined for the ER partially alleviates this stress. Such a model would also explain why the enhanced resistance to tunicamycin does not fully require Hac1 and the ER unfolded protein response. As noted above, however, we cannot rule out the possibility that tunicamycin is inhibiting growth by affecting cellular processes other than ER stress and that reduced mRNA translation is interacting with these additional processes to alleviate the growth-inhibitory effects of tunicamycin.

It is of particular interest that the extension of RLS in *afg3Δ* cells requires Gcn4, similar to ribosomal large subunit deletion mutants such as *rpl20bΔ*. While deletion of either *AFG3* or *RPL20B* results in a similar reduction in overall mRNA translation, the polysome profile of *afg3Δ* cells does not show the profound depletion of 60S ribosomal subunits seen in long-lived ribosomal protein gene deletion strains

[43]. Instead, the polysome profile of *afg3Δ* cells more resembles the general decrease in translation without an imbalance of free 40S and 60S subunits seen in *sch9Δ* cells; however, in the case of *SCH9* deletion the RLS extension is only partially dependent on Gcn4 [43]. The situation is made more complex by the observation that reduced mRNA translation is not always sufficient to extend RLS; for example, small ribosomal subunit protein gene deletions or treatment with the translation inhibitor cycloheximide do not extend RLS [43]. This may suggest that loss of *AFG3* extends life span via a reduction in mRNA translation that mimics the Gcn4-dependent component of RLS extension in *sch9Δ* cells, but not the Gcn4-independent component.

This study demonstrates the utility of stress response profiling as a method for classifying longevity mutants in yeast. The observation that loss of the highly conserved m-AAA protease Afg3 phenocopies the longevity extension, enhanced tunicamycin resistance, and mRNA translation deficit of ribosomal protein deletion mutants suggests a previously unknown mechanism for regulating these processes in response to a mitochondrial signal. It will be of interest to further define the detailed mechanisms linking Afg3 function and cytoplasmic mRNA translation, as well as the specificity of translation-inhibition in *afg3Δ* mother cells, which allows for enhanced longevity. These future studies are likely to provide key insights into the complex nature by which cells sense and respond to mitochondrial stress, and how such responses impact longevity and health.

Experimental Procedures:

Yeast strains

Yeast strains were derived from the *MAT*α ORF deletion collection and are isogenic to the parental BY4742 strain [48,49], with the following exceptions. The *SIR2OX* strain is a tandem two copy *SIR2* strain with a *URA3* marker generated by integration of a second copy of *SIR2* in BY4742 as previously described [135]. With concern for spontaneous suppressors, all ribosomal gene deletions were generated by sporulation from the heterozygous diploid deletion collection and are isogenic to the *MAT*α ORF deletion collection. The *afg3Δ* and mrpl32Δ mutants were remade through homologous recombination of a URA3 marker at the endogenous locus and then backcrossed to BY4741 and sporulated. The *sir2Δ fob1Δ afg3Δ* mutant was generated by homologous recombination of URA3 into a previously described [8] *sir2Δ fob1Δ* strain. The *afg3Δ gcn4Δ* and *afg3Δ hac1Δ* strains were made from standard sporulation and tetrad dissection procedures from the remade *afg3Δ* strain and deletion collection strains. The *rpl20bΔhac1Δ* strain was a gift from K. Steffen, and was made similarly from an *rpl20bΔ::HIS3* marked strain. Full genotypes are included in the strain list in **Table S5**.

Growth rate and viability analysis

Cultures were typically grown at 30°C overnight in a 96 well plate in YPD and then 2.5µl of the overnight culture was inoculated into 147.5µl of culture media (YPD+diluent or YPD+drug) in 100 well Bioscreen plates. Unless otherwise indicated, paraquat was used at a 5mM concentration, tunicamycin at a 1µg/ml concentration, and MMS at a 0.01% concentration.

Yeast growth rates were analyzed in the $OD_{420-580}$ range in the Bioscreen C MBR machine (Growth Curves USA) as previously described using the Yeast Outgrowth Data Analyzer (YODA)[58]. Reported doubling times in 30°C YPD are taken from interval readings from the $OD_{420-580}$ 0.2-0.5 range of maximum growth rate. Inhibition of growth in response to stress was calculated as described above using the formula:

$$GRC_s = \frac{D_s - D_u}{D_u} * 100$$

where D_s is the doubling time of the strain in rich growth medium (YPD) in the presence of the stressor and D_u is the doubling time of the strain in the same medium in the absence of the stressor.

Heat shock survival experiments were performed with 10 minutes of 55°C incubation of overnight cultures grown in 96 well plates and then placed into the Bioscreen analyzer and survival integrals calculated using YODA. While the Bioscreen C MBR machine only measures culture density, we have shown in the past that growth curves can quantitatively assay for cell viability. We utilized the chronological aging features of YODA to calculate the viability of cultures which had undergone heat shock, which we have previously verified as an equally quantitative measure of viability as counts of colony forming units (Murakami and Kaeberlein, 2009; Murakami et al., 2008).

Statistical significance was determined by applying a two tailed student t-test of GRC_s in YPD+drug media compared to wild type in YPD+drug media. Error bars are standard error of the mean (s.e.m.). A minimum of four biological replicate cultures were examined for each condition. Trendlines comparing change in replicative lifespan to stress phenotypes utilized Excel's Analysis ToolPak add-in using the P value generated in the ToolPak's regression analysis.

Cluster analysis

Clustering was performed using the Array Track™ clustering algorithms [129]. Complete linkage analysis using Euclidean distances was used in the settings. Vectors are the $\log_2(V_s)$ value, where the percent difference between the long lived mutant and wild type was calculated (V_s= (GRC_s BY4742-GRC_s mutant)/(GRC_s BY4742)) and then $\log_2$ was taken of this value to mimic microarray style data. Heat maps are shown by taking the minimum values and assigning them the brightest green color and the maximum values as the brightest red color, and black represents a $\log_2(V_s)$=0.

Replicative lifespan analysis

Yeast replicative lifespan assays were performed as previously described [8,60]. In short, virgin daughter cells were isolated from each strain and then allowed to grow into mother cells while their corresponding daughters were microdissected and counted until the mother cell could no longer divide. YEP agar plates (1% yeast extract, 2% bacto-peptone, 2% agar) containing 2% glucose were utilized and strains were grown at 30°C. Statistical significance was determined using the Wilcoxon Rank-Sum test.

Polysome Analysis

Polysome analysis was carried out as described previously [43,136]. Briefly, 125ml of log phase (0.4-0.6 OD, as close to 0.5 OD as possible) yeast were quickly cooled by addition of 60ml frozen YPD containing 133µg/ml cycloheximide to halt translation immediately and prevent ribosomes from dissociating from RNA. Yeast were spun down and then lysed by glass beads and protein-containing fractions were isolated. 20 OD_{260} units were used for each polysome run by adding the lysate to 7-47% sucrose gradients. Gradients were spun for 2 hours at 39k rpm in a Beckmann ultracentrifuge. The resulting gradients were then fractionated and the A_{254} read, resulting in the polysome graphs in **Figure 7a**.

Acknowledgements – We thank K. Steffen for remade ribosomal gene deletion strains and V. MacKay for technical assistance with polysome analysis. This work was supported by NIH Grant R01AG039390 to MK. JRD and GLS were supported by NIH Training Grant T32AG000057. JS was supported by NIH Training Grant T32ES007032. MK is an Ellison Medical Foundation New Scholar in Aging.

Figures:

Figure 1: Growth inhibition of long lived strains in response to tunicamycin.

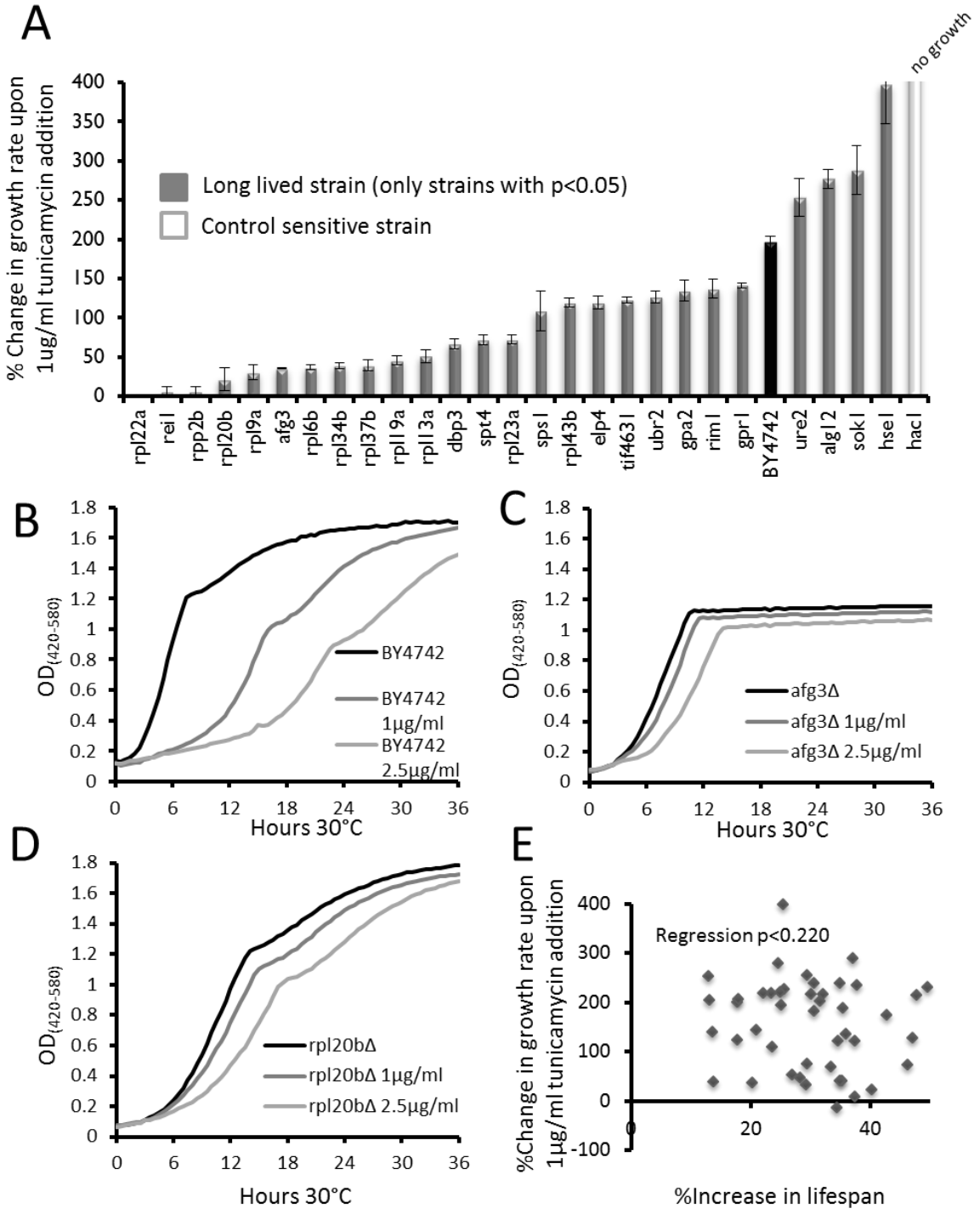

a) Long lived strains which showed significant ($p < 0.05$) changes in relative growth inhibition compared to wild type BY4742 are shown. The control sensitive strain *hac1Δ* did not grow in the media and thus is displayed as an infinite doubling time. Error bars are s.e.m. b-d) Representative outgrowth curves for wild type, *rpl20bΔ*, and *afg3Δ* strains in 0, 1, or 5 μg/mL tunicamycin. e) Scatter plot comparing the percent change in replicative lifespan to percent change in growth rate for each long-lived mutant.

Figure 2: Growth inhibition of long lived strains in response to paraquat.

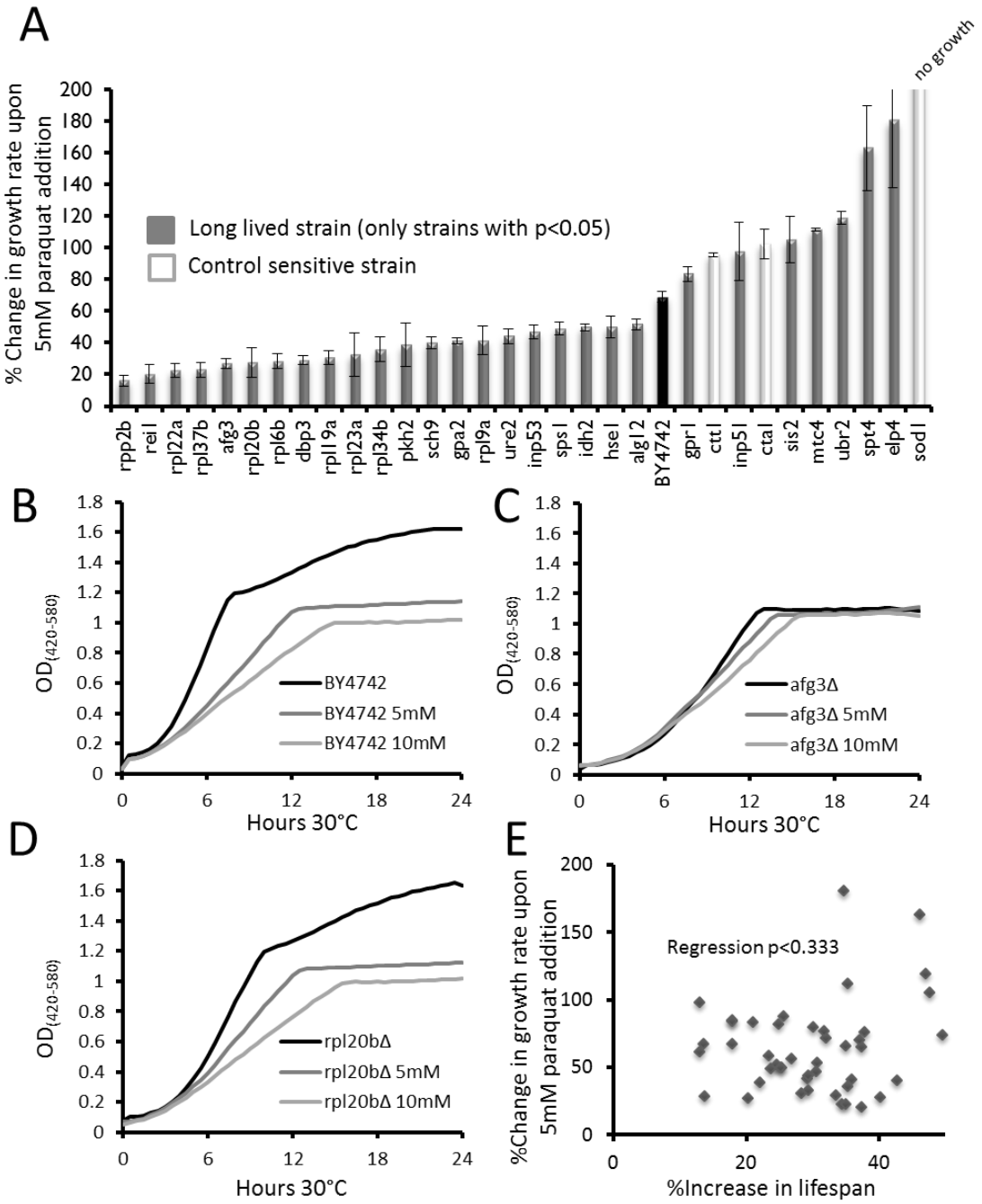

a) Long lived strains which showed significant ($p < 0.05$) changes in relative growth inhibition compared to wild type BY4742 are shown. The control sensitive strains *ctt1Δ,cta1Δ,* and *sod1Δ* are shown for comparison. Error bars are s.e.m. b-d) Representative outgrowth curves for wild type, *rpl20bΔ*, and

afg3Δ strains in 0, 5, or 10 mM paraquat. c) Scatter plot comparing the percent change in replicative lifespan to percent change in growth rate for each long-lived mutant.

Figure 3: Growth inhibition of long lived strains in response to MMS.

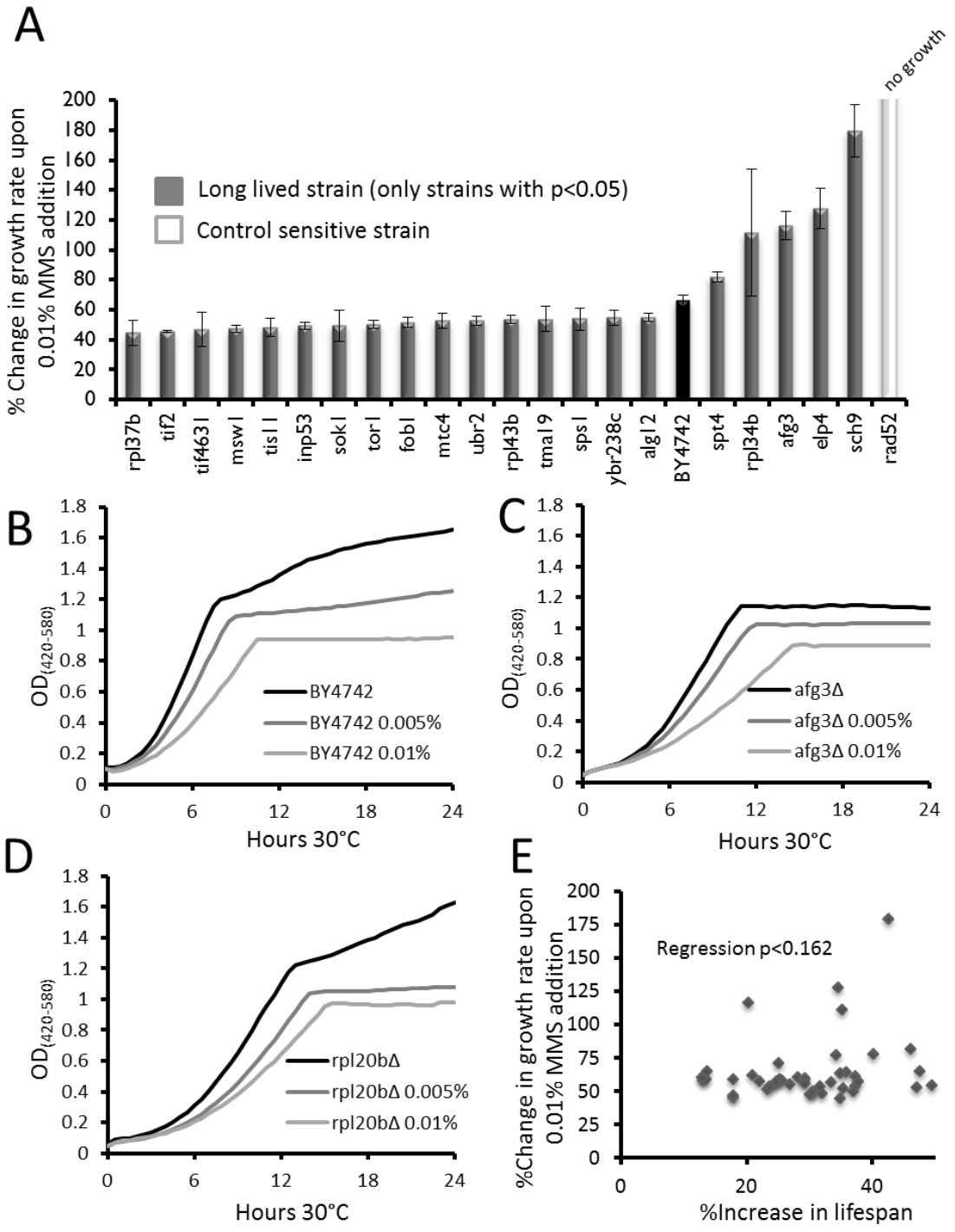

a) Long lived strains which showed significant ($p < 0.05$) changes in relative growth inhibition compared to wild type BY4742 are shown. The control sensitive *rad52Δ* strain is shown for comparison. Error bars

are s.e.m. b-d) Representative outgrowth curves for wild type, *rpl20bΔ*, and *afg3Δ* strains in 0, 0.005%, or 0.01% MMS. c) Scatter plot comparing the percent change in replicative lifespan to percent change in growth rate for each long-lived mutant.

Figure 4: Survival of long-lived strains following transient heat shock.

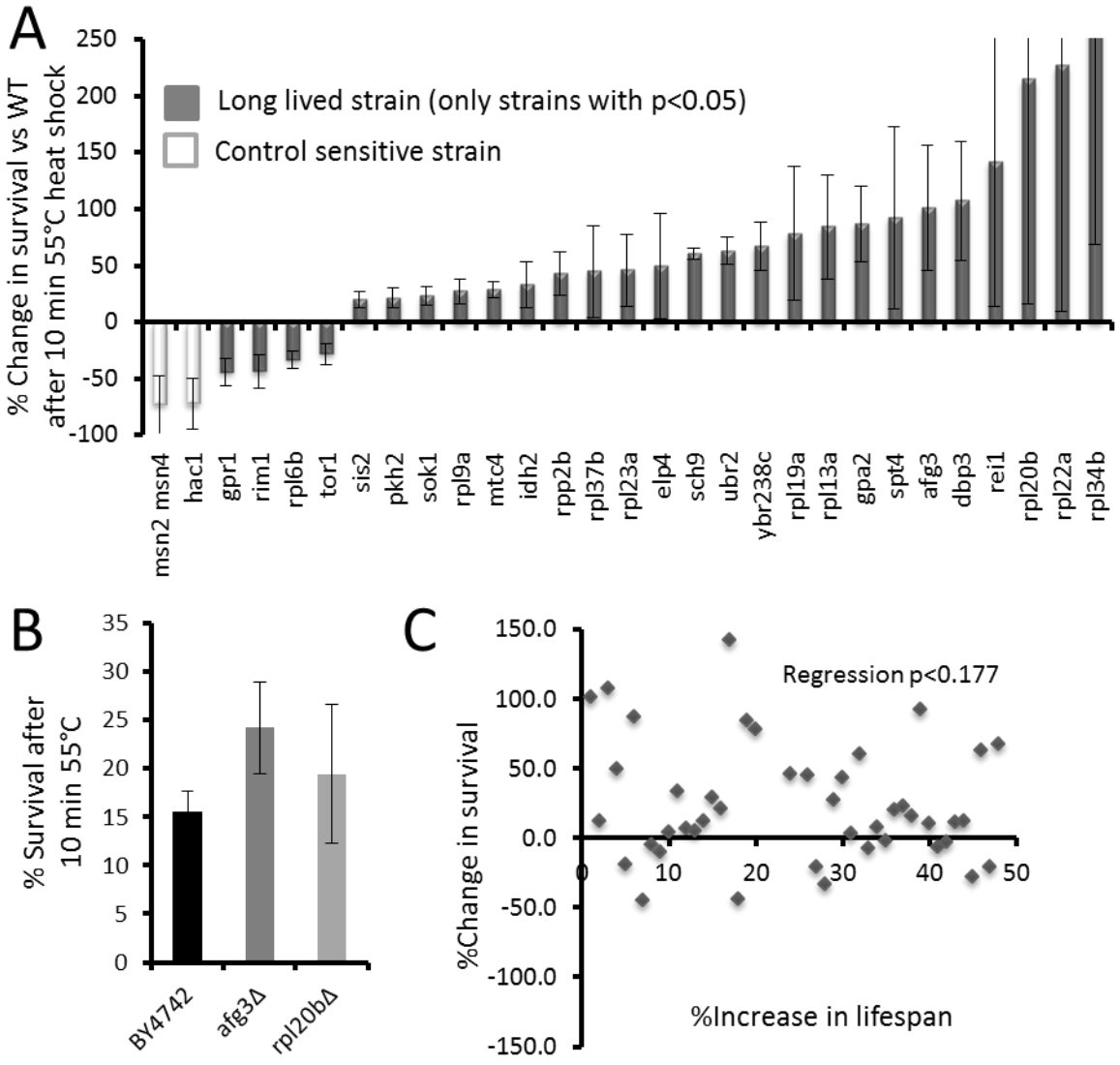

a) Long lived strains which showed significant ($p < 0.05$) changes in relative growth inhibition compared to wild type BY4742 are shown. The control sensitive *msn2Δmsn4Δ* and *hac1Δ* strains are shown for comparison. Error bars are s.e.m. Data for all strains tested can be found in b) Percent survival after

heat shock is shown for wild type BY4742 and long lived strains *rpl20bΔ* and *afg3Δ* cells. c) Scatter plot comparing the percent change in replicative lifespan to percent change in survival for each long-lived mutant.

Figure 5: Clustering of long lived mutants based on their stress response profiles.

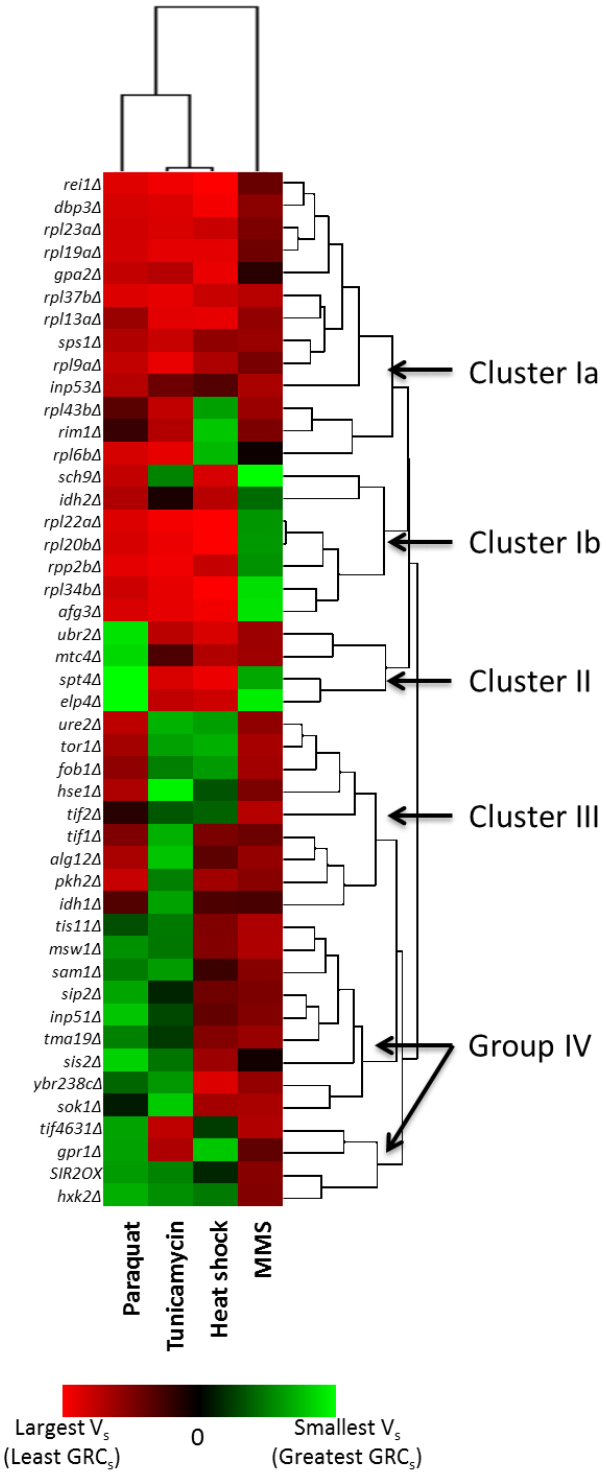

Clusters were formed using Euclidean distance calculations of vectors constructed from the percent difference in sensitivity of a mutant strain compared to wild type, as described in **Methods**.

Figure 6: Hac1-independent resistance to tunicamycin in afg3Δ and rpl20bΔ cells.

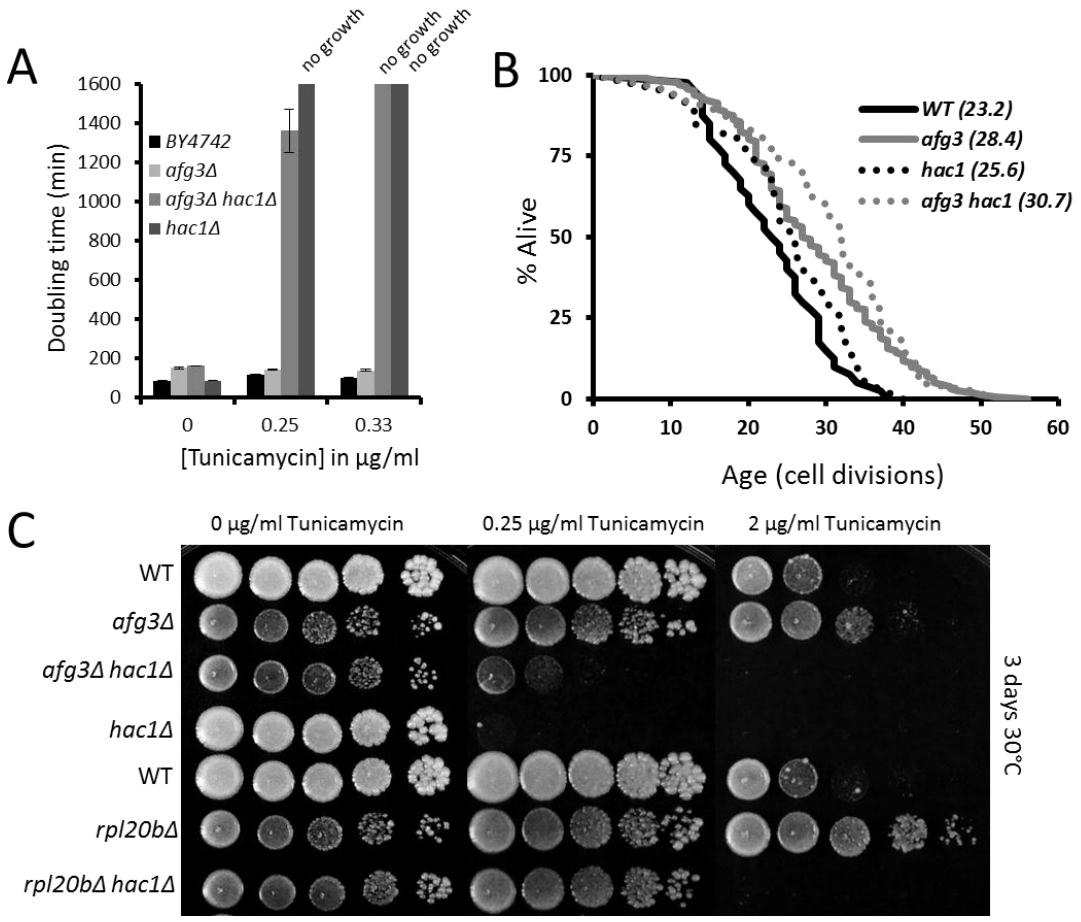

a) Average doubling times for wild type BY4742, *afg3Δ*, *hac1Δ*, and *afg3Δ hac1Δ* strains at the indicated concentrations of tunicamcycin. Note how *afg3Δ hac1Δ* double mutant cells can grow, albeit very slowly, at 0.25µg/ml tunicamycin, while *hac1Δ* cells cannot, indicating Hac1-independent tunicamycin resistance. b) Replicative lifespan curves of the indicated strains. Parentheses denote mean lifespan. *afg3Δ* does not require Hac1 for lifespan extension. c) Spot assays of the indicated strains across tunicamycin concentrations. Spots were diluted 1:10. Panels were grown for 3 days at 30°C.

Figure 7: Deletion of *AFG3* reduces cytoplasmic mRNA translation and extends life span by a Sir2-independent, Gcn4-dependent mechanism.

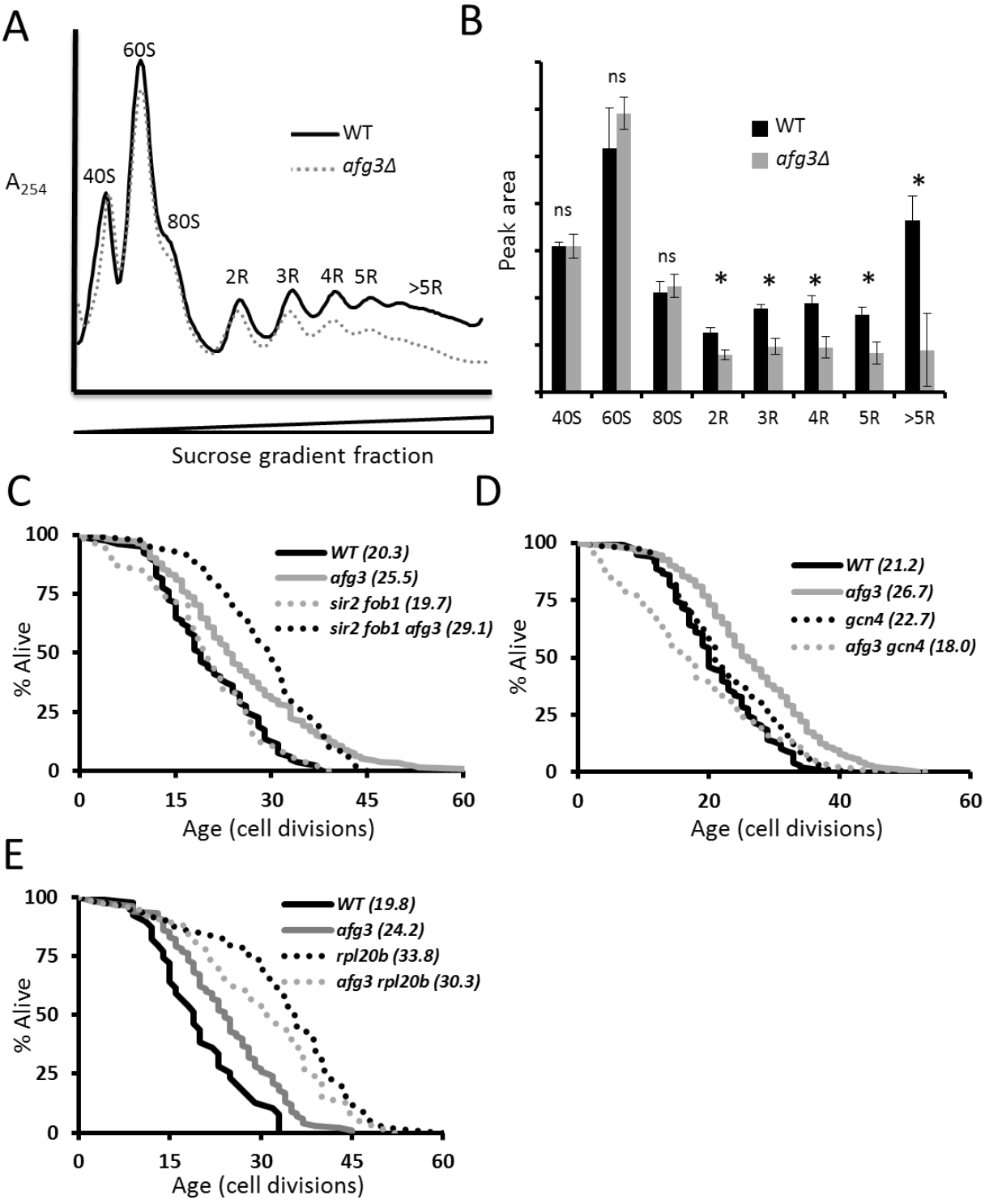

a) Representative polysome profiles of log phase wild type BY4742 yeast and *afg3Δ* mutant yeast grown in YPD at 30°C. Deletion of AFG3 causes a shift of ribosomes from highly translated mRNA to unbound forms. Curves are normalized by the minima between 80S free subunits and 2R disomes. b) Quantitation of peak areas from triplicate polysomes. *$p<0.05$, ns= not significant, error bars are s.e.m. c-e) Replicative lifespan curves of the indicated strains. Parentheses denote mean lifespan. *afg3Δ* requires Gcn4 for lifespan extension but does not require Sir2 or Fob1. *afg3Δ* is not additive with *rpl20bΔ* for lifespan extension.

Figure 8: Replicative lifespan curves of control strains sensitive to the tested stresses. Parentheses denote mean lifespan.

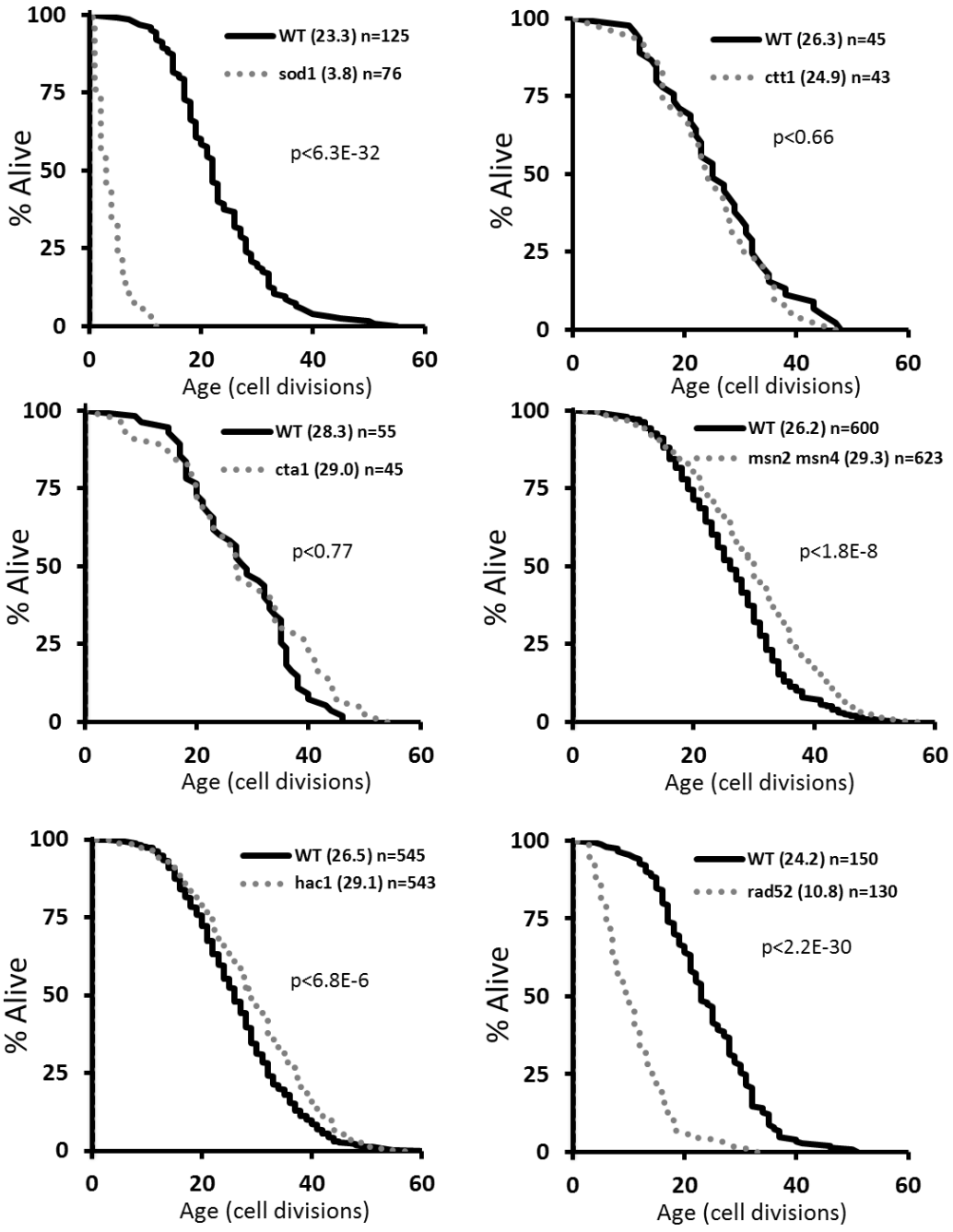

Figure 9: Growth curves and lifespan curves of respiratory dead or deficient strains.

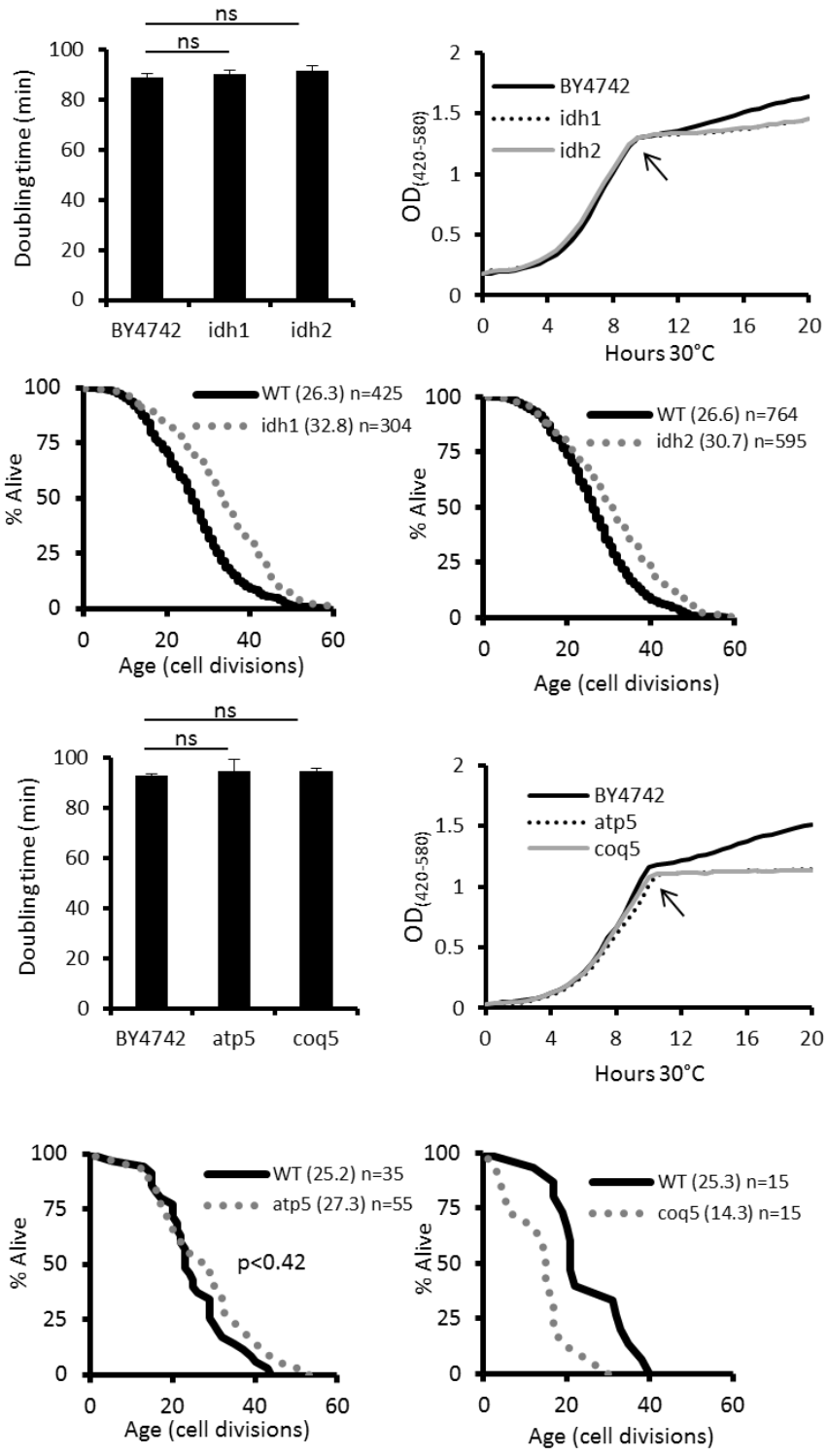

Parentheses denote mean lifespan, arrows indicate when the cultures shift to respiration.

Figure 10: Unsuppressed growth of *afg3Δ*, *yta12Δ*, and *mrpl32Δ* and corresponding lifespan curves.

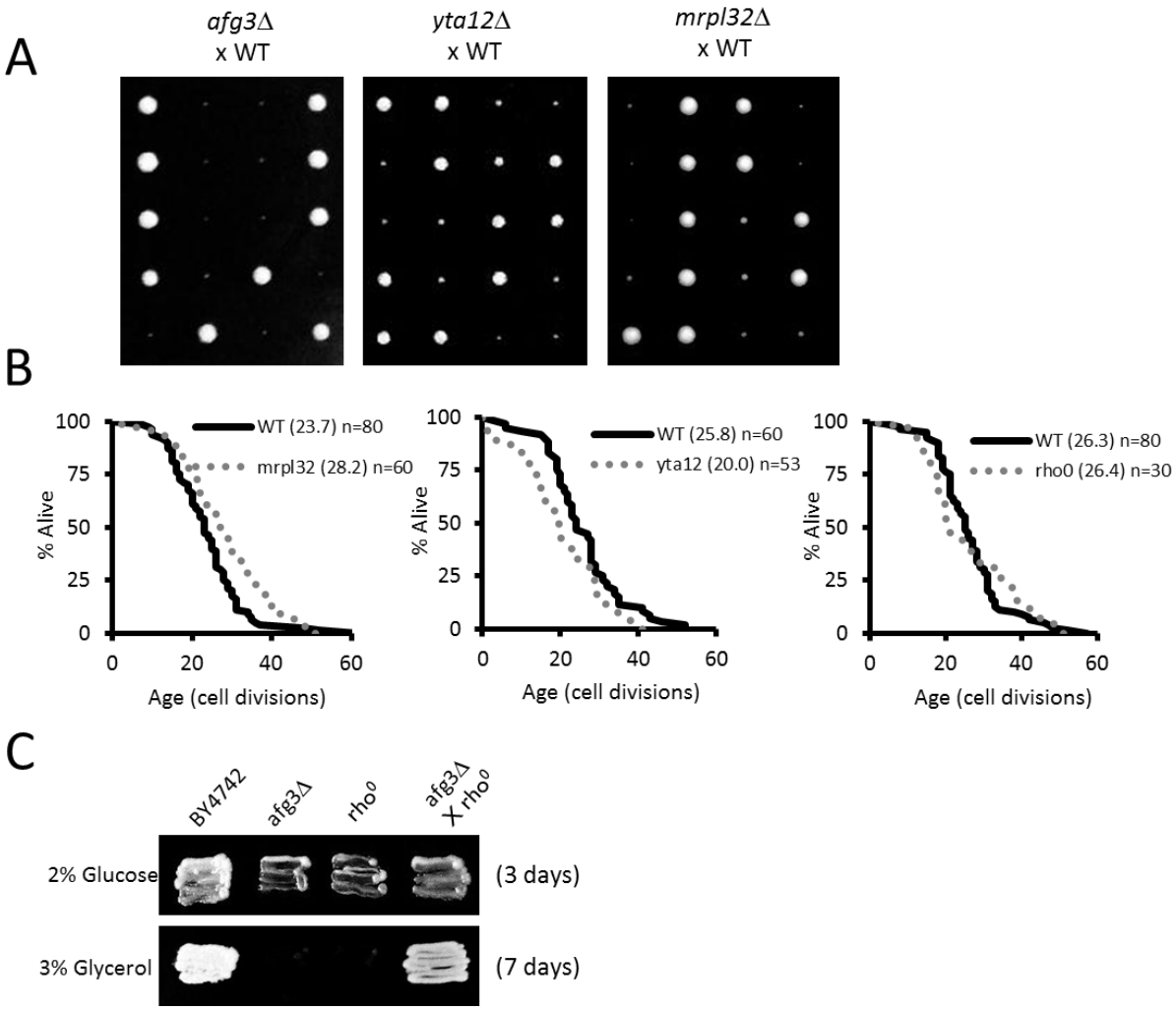

a) Pictures of replica plated tetrads resulting from *afg3Δ*, *yta12Δ*, and *mrpl32Δ* crosses. b) Lifespans of indicated strains. Parentheses denote mean lifespans. c) Patches of yeast grown at 30°C indicate that *rho*^{0} cells can be complemented by *afg3Δ* mutants, indicating *afg3Δ* contains functional mtDNA

Section V: Rad53 and Los1 Mediate Longevity from Dietary Restriction through Gln3

Transitioning introduction:

While it was interesting that Afg3, a mitochondrial protease, could regulate lifespan in a very similar manner as large ribosomal protein subunit deletions, we continued studying other pathways which may regulate dietary restriction mediated lifespan extension. We were delighted to find that nuclear tRNA regulation was central to the longevity process, and that it could regulate lifespan independent of translation. We found that the ATR pathway, a DNA damage response pathway, was tightly integrated in this response, and that the nitrogen catabolite repression transcription factor Gln3 was downstream of nuclear tRNA signaling. The findings were incredibly novel, undeniably consistent, and remarkable in the magnitude of their effects. So this dissertation concludes in the discussion of these findings.

The following section is based on a publication submitted to Nature.

Abstract:

Dietary restriction (DR) is the best-characterized intervention for slowing aging in organisms from yeast to mammals. Here we describe roles for the tRNA exporter Los1 and the DNA damage response factor Rad53 in yeast replicative lifespan (RLS) extension from DR. DR caused Los1 to become depleted from the nucleus in a Rad53-dependent manner. Deletion of *LOS1* or overexpression of *RAD53* was sufficient to extend RLS. Deletion of *LOS1* had no detectable effect on global mRNA translation, but instead resulted in activation of the nitrogen responsive transcription factor Gln3. Gln3 was required by for lifespan extension from DR, and overexpression of Gln3 extended RLS by approximately 50% under non-restricted conditions. These findings further define the mechanistic basis for lifespan extension from

DR in yeast and demonstrate new functions for Los1, Rad53, and Gln3 as key mediators of the response to DR.

Introduction:

Aging is a complex process, even in one of the simplest model eukaryotes, the budding yeast *Saccharomyces cerevisiae*. Aging in yeast can be studied by determining the RLS of a mother cell, defined as the number of daughters the cell produces prior to irreversible arrest[19]. At least three types of molecular damage are asymmetrically retained in the yeast mother cell during cell division and have been proposed to contribute to replicative aging in yeast: nuclear extrachromosomal rDNA circles (ERCs), cytoplasmic protein aggregates, and degenerate mitochondria[19]. Several genetic pathways that modulate RLS also modulate aging in multicellular eukaryotes, suggesting that aspects of cellular aging have been conserved across broad evolutionary distances. Most notably, inhibition of the target of rapamycin (TOR) kinase extends lifespan in yeast, worms, fruit flies, and mice[137,138].

Dietary restriction (DR), defined as a reduction in nutrient availability without malnutrition, has been reported to slow aging in many different species, including yeast, worms, flies, mice, rats, and rhesus monkeys[139]. One method of DR in yeast is accomplished by reducing the glucose present in the medium from 2% to 0.05%[8]. In yeast, as in other organisms, lifespan extension from DR is thought to be mediated, at least in part, through inhibition of TOR signaling[137,138]. Evidence for this model in yeast includes observations that DR is sufficient to reduce TOR activity, mutations in the gene encoding the TOR kinase, *TOR1*, extend lifespan under control but not DR conditions, and both DR and *tor1*Δ further increase the RLS of cells with low levels of ERCs from deletion of the gene encoding the replication fork block protein *FOB1*[8,41].

Results:

From an ongoing, unbiased screen of the yeast ORF deletion collection, we found that deletion of the *LOS1* gene resulted in a significant increase in RLS ($p<0.001$, **Fig. 1a**). *LOS1* encodes a homolog of human exportin-t that mediates nuclear export of tRNA[140]. In yeast, pre-tRNA is transcribed in the nucleus and must be exported to the cytoplasm in order to be processed into mature uncharged tRNA[141]. The mature, uncharged tRNA is then reimported into the nucleus by Mtr10 and other tRNA import factors[21]. Within the nucleus, tRNA synthetases attach the cognate amino acids, at which point Los1 then functions to re-export charged tRNAs from the nucleus to the cytoplasm, allowing for mRNA translation at the ribosome[22]. The fact that *los1*Δ cells are viable, and indeed long-lived, suggests that additional factors must also participate in export of tRNA from the nucleus. Los1 clearly plays a primary role in this process, however, as evidenced by the fact that *los1*Δ cells show a significant increase in accumulation of tRNA within the nucleus[140]. Los1 also plays an important role in regulating nuclear accumulation of tRNA in response to environmental stress; reduction of amino acid availability or DNA damage causes Los1 to relocalize from the nucleus to the cytoplasm, resulting in accumulation of tRNA in the nucleus[142,143].

DR and Los1 similarly modulate RLS

We first set out to determine whether deletion of *LOS1* increases RLS by a mechanism similar to DR. Using a strain expressing a GFP-fusion to Los1, we found that DR decreased the relative amount of Los1-GFP present in the nucleus compared to Los1 in the cytoplasm ($p<0.001$, **Fig. 1b**). These data indicate that Los1 localization is regulated by DR. Prior studies have shown that DR fails to increase the RLS of *sir2*Δ single mutant cells lacking the Sir2 histone deacetylase, but robustly increases RLS of *sir2*Δ *fob1*Δ double mutant cells[8,61]. Like DR, deletion of *LOS1* does not increase the RLS of *sir2*Δ cells ($p=0.07$), but significantly increases the RLS of *sir2*Δ *fob1*Δ cells ($p<0.001$, **Fig. 1c,d**). DR failed to further extend the RLS of *sir2*Δ *fob1*Δ *los1*Δ cells ($p=0.3$, **Fig. 1d**), supporting the model that Los1 and DR modulate

longevity by a similar mechanism. Two genetic mimetics of DR, deletion of *TOR1* or deletion of the yeast S6 kinase/Akt homolog, *SCH9*, also failed to further increase RLS in *los1*Δ mother cells (p=0.1, 0.5, respectively, **Fig. 1e,f**).

Mtr10 is a nuclear import receptor involved in retrograde transport of tRNAs from the cytoplasm back into the nucleus[144]. As a further test of the importance of nuclear sequestration of tRNA in RLS and DR, we examined the effect of *MTR10* deletion or overexpression on lifespan. Overexpression of *MTR10* under its native promoter from a low copy plasmid significantly increased RLS relative to a control plasmid containing the same sequence but lacking *MTR10* (p<0.001, **Fig. 1g**). Deletion of *MTR10* also prevented RLS extension from DR (p=0.9, **Fig. 1h**). Taken together, these data indicate that altering tRNA transport protein levels to favor accumulation of nuclear tRNA is sufficient to extend RLS and support a model in which nuclear sequestration of tRNA via regulation of Los1 localization is one mechanism by which DR slows aging in yeast.

Rad53, Tor1 regulate Los1 Localization

Rad53 is a conserved DNA response factor downstream of ATR that also functions to regulate nuclear tRNA[143,145]. In response to DNA damage, Rad53 signaling causes Los1 to be exported to the cytoplasm, resulting in sequestration of tRNA in the nucleus[143]. We therefore wondered whether Rad53 might also be important for regulating Los1 localization in response to DR. Utilizing the Los1-GFP strain, we observed that relocalization of Los1 to the nucleus in response to DR was prevented in cells lacking *RAD53* (p=0.1, **Fig 2a**). Deletion of *RAD53* also prevented RLS extension from DR, even in the DR sensitized *fob1*Δ background (p=0.3), but did not prevent RLS extension from deletion of *LOS1* (p<0.001), consistent with the model that Rad53 acts between DR and Los1 to modulate RLS (**Fig. 2b,c**). Importantly, overexpression of *RAD53* was also sufficient to extend RLS, comparable to the effect of *MTR10* overexpression or *LOS1* deletion (p<0.001, **Fig. 2d**).

Since reduced TOR signaling is believed to play a key role in mediating RLS extension from DR[41], we wished to place TOR genetically within the longevity pathway containing DR, Los1, and Rad53. Rad53 is not required for deletion of *TOR1* to extend RLS ($p=0.005$, **Fig. 2e**), suggesting *tor1*Δ acts independently of Rad53. Interestingly, Los1-GFP is enriched in the cytoplasm in a *tor1*Δ mutant under nutrient rich conditions, albeit to a lesser extent than in wild type cells subjected to DR ($p<0.001$, **Fig. 2f**). Unlike DR, however, cytoplasmic localization of Los1-GFP in *tor1*Δ cells does not require Rad53 ($p<0.001$). Rapamycin, a well established inhibitor of the TOR complex[146], also causes Los1-GFP to become enriched in the cytoplasm in a Rad53-independent manner ($p<0.001$).

Since Rad53 was required for the translocation of Los1 by DR, we tested if DR could affect Rad53 directly. We examined the effect of DR or deletion of *TOR1* on Rad53 abundance and localization by utilizing a strain expressing a Rad53-GFP fusion protein under the control of the *RAD53* promoter. As expected, total Rad53-GFP abundance and the proportion of Rad53 in the nucleus was increased by treatment with methyl methane sulfonate (MMS) ($p<0.001$, **Fig. 2g**). DR had a similar effect on Rad53 nuclear abundance ($p<0.001$). Deletion of either *TOR1* or *LOS1*, in contrast, did not change levels of nuclear Rad53-GFP ($p=0.9$, $p=0.3$, respectively). These data suggest that both *TOR1* and *RAD53* act in parallel downstream of DR to regulate Los1 and RLS.

*los1*Δ *affects RLS, not translation*

We next considered the possibility that nuclear sequestration of tRNA in *los1*Δ cells might increase RLS by impairing global mRNA translation, which has been associated with longevity in yeast and other organisms [54]. Surprisingly, deletion of *LOS1* had no detectable effect on mRNA translation, as measured by maximal doubling time, colony growth rates, polysome analysis, and cell cycle progression (**Fig. 3a-d)**. Experiments using a long-lived, slow growing *afg3*Δ mutant are shown for comparison[23]. These data

suggest that a pool of charged tRNA sufficient to support rapid growth must remain in *los1*Δ cells, and that deletion of *LOS1* induces a longevity signal distinct from mRNA translation.

To find the potential signal, we utilized microarray analysis to compare the gene expression profiles of wild type and *los1*Δ cells under non-restricted conditions. From this study, 60 genes were expressed more highly in *los1*Δ cells, and 31 showed reduced expression. Gene ontology analysis indicated that a majority of the *LOS1* regulated mRNAs encoded proteins involved in amino acid biosynthesis and nitrogen metabolism**.** Of the 60 genes upregulated in *los1*Δ cells, 88% are known targets of the Gcn4 transcription factor as annotated on Yeastract[147] (**Fig. 3e**), supporting the idea that Gcn4 is activated by loss of Los1.

We have previously reported that activation of Gcn4 plays a key role in mediating RLS extension in mutants with reduced mRNA translation resulting from deficiency for the large (60S) ribosomal subunit[43]. For example, deletion of Gcn4 completely blocks lifespan extension in cells lacking the ribosomal large subunit protein Rpl20b; however, deletion of Gcn4 only partially prevents lifespan extension from deletion of *TOR1* or in response to DR[43]. We have interpreted this to imply that Gcn4 is one factor important for lifespan extension from DR or inhibition of TOR, but that additional factors must also act to mediate lifespan extension in these cases. Consistent with this interpretation, we find that deletion of *GCN4* does not significantly reduce the long RLS of *los1*Δcells (p=0.1), although lifespan appears to be partially suppressed (**Fig. 3f**).

Gln3 promotes longevity in yeast

In addition to enrichment for Gcn4 target genes, analysis of our microarray data indicated that 13 (22%) of the *los1*Δ upregulated mRNAs are also co-regulated by Gln3, the primary transcription factor involved in promoting expression of genes repressed by nitrogen catabolite repression (NCR)[148]. Increased

expression of all 13 of these Gln3-target genes following deletion of *LOS1* was confirmed by RT-qPCR (**Fig. 3g,h**). Gln3 and NCR have not been previously associated with Los1 or sequestration of nuclear tRNA.

Our observation that deletion of *LOS1* induces Gln3 target genes, combined with the prior data placing TOR as a regulator of Gln3[149,150], suggested the hypothesis that Gln3 might serve as a primary factor upon which DR, TOR signaling, and Los1 converge to influence RLS. Consistent with this hypothesis, the abundance of GFP-tagged Gln3 was increased by DR, deletion of *LOS1*, or deletion of *TOR1* (**Fig. 4a**), as was the ratio of nuclear Gln3 to cytoplasmic Gln3. Further support for this model is provided by the observation that deletion of Gln3 prevents RLS extension from deletion of *TOR1* (p=0.3, **Fig. 4b**) and in response to DR, even in the DR-sensitized *sir2*Δ *fob1*Δ background (p=0.3, **Fig. 4c**). Ure2 is a negative regulator of Gln3 that binds to Gln3 preferentially after phosphorylation of Gln3 by TOR and retains it in the cytoplasm[149]. Deletion of *URE2* also increased RLS (p<0.001, **Fig. 4d**) and enhanced nuclear abundance of Gln3, further suggesting that enhanced Gln3 activity may extend RLS. To test this directly, we overexpressed Gln3 and observed a striking 50% increase in RLS (p<0.001, **Fig. 4e**).

In contrast to deletion of *TOR1*, deletion of *GLN3* did not completely block RLS extension from deletion of *LOS1* (p<0.001, **Fig. 4f**). Based on this observation, along with the microarray data, we considered the possibility that *GCN4* and *GLN3* might act redundantly to increase RLS following loss of Los1. Unexpectedly, the *gln3*Δ *gcn4*Δ double mutant had a significantly reduced RLS, relative to wild type or either single mutant (p<0.001 in each case, **Fig. 4f**). In this double mutant background RLS extension from deletion of *LOS1* was completely suppressed, supporting the idea that both transcription factors can act redundantly to promote RLS extension in *los1*Δ cells.

DNA repair has been suggested to play an important role in aging based, in part, on apparent premature aging resulting from deficiencies in DNA repair enzymes[151-153]. Our data demonstrate that increased

expression of the Rad53 DNA damage sensor is sufficient to extend RLS (**Fig. 2d**) and suggest that Rad53 plays an important role mediating the pro-longevity effects of DR. As a further test of this relationship, we examined whether additional components of this pathway, including Gln3, also play a role in protection against DNA damage. Relative to wild type cells, deletion of *TOR1* or *LOS1* or overexpression of *MTR10*, *RAD53*, or G*LN3* all significantly enhanced resistance to the DNA alkylating agent MMS (**Fig. 5a**). Deletion of either *TOR1* or *LOS1* partially rescued the MMS sensitivity of *rad53*Δ cells (**Fig. 5b**), mirroring their effects on RLS. These data suggest an unexpected mechanistic link between the Rad53 DNA damage response and DR, likely involving nuclear sequestration of tRNA. Given the highly conserved nature of these factors, it will be of interest to determine the relevance of this pathway for mammalian aging.

Discussion:

The data presented above allow us to propose a comprehensive model for DR in yeast that has previously been elusive (**Fig 5c**). By this model, Gln3 is the primary factor acting downstream of DR to extend RLS, and deletion of either *LOS1* or *TOR1* mimic the pro-longevity response from DR by causing Gln3 to become activated. Loss of *TOR1* frees Gln3 from being retained in the cytoplasm by Ure2, as previously described[149]. The precise mechanism by which deletion of *LOS1* activates Gcn3 will be important to determine in future studies, but may involve nuclear activation of Gln3, perhaps by a mechanism akin to Gcn4 activation by tRNA-bound Gcn2. This model explains the previously perplexing observation that Gcn4 was completely required for RLS extension in the case of long-lived 60S ribosomal protein deletions, but only partially required for RLS extension from DR or deletion of *TOR1*[43]. DR and *TOR1* deletion may moderately activate Gcn4 relative to 60S ribosomal protein deletions[43]; however, the fact that only Gln3 and not Gcn4 is required for RLS extension in these cases clearly suggests that Gln3 is the key downstream factor in this branch of the pathway.

Methods:

Yeast strains:

The background strain for all experiments was BY4742 unless otherwise indicated. The strain list with full genotype and frozen stocks are included in Supplemental Table 4. Prototrophic deletions were made using homologous recombination following amplification of the marker from pRS303, pRS305, or pRS306. All deletions, plasmids, and spore clones were verified by PCR or sequencing prior to analysis. Over expression plasmids were taken from the Princeton pMoBY collection[154] as a generous gift from Maitreya Dunham. GFP genomically tagged strains were generated by backcrossing from the collection[155]; initial strains were a gift from Stan Fields.

Replicative lifespans:

Yeast replicative lifespan assays were performed as previously described[8,156]. In short, virgin daughter cells were isolated from each strain and then allowed to grow into mother cells while their corresponding daughters were microdissected and counted until the mother cell could no longer divide. In any plasmid containing lifespan, we assured cells began their lifespan with a plasmid by patching onto selective plates prior to analysis, and performed lifespans on mother cells transferred directly from the selective media to YEPD lifespan plates. YEP agar plates (1% yeast extract, 2% bacto-peptone, 2% agar) containing 2% glucose were utilized and strains were grown at 30°C. The control plasmid alone slightly shortened RLS, as previously reported[157]. However, in a series of control experiments we confirmed that the well-established RLS extension from *SIR2* overexpression is maintained using this system while overexpression of other genes (e.g. *MSN4*) does not extend RLS, and that plasmid loss from the mother cell is equal between plasmids (**Fig. S1a,b, c**). Statistical significance was determined using the Wilcoxon Rank-Sum test.

Fluorescence microscopy:

Cells were grown to log phase by dilute streaking on SC-HIS plates (to select for GFP+ cells) 16 hours prior to analysis. Cells were resuspended in 30µl SC media containing 1µM DAPI and 2.5µl of the cell suspension were used in a Teflon printed slide 6mm well. Pictures were taken using a Zeiss Axiovert 200M fluorescence microscope using AxioVision 4.8 software. Images were analysed on AxioVision and GFP pixels overlapping strong, nuclear DAPI signals were chosen to measure pixel intensity for nuclear GFP, and a non-vacuolar (and extra-nuclear) GFP pixel was chosen as a cytosolic measurement. A pixel nearby the cell was chosen to subtract background from all measurements. Pictures were analyzed in sets of 20 cells and the results were pooled for statistical analysis, with the pooled statistics shown in **Table S6**. Statistics were performed by comparing individual cell fluorescence ratios by student's t-test.

Flow cytometry:

For cell cycle analysis, samples were prepared following a protocol previously described[23]. GFP quantitation by flow cytometry was performed on live cells prepared as in microscopy experiments, except instead of resuspending cells in SC media with DAPI, they were resuspended in ice water and immediately run through the flow cytometer. GFP intensity values were calculated as mean raw GFP intensity subtracted by GFP auto fluorescence of isogenic cells grown under identical conditions. All values were also normalized to relative cell size, as measured by forward scatter. Fold changes were normalized to normal 2% glucose growth conditions of WT (but GFP tagged) cells as an intensity of "1". Values were compared by student's t-test for statistical analysis. At least 20,000 cells were counted on multiple, independent days. FCS Express was used for flow cytometry data analysis. Strains in Fig. 5b,c were in the BY4741 background.

Growth curves:

Cultures were grown at 30°C overnight in a 96 well plate in YPD and then 2.5µl of the overnight culture was inoculated into 147.5µl of culture media in 100 well Bioscreen plates. Yeast growth rates were analyzed in the $OD_{420-580}$ range in the Bioscreen C MBR machine (Growth Curves USA) as previously described using the Yeast Outgrowth Data Analyzer (YODA)[104].

Polysome profiles:

Polysome analysis was carried out as described previously[43,136]. Briefly, 125ml of log phase (0.4-0.6 OD, as close to 0.5 OD as possible) yeast were quickly cooled by addition of 60ml frozen YPD containing 133µg/ml cycloheximide to halt translation immediately and prevent ribosomes from dissociating from RNA. Yeast were spun down and then lysed by glass beads and protein-containing fractions were isolated. 20 OD260 units were used for each polysome run by adding the lysate to 7-47% sucrose gradients. Gradients were spun for 2 hours at 39k rpm in a Beckmann ultracentrifuge. The resulting gradients were then fractionated and the A254 read, resulting in the polysome graphs in Fig. 3C.

Microarrays:

Wild type and *los1*Δ cells were inoculated in 5ml YEPD overnight culture. Three isolates of each strain were tested, with six cultures (duplicates) for wild type cells and three cultures for *los1*Δ cells. Overnight cultures were then diluted to <0.05 OD_{600} in 50ml YEPD and shaken at 225 rpm at 30°C until exactly 0.5 OD_{600} was reached. The entire cuture was then transferred to conical tubes and centrifuged at 4°C for 2 minutes at 3000g in a counter top centrifuge. Supernatant was removed and resuspended in 1 ml ice cold Martin Lysis buffer (40mM KCl, 7.5 mM $MgCl_2$, 1 mM DTT, 25 mM Tris-HCl pH7.5, 0.5 mg/ml heparin, 100µg/ml cycloheximide, in ddH_2O). Suspensions were transferred to microfuge tubes containing 0.4g glass beads (Sigma) and vortexed for 30 seconds, 8 times with 30 seconds on ice between vortex steps. 10µl of 20% triton X-100 and 10µl 20% Na deoxycholate were added to each tube and

vortexed for 15 seconds. Lysate was cleared of debris by centrifugation at 17k g in a microcentrifuge at 4°C for 2 minutes. Cleared lysate was then treated by the RNeasy Qiagen RNA prep following the manufacturer's protocol. Integrity of RNA samples was assessed with an Agilent 2100 Bioanalyzer. The Affymetrix 3'-IVT Express Kit was used to process the samples using 100 ng total RNA starting material. Manufacturer protocols were used to process Affymetrix GeneChip Yeast Genome 2.0 Arrays (Santa Clara, CA). Hybridized arrays were scanned with an Affymetrix GeneChip® 3000 scanner. Image generation and feature extraction were performed using the Affymetrix Gene Chip Command Console (AGCC) software.

Raw microarray data was processed and analyzed with Bioconductor (http://www.bioconductor.org/). The data were normalized with the Bioconductor oligo package [158]. From the normalized data, genes with significant evidence for differential expression were identified using the Bioconductor limma package[159]. P-values were calculated with a modified t-test in conjunction with an empirical Bayes method to moderate the standard errors of the estimated log-fold changes. P-values were adjusted for multiplicity with the Bioconductor package qvalue[160], which allows for selecting statistically significant genes while controlling the estimated false discovery rate. The microarray data were deposited in the GEO public database, GEO accession number GSE37241.

To check expression by RT-qPCR, cells and RNA were harvested as in the microarray preparations. Superscript III (Invitrogen) reverse transcriptase was used according to manufacturer specifications to synthesize cDNA. SYBR Green (Invitrogen) was used to assay the qPCR steps also according to manufacturer specifications. A Roto-Gene 3000 (Corbett Research) was used to perform the reaction steps and default automated analysis was utilized to calculate Ct values. A single unit difference in Ct was defined as a two fold change, and fold changes were based on subtracting the Ct values for the housekeeping gene (*PRP8*) to equalize loading between genotypes. At least triplicate runs were performed and mean values are represented on Figure 3F. Primers used are listed in Table S5.

DNA damage resistance assays:

Cells were grown overnight at 30°C in 150µl YEPD (or in 150µl SC-URA if containing a pMoBY plasmid) in 96 well plates before serial dilution to ~300 colonies per plate during colony forming unit (CFU) analysis. Plates without MMS were used to measure 100% viability CFU counts and plates containing 0.01% or 0.001% MMS were used to gather CFU counts to compare to untreated plates to yield a % viable count. At least two independent experiments were performed. Percent viable counts were used for statistical analysis via student's t-test.

Figures:

Figure 1: Regulators of nuclear tRNA import and export influence lifespan.

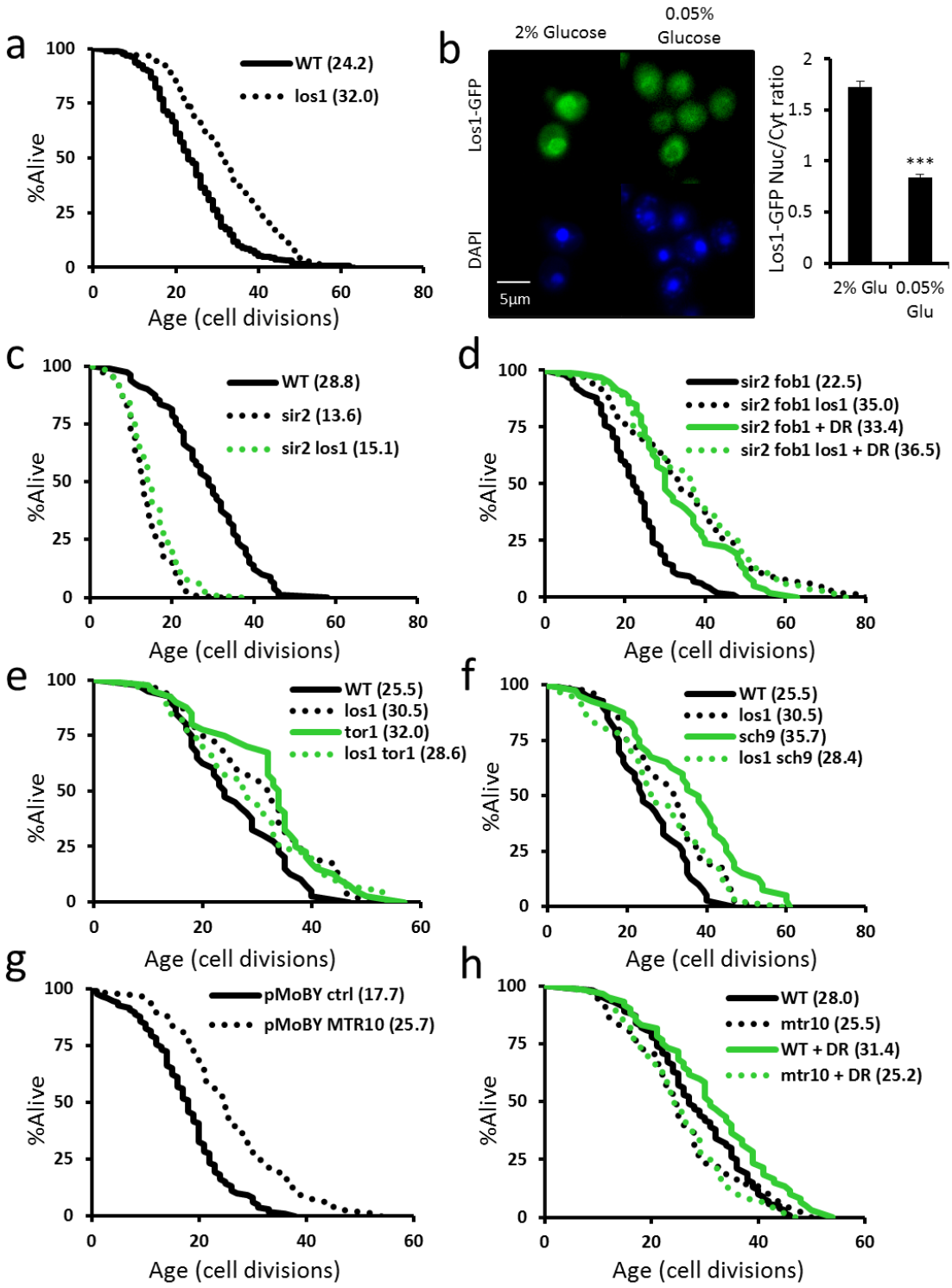

a, Deletion of the nuclear tRNA exporter gene *LOS1* extends RLS **b**, Fluorescence microscopy reveals that DR (0.05% glucose) reduces nuclear Los1-GFP ***p<0.001. **c-f**, Replicative lifespan analysis indicates that deletion of LOS1 acts similarly to DR. Deletion of *LOS1* fails to extend RLS of *sir2*Δ cells, but robustly extends RLS of *sir2*Δ*fob1*Δ cells. Deletion of *LOS1* does not increase RLS additively with DR or with genetic mimics of DR (*tor1*Δ and *sch9*Δ). **g,** Overexpression of the nuclear tRNA importer *MTR10*, which functions antagonistically to *LOS1*, extends RLS, and **h,** deletion of *MTR10* blocks RLS extension from DR. All RLS statistics are provided in Table S1 and microscopy statistics in Table S6.

Figure 2: Rad53 acts between DR and Los1

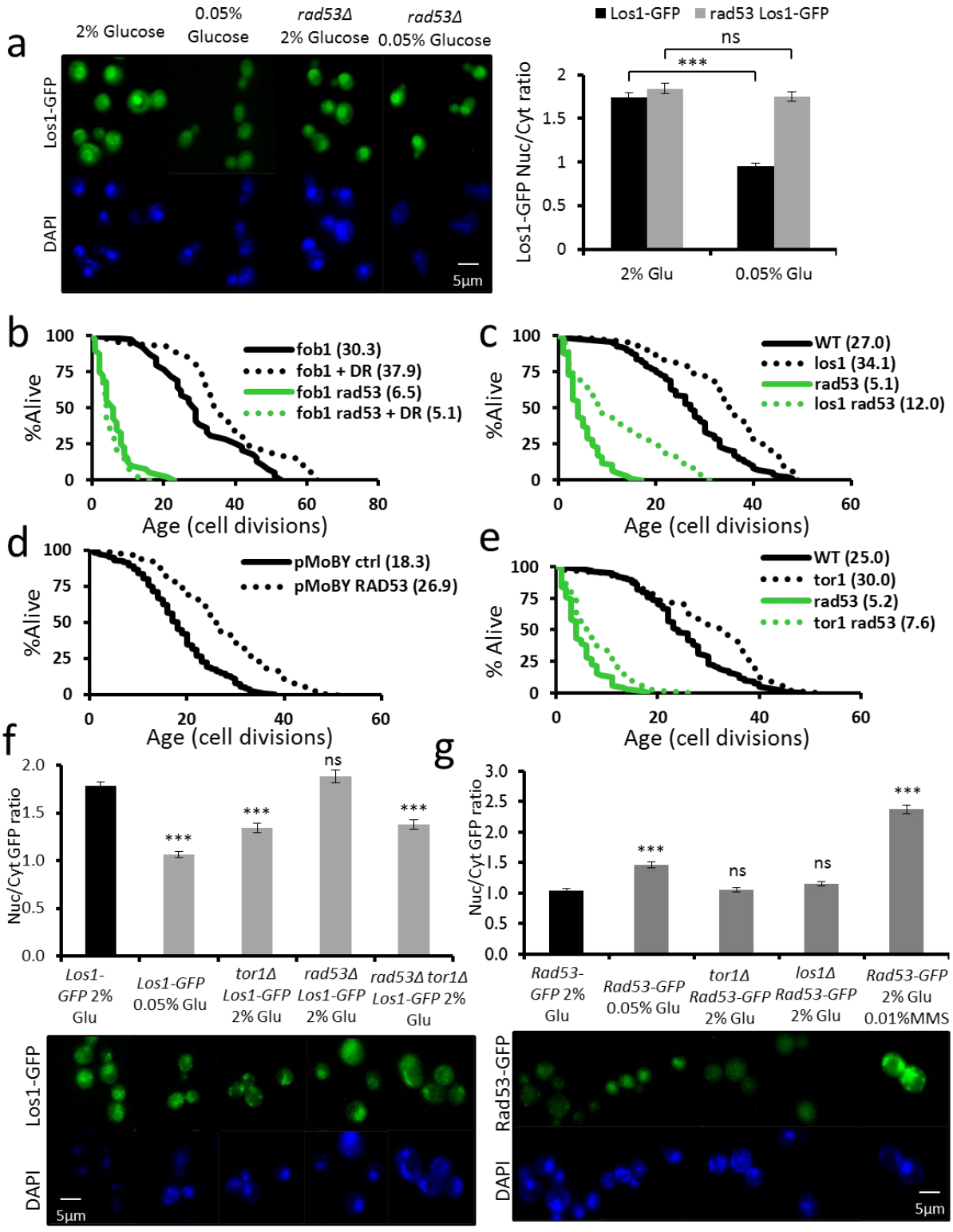

a, Fluorescence microscopy indicates that Rad53 is required for nuclear exclusion of Los1-GFP in response to DR. **b-c**, Replicative lifespan analysis demonstrates that Rad53 is required for RLS extension from DR, but not from deletion of *LOS1*. **d,** Overexpression of *RAD53* extends RLS. **e,** Rad53 is not required for RLS extension from deletion of *TOR1*. **f,** Fluorescence microscopy indicates that Rad53 is not required for nuclear exclusion of Los1-GFP in response to deletion of *TOR1*. **g**,GFP-tagged Rad53 is enriched in the nucleus by DR but not by deletion of *TOR1* or *LOS1*. All RLS statistics are provided in Table S1 and microscopy statistics in Table S6. ***$p<0.001$, ns indicates $p>0.05$.

Figure 3: Deletion of *LOS1* activates *GLN3* without reducing global mRNA translation.

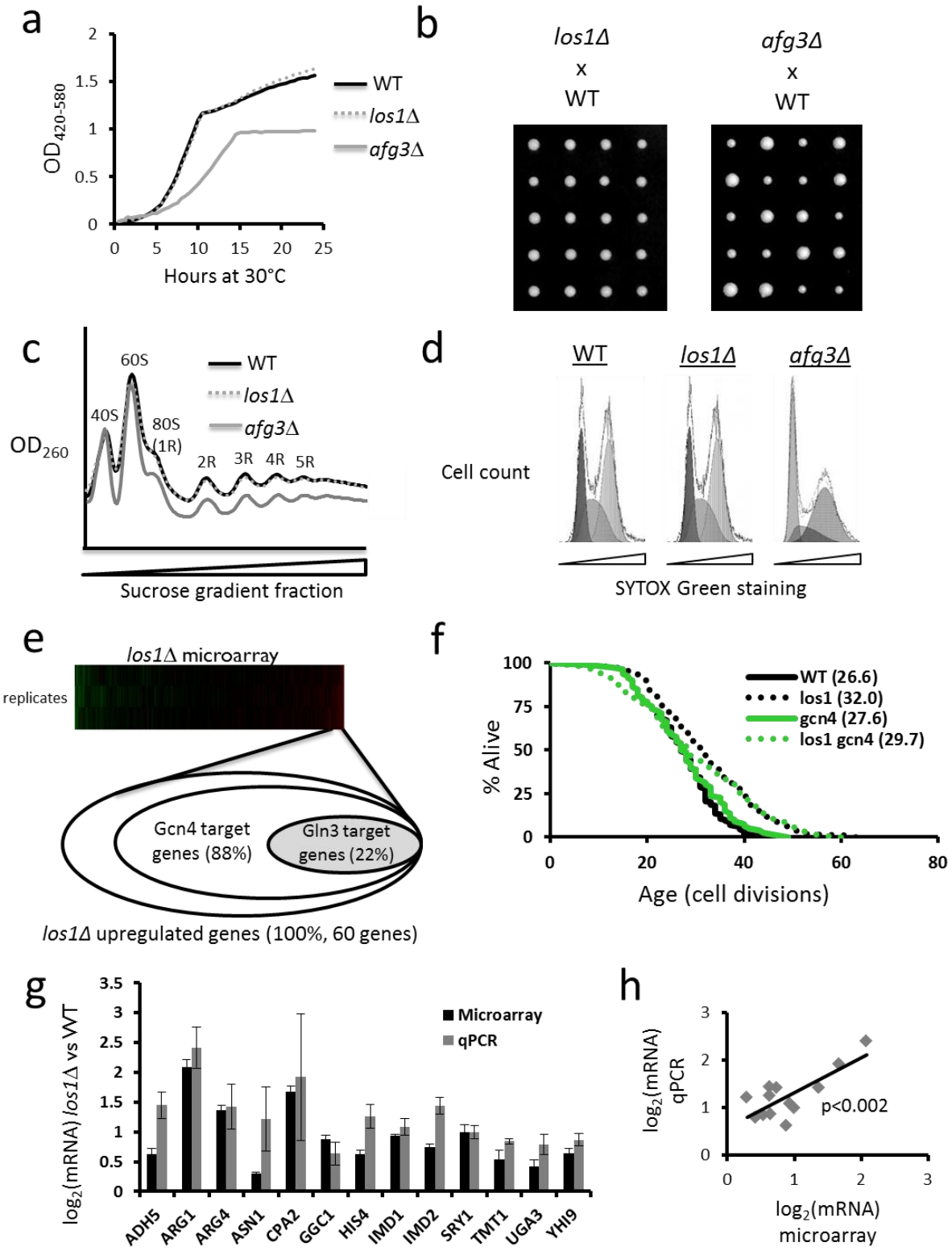

a-d, Representative growth curves, haploid spore clones from a tetrad dissection, polysome profiles, and cell cycle profiles of *los1*Δ and WT yeast indicate that *los1*Δ cells do not have a significant defect in mRNA translation. For comparison, a translation-deficient *afg3*Δ mutant is shown in each case. The R values in part c correspond to the number of ribosomes bound to a particular mRNA. **e**, Diagram highlighting the relative proportions of Gcn4 and Gln3 regulated genes within the subset of genes found to be upregulated in *los1*Δ yeast. **f,** Deletion of *GCN4* does not block RLS extension from deletion of *LOS1*. All RLS statistics are provided in Table S1. **g,** RT-qPCR verification of the Gln3 target genes found to be upregulated bymicroarray analysis of *los1*Δ cells. **h,** Comparison of the qPCR results with those of the microarray.

Figure 4: Gln3 activation mediates RLS extension by DR

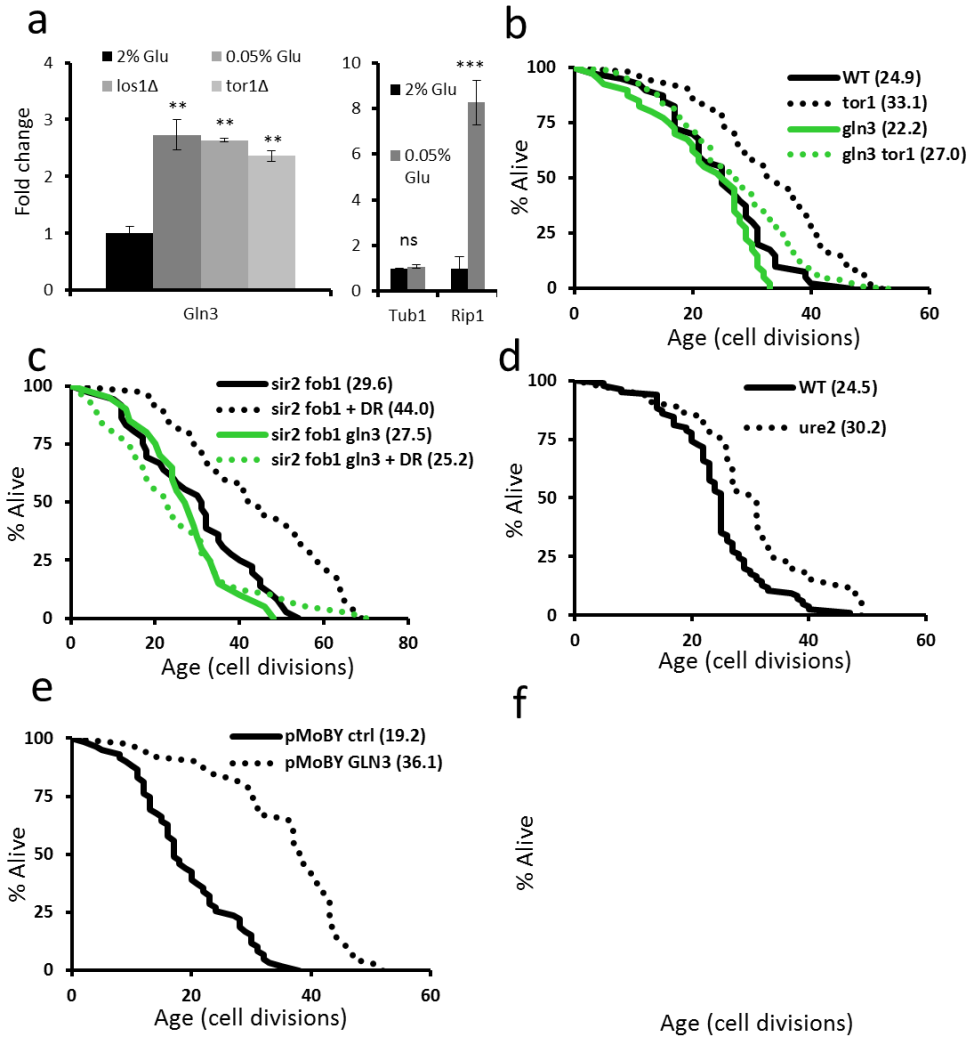

a, Flow cytometry experiments quantifying the amount of endogenously tagged GFP proteins from thousands of cells. Gln3 abundance is increased in DR and DR mimetics *los1*Δ and *tor1*Δ. Positive and negative controls for abundance, Rip1 and Tub1, respectively, are also shown. **p<0.01, ***p<0.001, ns indicates p>0.05. **b,** Deletion of *GLN3* blocks RLS extension from deletion of *TOR1*. **c,** Deletion of *GLN3* blocks RLS extension from DR. **d,** Deletion of the negative regulator of *GLN3*, *URE2*, extends RLS. **e,** Overexpression of *GLN3* is sufficient to extend RLS. **f,** Double deletion of both *GLN3* and *GCN4* blocks RLS extension from deletion of *LOS1*. All RLS statistics are provided in Table S1.

Figure 5: Gln3 pathway protects against DNA damage

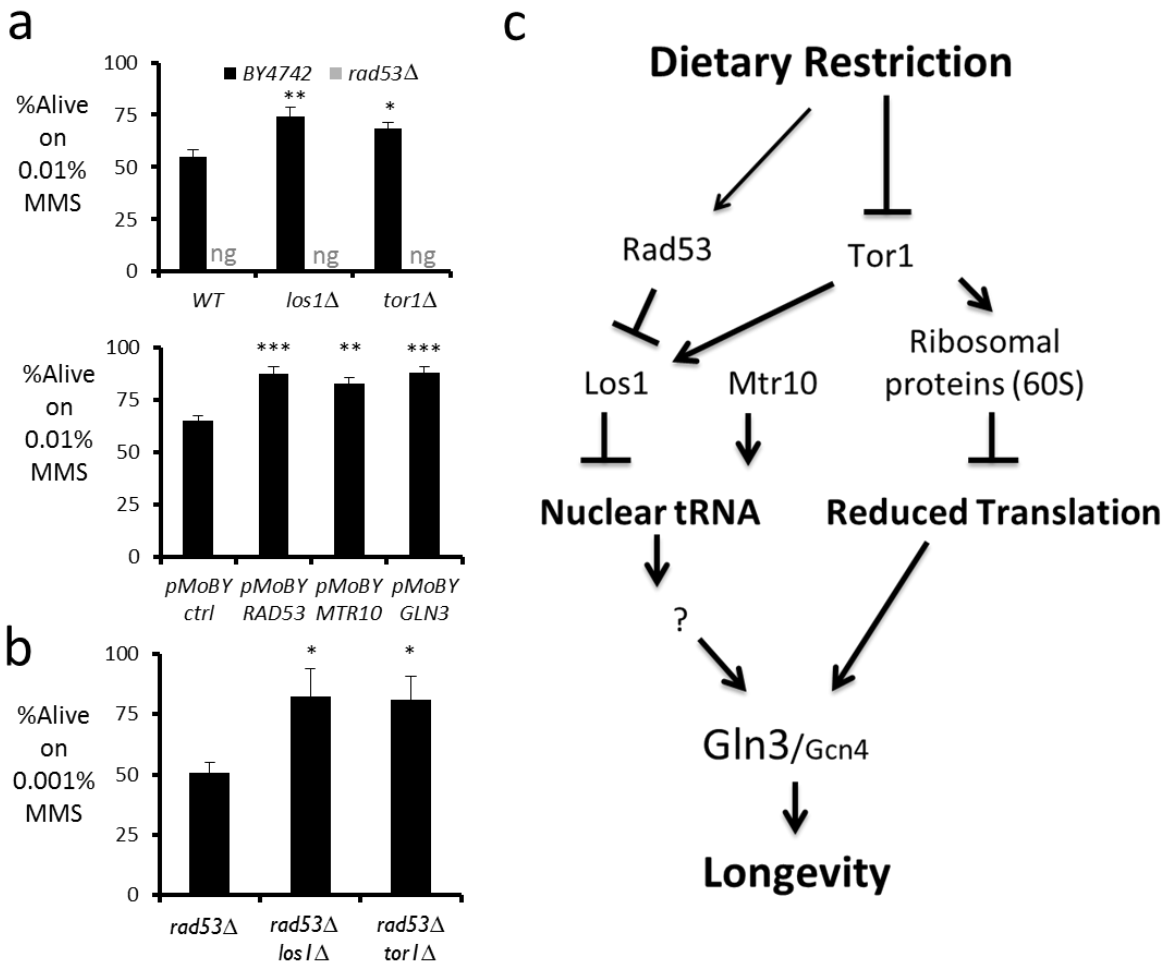

a,b, Quantitation of colony forming units of WT or mutant yeast stressed with the DNA alkylating agent MMS. p values are compared to WT or pMoBY WT controls. ng indicates no survival, *p<0.05, **p<0.01, ***p<0.001. **c,** Diagram summarizing a simplistic view of the main results supported by the data in this publication.

Concluding remarks and discussion

In the short time I have had the benefit of studying yeast lifespan in the Kaeberlein lab, we have dramatically advanced our understanding of how yeast lifespan is regulated. Certainly the most interesting finding was the identification of "the" transcription factor which regulates yeast lifespan through 0.05% glucose mediated dietary restriction (DR). Gln3 was found because its targets were upregulated in the long lived *los1*Δ mutant, which we showed extended replicative lifespan (RLS) in a pathway overlapping DR. In addition to the novelty of Gln3 being not only necessary but sufficient for RLS extension, this project revealed novel nodes to the DR pathway. DR signals through a DNA damage response factor Rad53 as well as through the nuclear tRNA exporter Los1. No parts of these pathways were previously implicated in lifespan extension and would have taken much longer to find without the unbiased screen the Kennedy lab pioneered in conjunction with our own. As with every good find in science, this study opens up just as many questions as were answered. If Gln3 is the only transcription factor necessary for RLS extension by DR, which of its targets are responsible for this? We are attempting to answer this question by making double mutants with *los1*Δ and a deletion of one of the 13 targets of Gln3 upregulated in *los1*Δ mutants. We are simultaneously constructing overexpression strains of these 13 targets in the hope that some will extend RLS. Nuclear tRNA can occur in any organism, so can it induce similar longevity enhancing signals in other organisms? If so, what senses tRNA and passes the signal to a Gln3-like transcription factor? On that note, Gln3 is modestly conserved at best in mammals (10% homology at most), so what is the target transcription factor in higher eukaryotes? We at least have an idea in yeast that Gcn2 can bind nuclear, uncharged tRNA and induce phosphorylation events, so it will be very interesting to see if this can activate Gln3 in yeast and what its targets are in other organisms.

While the tRNA/Los1/Gln3 project undoubtedly caps my achievements in the Kaeberlein lab, all the other projects mentioned in the above sections were valuable and welcome additions to longevity studies. We

were somewhat surprised the paper supporting antagonistic pleiotropy did not draw more praise from reviewers on previous submissions of that paper; it truly was the first study systematically searching for evidence supporting the evolutionary theory of aging. 32 out of 49 mutants fit the tenets of the theory with just a simple outgrowth test followed by periodic short bursts of low nutrients, and the other mutants could easily be found to support the theory if additional stresses were tested for fitness. Since it is still widely debated about whether or not there is any selection for aging related processes in nature, this study should be included in further reviews of the subject. It also places into context what types of problems we may encounter through longevity interventions; what are the consequences of reduced translation aside from enhanced lifespan potential? This is particularly an issue for the TOR pathway, since rapamycin was initially used to aid in immunosuppression. While humankind certainly is evolving in ways unique to the history of biology, there will undoubtedly be problems with interventions we think should extend lifespan and understanding the risks will be crucial to appropriately using them in medicine. In light of the Gln3 story, it may be possible to activate longevity pathways without reducing translation. This should reduce the risks of longevity interventions substantially, although further studies of course will have to be done to support this hypothesis.

As I continue to point out, science evolves just as species do, although we certainly hope it does so at a faster rate! Sirtuins were promising mediators of lifespan extension by caloric restriction a decade ago, however we have thoroughly shown the fallacy of that notion in yeast. Knockouts of *SIR2* made every one of 32 long lived mutants tested fail to extend lifespan, but this was shown not to be because all of them acted through Sir2. A deletion of *FOB1* relieved the damage in *sir2*Δ mutants and allowed interventions to extend lifespan in a *sir2*Δ*fob1*Δ double mutant, indicating Sir2 is dispensable for many forms of lifespan extension. With this in mind, it is unlikely that the homologue SIRT1 regulates aging similarly in mice. Nonetheless, since it is a NAD+ dependent deacetylase and certainly has roles important roles regulating p53[161] and other tumor suppressors[162], it will continue to be an interesting protein to study, but probably in an aging independent manner. There are also emerging studies

suggesting that the closely related protein SIRT6 may be a more promising Sirtuin which can regulate aging related processes[163,164]. It is the opinion of this author, however, that there are much more promising longevity interventions within the TOR pathway and the sirtuin studies may be heavily biased.

The TOR pathway is ever expanding and there is no doubt it will take many more years to figure out how it functions in longevity across the different species. Our phenotype clustering study presented here implicates the mitochondria AAA protease as being involved in lifespan extension in an overlapping pathway. This result was completely unexpected and raises far more questions than it answers. How would *dys*function at the mitochondria signal for something which increases lifespan? It is clear from work by the Dillon lab that a mitochondria unfolded protein response may be able to extend lifespan in worms, and it is possible that a similar mechanism is working in yeast. Indeed, another report from Jennifer Schleit and Simon Johnson from our lab (to be published soon), suggests there is a sort of mitochondria unfolded protein response in yeast and it may be moderating some genotype specific increases in lifespan by DR. We showed in Section IV that *afg3*Δ mutants have some capacity to resist ER stress independent of Hac1, and it may be due to activation of another type of unfolded protein response. Perhaps most the interesting piece of data aside from the aging context is that *afg3*Δ mutants have a translational defect, suggesting signaling from the mitochondria to the translation machinery. This defect is not resulting from a simple lack of ATP since we can isolate suppressors which restore normal translation rates in an *afg3*Δ mutant without restoring their ability to respire. We have been attempting to isolate the identity of this suppressor and know that once discovered, it will be a finding which will bring a completely new translation regulatory pathway into the view of molecular biologists. Hopefully, it will also enable us to regulate lifespan without reducing mitochondria function or translation. Time will tell.

The general findings of the sections in this dissertation are summarized in the figure below. Newly discovered or supported connections are highlighted in green. Interesting related studies which should be done are highlighted with red question marks. Thank you for reading!

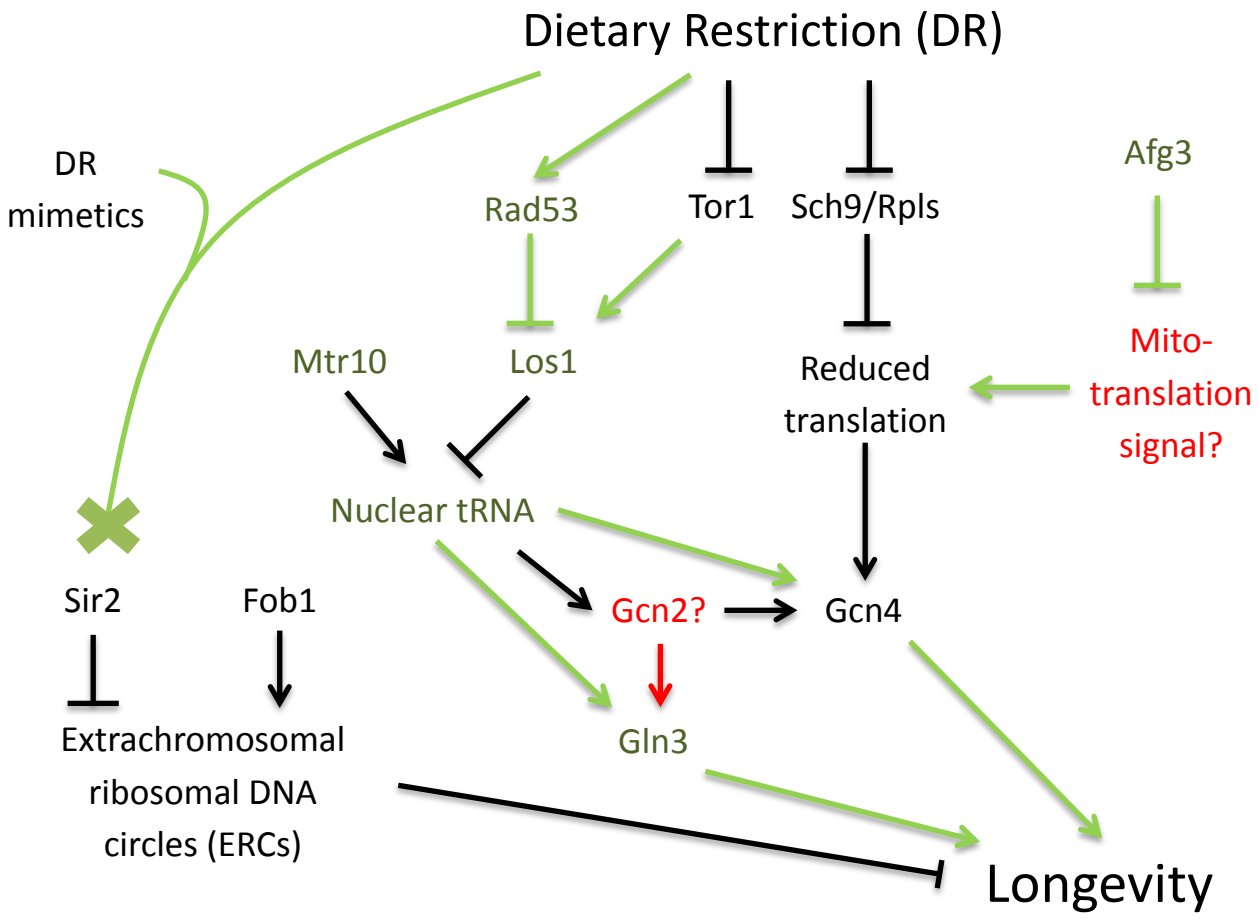

List of Abbreviations:

In alphabetical order:

CLS, Chronological lifespan

DR, Dietary restriction

RLS, Replicative lifespan

TOR, Target of rapamycin

Acknowledgements:

I would like to thank everyone who has helped make my PhD possible and made my experience at UW an exciting research endeavor. Matt Kaeberlein has routinely surprised me by his ability to hang out in our corner of the lab for five minutes and shoot off a number of great ideas we all could actively pursue to make our projects better. He has been extremely helpful in getting all the material present here published in higher profile journals than I ever expected them to. I have been given limitless opportunity thanks to his support, and cannot thank him enough for that, and the fact that he never showed anger beyond sarcasm is rare in science. The undergraduate researchers who have worked directly with me (my team!), Annie Chou, Umema Ahmed, and Sylvia Sim probably did more hands on work than I in many of the projects and were the most reliable and friendly people I could ask for. All the members on my committee who have supported me throughout my graduate career, including Peter Rabinovitch, Brian Kennedy, Maitreya Dunham, Rich Gardner, and Weiqing Li have also helped make my UW experience the best of my career so far and extended my collaborative potential. The people at the Institute of Aging Research at Guangdong Medical College also expanded my collaborative potential and opened my eyes to international research. I could not have produced the publications I have without the tremendous help from my colleagues within the Kaeberlein lab and its affiliated labs and they deserve acknowledgement as well. Chris Murakami managed the lab to be a place of efficiency against many obstacles, and has provided both ideas and talented bench work to aid in the majority of projects within this dissertation. George Sutphin, a fellow MCB PhD student, helped me understand the potential in working with an equal on a project from beginning to end, and we both hope to continue publishing together in the future. Brady Olsen, despite working as many programmers do in the dungeons at night, was integral in allowing for data analysis he made possible through extensive database management and statistical assistance. There are too many replicative lifespan dissectors to thank than can fit on this page, but I hope they know their work is appreciated through their inclusion as authors on all manuscripts included here and through the stories I will pass on in my career. I might have gone insane if it were not for their random conversations

in D600 which made dissecting with them the best part of any day. Of course the management of Daniel Carr and the initial help of Jenn Schleit to help the replicative lifespan team meet their full potential was a godsend. I have benefitted from the contact of all other members of the Kaeberlein lab and thank them all for helping me get where I am today.

Bibliography:

1 Jones, W. Longevity in a fasting spider. *Science* **3**, 4, doi:10.1126/science.ns-3.48.4-c (1884).
2 Williams, G. C. Pleiotropy, natural selection, and the evolution of senescence. *Evolution* **11**, 398-411 (1957).
3 Kenyon, C., Chang, J., Gensch, E., Rudner, A. & Tabtiang, R. A C. elegans mutant that lives twice as long as wild type. *Nature* **366**, 461-464 (1993).
4 Walker, D. W., McColl, G., Jenkins, N. L., Harris, J. & Lithgow, G. J. Evolution of lifespan in C. elegans. *Nature* **405**, 296-297 (2000).
5 Kaeberlein, M. *et al.* Substrate specific activation of sirtuins by resveratrol. *The Journal of biological chemistry* **280**, 17038-17045 (2005).
6 Anderson, R. M., Bitterman, K. J., Wood, J. G., Medvedik, O. & Sinclair, D. A. Nicotinamide and PNC1 govern lifespan extension by calorie restriction in Saccharomyces cerevisiae. *Nature* **423**, 181-185, doi:10.1038/nature01578 (2003).
7 Boily, G. *et al.* SirT1 regulates energy metabolism and response to caloric restriction in mice. *PLoS One* **3**, e1759, doi:10.1371/journal.pone.0001759 (2008).
8 Kaeberlein, M., Kirkland, K. T., Fields, S. & Kennedy, B. K. Sir2-independent life span extension by calorie restriction in yeast. *PLoS Biol* **2**, E296 (2004).
9 Burtner, C. R., Murakami, C. J., Kennedy, B. K. & Kaeberlein, M. A molecular mechanism of chronological aging in yeast. *Cell Cycle* **8**, 1256-1270 (2009).
10 Burhans, W. C. & Weinberger, M. Acetic acid effects on aging in budding yeast: are they relevant to aging in higher eukaryotes? *Cell Cycle* **8**, 2300-2302 (2009).
11 Burtner, C. R., Murakami, C. J., Olsen, B., Kennedy, B. K. & Kaeberlein, M. A genomic analysis of chronological longevity factors in budding yeast. *Cell Cycle* **10**, 1385-1396 (2011).
12 Smith, E. D. *et al.* Quantitative evidence for conserved longevity pathways between divergent eukaryotic species. *Genome research* **18**, 564-570, doi:10.1101/gr.074724.107 (2008).
13 Sutphin, G. L., Olsen, B. A., Kennedy, B. K. & Kaeberlein, M. Genome-wide analysis of yeast aging. *Subcell Biochem* **57**, 251-289, doi:10.1007/978-94-007-2561-4_12 (2012).
14 Ashrafi, K., Sinclair, D., Gordon, J. I. & Guarente, L. Passage through stationary phase advances replicative aging in Saccharomyces cerevisiae. *Proceedings of the National Academy of Sciences of the United States of America* **96**, 9100-9105 (1999).
15 Weinberger, M. *et al.* DNA replication stress is a determinant of chronological lifespan in budding yeast. *PloS one* **2**, e748, doi:10.1371/journal.pone.0000748 (2007).
16 Zhou, K. I., Pincus, Z. & Slack, F. J. Longevity and stress in Caenorhabditis elegans. *Aging (Albany NY)* **3**, 733-753 (2011).
17 Nakagawa, S., Lagisz, M., Hector, K. L. & Spencer, H. G. Comparative and meta-analytic insights into life extension via dietary restriction. *Aging Cell* **11**, 401-409, doi:10.1111/j.1474-9726.2012.00798.x (2012).
18 Fontana, L., Partridge, L. & Longo, V. D. Extending healthy life span--from yeast to humans. *Science* **328**, 321-326, doi:10.1126/science.1172539 (2010).
19 Kaeberlein, M. Lessons on longevity from budding yeast. *Nature* **464**, 513-519, doi:nature08981 [pii]
10.1038/nature08981 (2010).
20 Hellmuth, K. *et al.* Yeast Los1p has properties of an exportin-like nucleocytoplasmic transport factor for tRNA. *Molecular and cellular biology* **18**, 6374-6386 (1998).
21 Murthi, A. *et al.* Regulation of tRNA bidirectional nuclear-cytoplasmic trafficking in Saccharomyces cerevisiae. *Molecular biology of the cell* **21**, 639-649, doi:10.1091/mbc.E09-07-0551 (2010).
22 Shaheen, H. H. & Hopper, A. K. Retrograde movement of tRNAs from the cytoplasm to the nucleus in Saccharomyces cerevisiae. *Proc Natl Acad Sci U S A* **102**, 11290-11295, doi:10.1073/pnas.0503836102 (2005).

23 Delaney, J. R., Murakami, C. J., Olsen, B., Kennedy, B. K. & Kaeberlein, M. Quantitative evidence for early life fitness defects from 32 longevity-associated alleles in yeast. *Cell Cycle* **10**, 156-165 (2011).

24 Nystrom, T. Translational fidelity, protein oxidation, and senescence: lessons from bacteria. *Ageing Res Rev* **1**, 693-703 (2002).

25 He, K. W., Shen, L. L., Zhou, W. W. & Wang, D. Y. Regulation of aging by unc-13 and sbt-1 in Caenorhabditis elegans is temperature-dependent. *Neurosci Bull* **25**, 335-342 (2009).

26 Van Raamsdonk, J. M. & Hekimi, S. Deletion of the mitochondrial superoxide dismutase sod-2 extends lifespan in Caenorhabditis elegans. *PLoS Genet* **5**, e1000361 (2009).

27 Clancy, D. J. *et al.* Extension of life-span by loss of CHICO, a Drosophila insulin receptor substrate protein. *Science* **292**, 104-106 (2001).

28 Tatar, M. *et al.* A mutant Drosophila insulin receptor homolog that extends life-span and impairs neuroendocrine function. *Science* **292**, 107-110 (2001).

29 Brown-Borg, H. M., Borg, K. E., Meliska, C. J. & Bartke, A. Dwarf mice and the ageing process. *Nature* **384**, 33 (1996).

30 Rose, M. & Charlesworth, B. A test of evolutionary theories of senescence. *Nature* **287**, 141-142 (1980).

31 Partridge, L., Prowse, N. & Pignatelli, P. Another set of responses and correlated responses to selection on age at reproduction in Drosophila melanogaster. *Proc Biol Sci* **266**, 255-261 (1999).

32 Buck, S., Vettraino, J., Force, A. G. & Arking, R. Extended longevity in Drosophila is consistently associated with a decrease in developmental viability. *J Gerontol A Biol Sci Med Sci* **55**, B292-301 (2000).

33 Zwaan, B. J., Bijlsma, R. & Hoekstra, R. F. Direct selection on lifespan in Drosophila melanogaster. *Evolution* **49**, 649-659 (1995).

34 Stearns, S. C., Ackermann, M., Doebeli, M. & Kaiser, M. Experimental evolution of aging, growth, and reproduction in fruitflies. *Proc Natl Acad Sci U S A* **97**, 3309-3313 (2000).

35 Giannakou, M. E. *et al.* Dynamics of the action of dFOXO on adult mortality in Drosophila. *Aging Cell* **6**, 429-438 (2007).

36 Liu, X. *et al.* Evolutionary conservation of the clk-1-dependent mechanism of longevity: loss of mclk1 increases cellular fitness and lifespan in mice. *Genes Dev* **19**, 2424-2434 (2005).

37 Jenkins, N. L., McColl, G. & Lithgow, G. J. Fitness cost of extended lifespan in Caenorhabditis elegans. *Proc Biol Sci* **271**, 2523-2526 (2004).

38 Marden, J. H., Rogina, B., Montooth, K. L. & Helfand, S. L. Conditional tradeoffs between aging and organismal performance of Indy long-lived mutant flies. *Proc Natl Acad Sci U S A* **100**, 3369-3373 (2003).

39 Toivonen, J. M., Gems, D. & Partridge, L. Longevity of Indy mutant Drosophila not attributable to Indy mutation. *Proc Natl Acad Sci U S A* **106**, E53; author reply E54 (2009).

40 Jazwinski, S. M. Yeast longevity and aging--the mitochondrial connection. *Mech Ageing Dev* **126**, 243-248 (2005).

41 Kaeberlein, M. *et al.* Regulation of yeast replicative life span by TOR and Sch9 in response to nutrients. *Science* **310**, 1193-1196 (2005).

42 Kaeberlein, M., Kirkland, K. T., Fields, S. & Kennedy, B. K. Genes determining yeast replicative life span in a long-lived genetic background. *Mech Ageing Dev* **126**, 491-504 (2005).

43 Steffen, K. K. *et al.* Yeast life span extension by depletion of 60s ribosomal subunits is mediated by Gcn4. *Cell* **133**, 292-302 (2008).

44 Smith, E. D. *et al.* Quantitative evidence for conserved longevity pathways between divergent eukaryotic species. *Genome Res* **18**, 564-570 (2008).

45 Managbanag, J. R. *et al.* Shortest-path network analysis is a useful approach toward identifying genetic determinants of longevity. *PLoS One* **3**, e3802 (2008).

46 Tsuchiya, M. *et al.* Sirtuin-independent effects of nicotinamide on lifespan extension from calorie restriction in yeast. *Aging Cell* **5**, 505-514 (2006).

47 Kaeberlein, M., McVey, M. & Guarente, L. The SIR2/3/4 complex and SIR2 alone promote longevity in Saccharomyces cerevisiae by two different mechanisms. *Genes Dev* **13**, 2570-2580 (1999).
48 Winzeler, E. A. *et al.* Functional characterization of the S. cerevisiae genome by gene deletion and parallel analysis. *Science* **285**, 901-906 (1999).
49 Brachmann, C. B. *et al.* Designer deletion strains derived from Saccharomyces cerevisiae S288C: a useful set of strains and plasmids for PCR-mediated gene disruption and other applications. *Yeast* **14**, 115-132 (1998).
50 R. Mortimer, M. P. On the origins of wine yeast. *Research in microbiology* **150**, 199-204 (1999).
51 Kirkwood, T. B. & Austad, S. N. Why do we age? *Nature* **408**, 233-238 (2000).
52 Kirkwood, T. B. Evolution of ageing. *Mech Ageing Dev* **123**, 737-745 (2002).
53 Kirkwood, T. B. & Holliday, R. The evolution of ageing and longevity. *Proc R Soc Lond B Biol Sci* **205**, 531-546 (1979).
54 Kennedy, B. K. & Kaeberlein, M. Hot topics in aging research: protein translation, 2009. *Aging Cell* **8**, 617-623, doi:ACE522 [pii]
10.1111/j.1474-9726.2009.00522.x (2009).
55 Barbet, N. C. *et al.* TOR controls translation initiation and early G1 progression in yeast. *Mol Biol Cell* **7**, 25-42 (1996).
56 Tyers, M., Tokiwa, G. & Futcher, B. Comparison of the Saccharomyces cerevisiae G1 cyclins: Cln3 may be an upstream activator of Cln1, Cln2 and other cyclins. *Embo J* **12**, 1955-1968 (1993).
57 Gallego, C., Gari, E., Colomina, N., Herrero, E. & Aldea, M. The Cln3 cyclin is down-regulated by translational repression and degradation during the G1 arrest caused by nitrogen deprivation in budding yeast. *Embo J* **16**, 7196-7206 (1997).
58 Olsen B, M. C., Kaeberlein M. YODA: Software to facilitate high-throughput analysis of chronological life span, growth rate, and survival in budding yeast. *BMC Bioinformatics* **11** (2010).
59 Haase, S. B. & Reed, S. I. Improved flow cytometric analysis of the budding yeast cell cycle. *Cell Cycle* **1**, 132-136 (2002).
60 Steffen, K. K., Kennedy, B. K. & Kaeberlein, M. Measuring replicative life span in the budding yeast. *J Vis Exp*, doi:1209 [pii]
10.3791/1209 (2009).
61 Delaney, J. R. *et al.* Sir2 deletion prevents lifespan extension in 32 long-lived mutants. *Aging Cell* **10**, 1089-1091, doi:10.1111/j.1474-9726.2011.00742.x (2011).
62 Lin, S. J., Defossez, P. A. & Guarente, L. Requirement of NAD and SIR2 for life-span extension by calorie restriction in Saccharomyces cerevisiae. *Science* **289**, 2126-2128. (2000).
63 Rogina, B. & Helfand, S. L. Sir2 mediates longevity in the fly through a pathway related to calorie restriction. *Proceedings of the National Academy of Sciences of the United States of America* **101**, 15998-16003 (2004).
64 Wang, Y. & Tissenbaum, H. A. Overlapping and distinct functions for a Caenorhabditis elegans SIR2 and DAF-16/FOXO. *Mechanisms of ageing and development* **127**, 48-56 (2006).
65 Li, Y., Xu, W., McBurney, M. W. & Longo, V. D. SirT1 inhibition reduces IGF-I/IRS-2/Ras/ERK1/2 signaling and protects neurons. *Cell Metab* **8**, 38-48 (2008).
66 Baur, J. A. *et al.* Dietary restriction: standing up for sirtuins. *Science* **329**, 1012-1013; author reply 1013-1014 (2010).
67 Smith, D. L., Jr. *et al.* Calorie restriction effects on silencing and recombination at the yeast rDNA. *Aging Cell* **8**, 633-642, doi:ACE516 [pii]
10.1111/j.1474-9726.2009.00516.x (2009).
68 Riesen, M. & Morgan, A. Calorie restriction reduces rDNA recombination independently of rDNA silencing. *Aging Cell* **8**, 624-632, doi:ACE514 [pii]
10.1111/j.1474-9726.2009.00514.x (2009).

69 Gottlieb, S. & Esposito, R. E. A new role for a yeast transcriptional silencer gene, SIR2, in regulation of recombination in ribosomal DNA. *Cell* **56**, 771-776, doi:0092-8674(89)90681-8 [pii] (1989).
70 Smith, J. S. & Boeke, J. D. An unusual form of transcriptional silencing in yeast ribosomal DNA. *Genes Dev* **11**, 241-254 (1997).
71 Aguilaniu, H., Gustafsson, L., Rigoulet, M. & Nystrom, T. Asymmetric inheritance of oxidatively damaged proteins during cytokinesis. *Science* **299**, 1751-1753 (2003).
72 Dang, W. *et al.* Histone H4 lysine 16 acetylation regulates cellular lifespan. *Nature* **459**, 802-807, doi:nature08085 [pii]
10.1038/nature08085 (2009).
73 Erjavec, N., Larsson, L., Grantham, J. & Nystrom, T. Accelerated aging and failure to segregate damaged proteins in Sir2 mutants can be suppressed by overproducing the protein aggregation-remodeling factor Hsp104p. *Genes & development* **21**, 2410-2421, doi:10.1101/gad.439307 (2007).
74 Fabrizio, P. & Longo, V. D. The chronological life span of Saccharomyces cerevisiae. *Methods in molecular biology* **371**, 89-95, doi:1-59745-361-7:89 [pii] (2007).
75 Fabrizio, P. & Longo, V. D. The chronological life span of Saccharomyces cerevisiae. *Aging cell* **2**, 73-81 (2003).
76 Mortimer, R. K. & Johnston, J. R. Life span of individual yeast cells. *Nature* **183**, 1751-1752 (1959).
77 Steinkraus, K. A., Kaeberlein, M. & Kennedy, B. K. Replicative aging in yeast: the means to the end. *Annual review of cell and developmental biology* **24**, 29-54, doi:10.1146/annurev.cellbio.23.090506.123509 (2008).
78 Kaeberlein, M. & Kennedy, B. K. Large-scale identification in yeast of conserved ageing genes. *Mech Ageing Dev* **126**, 17-21 (2005).
79 Muller, I. Experiments on ageing in single cells of Saccharomyces cerevisiae. *Arch Mikrobiol* **77**, 20-25 (1971).
80 Kennedy, B. K. *et al.* Redistribution of silencing proteins from telomeres to the nucleolus is associated with extension of life span in S. cerevisiae. *Cell* **89**, 381-391 (1997).
81 Burtner, C. R., Murakami, C. J. & Kaeberlein, M. A genomic approach to yeast chronological aging. *Methods in molecular biology* **548**, 101-114, doi:10.1007/978-1-59745-540-4_6 (2009).
82 Murakami, C. J., Burtner, C. R., Kennedy, B. K. & Kaeberlein, M. A method for high-throughput quantitative analysis of yeast chronological life span. *The journals of gerontology. Series A, Biological sciences and medical sciences* **63**, 113-121 (2008).
83 Smith, D. L., Jr., McClure, J. M., Matecic, M. & Smith, J. S. Calorie restriction extends the chronological lifespan of Saccharomyces cerevisiae independently of the Sirtuins. *Aging cell* **6**, 649-662, doi:10.1111/j.1474-9726.2007.00326.x (2007).
84 Herker, E. *et al.* Chronological aging leads to apoptosis in yeast. *The Journal of cell biology* **164**, 501-507, doi:10.1083/jcb.200310014
jcb.200310014 [pii] (2004).
85 Laun, P. *et al.* Aged mother cells of Saccharomyces cerevisiae show markers of oxidative stress and apoptosis. *Mol Microbiol* **39**, 1166-1173 (2001).
86 Madeo, F., Frohlich, E. & Frohlich, K. U. A yeast mutant showing diagnostic markers of early and late apoptosis. *J. Cell Biol.* **139**, 729-734 (1997).
87 Fabrizio, P., Pozza, F., Pletcher, S. D., Gendron, C. M. & Longo, V. D. Regulation of longevity and stress resistance by Sch9 in yeast. *Science* **292**, 288-290 (2001).
88 Longo, V. D. & Fabrizio, P. Regulation of longevity and stress resistance: a molecular strategy conserved from yeast to humans? *Cellular and molecular life sciences : CMLS* **59**, 903-908 (2002).
89 Fabrizio, P. *et al.* Superoxide is a mediator of an altruistic aging program in Saccharomyces cerevisiae. *The Journal of cell biology* **166**, 1055-1067, doi:10.1083/jcb.200404002

jcb.200404002 [pii] (2004).
90 Pan, Y., Schroeder, E. A., Ocampo, A., Barrientos, A. & Shadel, G. S. Regulation of yeast chronological life span by TORC1 via adaptive mitochondrial ROS signaling. *Cell metabolism* **13**, 668-678, doi:10.1016/j.cmet.2011.03.018 (2011).
91 Murakami, C. J., Wall, V., Basisty, N. & Kaeberlein, M. Composition and acidification of the culture medium influences chronological aging similarly in vineyard and laboratory yeast. *PloS one* **6**, e24530, doi:10.1371/journal.pone.0024530 (2011).
92 Murakami, C. & Kaeberlein, M. Quantifying yeast chronological life span by outgrowth of aged cells. *J Vis Exp*, doi:1156 [pii]
10.3791/1156 (2009).
93 Yang, J. *et al.* Cell size and growth rate are major determinants of replicative lifespan. *Cell Cycle* **10**, 144-155, doi:10.4161/cc.10.1.14455 (2011).
94 Langsrud, S. & Sundheim, G. Flow cytometry for rapid assessment of viability after exposure to a quaternary ammonium compound. *J Appl Bacteriol* **81**, 411-418 (1996).
95 Roth, B. L., Poot, M., Yue, S. T. & Millard, P. J. Bacterial viability and antibiotic susceptibility testing with SYTOX green nucleic acid stain. *Appl Environ Microbiol* **63**, 2421-2431 (1997).
96 Madeo, F. *et al.* A caspase-related protease regulates apoptosis in yeast. *Molecular cell* **9**, 911-917, doi:S1097276502005014 [pii] (2002).
97 Mazzoni, C. & Falcone, C. Caspase-dependent apoptosis in yeast. *Biochim Biophys Acta* **1783**, 1320-1327, doi:10.1016/j.bbamcr.2008.02.015 (2008).
98 Reverter-Branchat, G., Cabiscol, E., Tamarit, J. & Ros, J. Oxidative damage to specific proteins in replicative and chronological-aged Saccharomyces cerevisiae: common targets and prevention by calorie restriction. *The Journal of biological chemistry* **279**, 31983-31989, doi:10.1074/jbc.M404849200 (2004).
99 Parrella, E. & Longo, V. D. The chronological life span of Saccharomyces cerevisiae to study mitochondrial dysfunction and disease. *Methods* **46**, 256-262, doi:10.1016/j.ymeth.2008.10.004 (2008).
100 Erjavec, N. & Nystrom, T. Sir2p-dependent protein segregation gives rise to a superior reactive oxygen species management in the progeny of Saccharomyces cerevisiae. *Proceedings of the National Academy of Sciences of the United States of America* **104**, 10877-10881, doi:0701634104 [pii]
10.1073/pnas.0701634104 (2007).
101 Lai, C. Y., Jaruga, E., Borghouts, C. & Jazwinski, S. M. A mutation in the ATP2 gene abrogates the age asymmetry between mother and daughter cells of the yeast Saccharomyces cerevisiae. *Genetics* **162**, 73-87 (2002).
102 Guaragnella, N., Antonacci, L., Passarella, S., Marra, E. & Giannattasio, S. Hydrogen peroxide and superoxide anion production during acetic acid-induced yeast programmed cell death. *Folia Microbiol (Praha)* **52**, 237-240 (2007).
103 Unal, E., Kinde, B. & Amon, A. Gametogenesis eliminates age-induced cellular damage and resets life span in yeast. *Science* **332**, 1554-1557, doi:10.1126/science.1204349 (2011).
104 Olsen, B., Murakami, C. J. & Kaeberlein, M. YODA: software to facilitate high-throughput analysis of chronological life span, growth rate, and survival in budding yeast. *BMC Bioinformatics* **11**, 141, doi:10.1186/1471-2105-11-141 (2010).
105 Kenyon, C. J. The genetics of ageing. *Nature* **464**, 504-512, doi:10.1038/nature08980 (2010).
106 Harper, J. M., Salmon, A. B., Leiser, S. F., Galecki, A. T. & Miller, R. A. Skin-derived fibroblasts from long-lived species are resistant to some, but not all, lethal stresses and to the mitochondrial inhibitor rotenone. *Aging Cell* **6**, 1-13, doi:10.1111/j.1474-9726.2006.00255.x (2007).
107 Salmon, A. B., Sadighi Akha, A. A., Buffenstein, R. & Miller, R. A. Fibroblasts from naked mole-rats are resistant to multiple forms of cell injury, but sensitive to peroxide, ultraviolet light, and endoplasmic reticulum stress. *J Gerontol A Biol Sci Med Sci* **63**, 232-241 (2008).

108 Harper, J. M. *et al.* Fibroblasts from long-lived bird species are resistant to multiple forms of stress. *J Exp Biol* **214**, 1902-1910, doi:10.1242/jeb.054643 (2011).

109 Powers, R. W., 3rd, Kaeberlein, M., Caldwell, S. D., Kennedy, B. K. & Fields, S. Extension of chronological life span in yeast by decreased TOR pathway signaling. *Genes Dev* **20**, 174-184 (2006).

110 Thorpe, G. W., Fong, C. S., Alic, N., Higgins, V. J. & Dawes, I. W. Cells have distinct mechanisms to maintain protection against different reactive oxygen species: oxidative-stress-response genes. *Proc Natl Acad Sci U S A* **101**, 6564-6569, doi:10.1073/pnas.0305888101 (2004).

111 Postma, L., Lehrach, H. & Ralser, M. Surviving in the cold: yeast mutants with extended hibernating lifespan are oxidant sensitive. *Aging (Albany NY)* **1**, 957-960 (2009).

112 Kaeberlein, M. & Kennedy, B. K. Large-scale identification in yeast of conserved aging genes. *Mech Ageing Dev* **126**, 17-21 (2005).

113 Kennedy, B. K., Steffen, K. K. & Kaeberlein, M. Ruminations on dietary restriction and aging. *Cell Mol Life Sci* **64**, 1323-1328 (2007).

114 Chiocchetti, A. *et al.* Ribosomal proteins Rpl10 and Rps6 are potent regulators of yeast replicative life span. *Exp Gerontol* **42**, 275-286, doi:S0531-5565(06)00342-1 [pii] 10.1016/j.exger.2006.11.002 (2007).

115 Delaney, J. R. *et al.* Sir2 deletion prevents lifespan extension in 32 long-lived mutants. *Aging Cell*, doi:10.1111/j.1474-9726.2011.00742.x (2011).

116 Hinnebusch, A. G. Translational regulation of yeast GCN4. A window on factors that control initiator-trna binding to the ribosome. *J Biol Chem* **272**, 21661-21664 (1997).

117 Nolden, M. *et al.* The m-AAA protease defective in hereditary spastic paraplegia controls ribosome assembly in mitochondria. *Cell* **123**, 277-289, doi:10.1016/j.cell.2005.08.003 (2005).

118 Arlt, H. *et al.* The formation of respiratory chain complexes in mitochondria is under the proteolytic control of the m-AAA protease. *Embo J* **17**, 4837-4847, doi:10.1093/emboj/17.16.4837 (1998).

119 Yoneda, T. *et al.* Compartment-specific perturbation of protein handling activates genes encoding mitochondrial chaperones. *J Cell Sci* **117**, 4055-4066, doi:10.1242/jcs.01275 (2004).

120 Kruegel, U. *et al.* Elevated Proteasome Capacity Extends Replicative Lifespan in Saccharomyces cerevisiae. *PLoS Genet* **7**, e1002253, doi:10.1371/journal.pgen.1002253 (2011).

121 Kaufman, R. J. Stress signaling from the lumen of the endoplasmic reticulum: coordination of gene transcriptional and translational controls. *Genes & development* **13**, 1211-1233 (1999).

122 Travers, K. J. *et al.* Functional and genomic analyses reveal an essential coordination between the unfolded protein response and ER-associated degradation. *Cell* **101**, 249-258 (2000).

123 Arlt, H., Tauer, R., Feldmann, H., Neupert, W. & Langer, T. The YTA10-12 complex, an AAA protease with chaperone-like activity in the inner membrane of mitochondria. *Cell* **85**, 875-885 (1996).

124 Guelin, E., Rep, M. & Grivell, L. A. Sequence of the AFG3 gene encoding a new member of the FtsH/Yme1/Tma subfamily of the AAA-protein family. *Yeast* **10**, 1389-1394, doi:10.1002/yea.320101016 (1994).

125 Cohen, G., Fessl, F., Traczyk, A., Rytka, J. & Ruis, H. Isolation of the catalase A gene of Saccharomyces cerevisiae by complementation of the cta1 mutation. *Mol Gen Genet* **200**, 74-79 (1985).

126 Slekar, K. H., Kosman, D. J. & Culotta, V. C. The yeast copper/zinc superoxide dismutase and the pentose phosphate pathway play overlapping roles in oxidative stress protection. *J Biol Chem* **271**, 28831-28836 (1996).

127 Steinman, H. M. The amino acid sequence of copper-zinc superoxide dismutase from bakers' yeast. *J Biol Chem* **255**, 6758-6765 (1980).

128 Hoopes, L. L., Budd, M., Choe, W., Weitao, T. & Campbell, J. L. Mutations in DNA replication genes reduce yeast life span. *Mol Cell Biol* **22**, 4136-4146 (2002).

129 Tong, W. *et al.* ArrayTrack--supporting toxicogenomic research at the U.S. Food and Drug Administration National Center for Toxicological Research. *Environ Health Perspect* **111**, 1819-1826 (2003).
130 Steffen, K. K. *et al.* Ribosome Deficiency Protects Against ER Stress in Saccharomyces cerevisiae. *Genetics*, doi:10.1534/genetics.111.136549 (2012).
131 Juhola, M. K., Shah, Z. H., Grivell, L. A. & Jacobs, H. T. The mitochondrial inner membrane AAA metalloprotease family in metazoans. *FEBS Lett* **481**, 91-95 (2000).
132 Andreou, A. M. & Tavernarakis, N. Protein metabolism and homeostasis in aging. Preface. *Adv Exp Med Biol* **694**, vii-viii (2010).
133 Kirchman, P. A., Kim, S., Lai, C. Y. & Jazwinski, S. M. Interorganelle signaling is a determinant of longevity in Saccharomyces cerevisiae. *Genetics* **152**, 179-190 (1999).
134 Heeren, G. *et al.* The mitochondrial ribosomal protein of the large subunit, Afo1p, determines cellular longevity through mitochondrial back-signaling via TOR1. *Aging (Albany NY)* **1**, 622-636 (2009).
135 Kaeberlein, M., McVey, M. & Guarente, L. The SIR2/3/4 complex and SIR2 alone promote longevity in Saccharomyces cerevisiae by two different mechanisms. *Genes Dev* **13**, 2570-2580. (1999).
136 MacKay, V. L. *et al.* Gene expression analyzed by high-resolution state array analysis and quantitative proteomics: response of yeast to mating pheromone. *Mol Cell Proteomics* **3**, 478-489, doi:10.1074/mcp.M300129-MCP200 (2004).
137 Stanfel, M. N., Shamieh, L. S., Kaeberlein, M. & Kennedy, B. K. The TOR pathway comes of age. *Biochim Biophys Acta* **1790**, 1067-1074, doi:S0304-4165(09)00173-1 [pii]
10.1016/j.bbagen.2009.06.007 (2009).
138 Kapahi, P. *et al.* With TOR, less is more: a key role for the conserved nutrient-sensing TOR pathway in aging. *Cell metabolism* **11**, 453-465, doi:S1550-4131(10)00153-1 [pii]
10.1016/j.cmet.2010.05.001 (2010).
139 Anderson, R. M. & Weindruch, R. Metabolic reprogramming, caloric restriction and aging. *Trends in endocrinology and metabolism: TEM* **21**, 134-141, doi:10.1016/j.tem.2009.11.005 (2010).
140 Sarkar, S. & Hopper, A. K. tRNA nuclear export in saccharomyces cerevisiae: in situ hybridization analysis. *Molecular biology of the cell* **9**, 3041-3055 (1998).
141 Yoshihisa, T., Yunoki-Esaki, K., Ohshima, C., Tanaka, N. & Endo, T. Possibility of cytoplasmic pre-tRNA splicing: the yeast tRNA splicing endonuclease mainly localizes on the mitochondria. *Molecular biology of the cell* **14**, 3266-3279, doi:10.1091/mbc.E02-11-0757 (2003).
142 Shaheen, H. H. *et al.* Retrograde nuclear accumulation of cytoplasmic tRNA in rat hepatoma cells in response to amino acid deprivation. *Proc Natl Acad Sci U S A* **104**, 8845-8850, doi:10.1073/pnas.0700765104 (2007).
143 Ghavidel, A. *et al.* Impaired tRNA nuclear export links DNA damage and cell-cycle checkpoint. *Cell* **131**, 915-926 (2007).
144 Shaheen, H. H. & Hopper, A. K. Retrograde movement of tRNAs from the cytoplasm to the nucleus in Saccharomyces cerevisiae. *Proc Natl Acad Sci U S A* **102**, 11290-11295, doi:10.1073/pnas.0503836102 (2005).
145 Sanchez, Y. *et al.* Regulation of RAD53 by the ATM-like kinases MEC1 and TEL1 in yeast cell cycle checkpoint pathways. *Science* **271**, 357-360 (1996).
146 Cox, L. S. & Mattison, J. A. Increasing longevity through caloric restriction or rapamycin feeding in mammals: common mechanisms for common outcomes? *Aging Cell* **8**, 607-613, doi:10.1111/j.1474-9726.2009.00509.x (2009).
147 Teixeira, M. C. *et al.* The YEASTRACT database: a tool for the analysis of transcription regulatory associations in Saccharomyces cerevisiae. *Nucleic Acids Res* **34**, D446-451, doi:10.1093/nar/gkj013 (2006).

148 Courchesne, W. E. & Magasanik, B. Regulation of nitrogen assimilation in Saccharomyces cerevisiae: roles of the URE2 and GLN3 genes. *Journal of bacteriology* **170**, 708-713 (1988).
149 Beck, T. & Hall, M. N. The TOR signalling pathway controls nuclear localization of nutrient-regulated transcription factors. *Nature* **402**, 689-692, doi:10.1038/45287 (1999).
150 Bertram, P. G. *et al.* Convergence of TOR-nitrogen and Snf1-glucose signaling pathways onto Gln3. *Molecular and cellular biology* **22**, 1246-1252 (2002).
151 Garinis, G. A., van der Horst, G. T., Vijg, J. & Hoeijmakers, J. H. DNA damage and ageing: new-age ideas for an age-old problem. *Nature cell biology* **10**, 1241-1247, doi:10.1038/ncb1108-1241 (2008).
152 Diderich, K., Alanazi, M. & Hoeijmakers, J. H. Premature aging and cancer in nucleotide excision repair-disorders. *DNA repair* **10**, 772-780, doi:10.1016/j.dnarep.2011.04.025 (2011).
153 Kennedy, S. R., Loeb, L. A. & Herr, A. J. Somatic mutations in aging, cancer and neurodegeneration. *Mechanisms of ageing and development*, doi:10.1016/j.mad.2011.10.009 (2011).
154 Ho, C. H. *et al.* A molecular barcoded yeast ORF library enables mode-of-action analysis of bioactive compounds. *Nat Biotechnol* **27**, 369-377, doi:10.1038/nbt.1534 (2009).
155 Huh, W. K. *et al.* Global analysis of protein localization in budding yeast. *Nature* **425**, 686-691 (2003).
156 Steffen, K. K., Kennedy, B. K. & Kaeberlein, M. Measuring replicative life span in the budding yeast. *J Vis Exp*, doi:10.3791/1209 (2009).
157 Sinclair, D. A. & Guarente, L. Extrachromosomal rDNA circles--a cause of aging in yeast. *Cell* **91**, 1033-1042 (1997).
158 Carvalho, B. S. & Irizarry, R. A. A framework for oligonucleotide microarray preprocessing. *Bioinformatics* **26**, 2363-2367, doi:10.1093/bioinformatics/btq431 (2010).
159 Smyth, G. K. Linear models and empirical bayes methods for assessing differential expression in microarray experiments. *Stat Appl Genet Mol Biol* **3**, Article3, doi:10.2202/1544-6115.1027 (2004).
160 Tusher, V. G., Tibshirani, R. & Chu, G. Significance analysis of microarrays applied to the ionizing radiation response. *Proceedings of the National Academy of Sciences of the United States of America* **98**, 5116-5121 (2001).
161 Vaziri, H. *et al.* hSIR2(SIRT1) functions as an NAD-dependent p53 deacetylase. *Cell* **107**, 149-159 (2001).
162 Yi, J. & Luo, J. SIRT1 and p53, effect on cancer, senescence and beyond. *Biochim Biophys Acta* **1804**, 1684-1689, doi:10.1016/j.bbapap.2010.05.002 (2010).
163 Mostoslavsky, R. *et al.* Genomic instability and aging-like phenotype in the absence of mammalian SIRT6. *Cell* **124**, 315-329, doi:10.1016/j.cell.2005.11.044 (2006).
164 Kanfi, Y. *et al.* The sirtuin SIRT6 regulates lifespan in male mice. *Nature* **483**, 218-221, doi:10.1038/nature10815 (2012).

VITA

Joseph Delaney was born in San Jose, CA. At the University of California at Berkeley he earned a Bachelor of Science degree in Chemical Biology, with honors in 2007. He participated in the post-baccalaureate program at the NIH working in the NCI in 2008. In 2012 he earned a Doctor of Philosophy at the University of Washington in Molecular and Cellular Biology.